Titre: Title:	Computational Musculoskeletal Finite Element Model Studies of a Knee Joint during Stair Ascent
Auteur: Author:	Amirhossein Makani
Date:	2022
Type:	Mémoire ou thèse / Dissertation or Thesis
Référence: Citation:	Makani, A. (2022). Computational Musculoskeletal Finite Element Model Studies of a Knee Joint during Stair Ascent [Master's thesis, Polytechnique Montréal]. PolyPublie. https://publications.polymtl.ca/10322/

URL de PolyPublie: PolyPublie URL:	https://publications.polymtl.ca/10322/
Directeurs de recherche: Advisors:	Aboulfazl Shirazi-Adl
Programme: Program:	Génie mécanique

POLYTECHNIQUE MONTRÉAL

affiliée à l'Université de Montréal

Computational Musculoskeletal Finite Element Model Studies of a Knee Joint During Stair Ascent

AMIRHOSSEIN MAKANI

Département de génie mécanique

Mémoire présenté en vue de l'obtention du diplôme de *Maîtrise ès sciences appliquées*

Génie mécanique

Avril 2022

POLYTECHNIQUE MONTRÉAL

affiliée à l'Université de Montréal

Ce mémoire intitulé :

Computational Musculoskeletal Finite Element Model Studies of a Knee Joint During Stair Ascent

présenté par **Amirhossein MAKANI**

en vue de l'obtention du diplôme de *Maîtrise ès sciences appliquées*

a été dûment accepté par le jury d'examen constitué de :

Aouni LAKIS, président
Aboulfazl SHIRAZI-ADL, membre et directeur de recherche
L'Hocine YAHIA, membre

ACKNOWLEDGEMENTS

Help of my dear friend, Dr. Masoud Sharifi is acknowledged.

RÉSUMÉ

Le genou est une articulation très chargée dans le corps humain qui subit de grands mouvements dans diverses activités quotidiennes. Les dommages aux structures du genou sont associées à des charges internes importantes. Environ un tiers des troubles articulaires proviennent de la région fémoropatellaire (FP) qui fait de la montée des escaliers une activité exigeante pour les patients. En tant que l'une des articulations les plus fréquemment blessées du corps humain, le genou souffre d'arthrose (OA) plus que toute autre articulation portante. L'arthrose est destructrice pour l'articulation du genou en dégradant sa lubrification, ses propriétés mécaniques, sa composition et sa morphologie. L'obésité, les tâches quotidiennes lourdes (montée d'escaliers par exemple) et les blessures existantes exposent le genou à un risque encore plus élevé d'initiation et de progression de l'arthrose. Les résultats de la 3e enquête nationale sur la santé et la nutrition (1988-1994) sur 6596 adultes âgés (> 60 ans) ont révélé que 18,1 % des hommes américains et 23,5 % des femmes américaines souffraient de douleurs au genou, la prévalence augmentant avec l'âge. Les douleurs au genou sont également plus fréquentes chez les femmes que chez les hommes. Une hypothèse raisonnable et généralement acceptée est que l'initiation et la progression de l'arthrose sont associées à la fois à des changements anormaux dans les zones de contact et à une amplitude élevée des contraintes de contact. Il existe une corrélation dose-réponse claire entre les symptômes de l'arthrose du genou et les activités de travail pénibles telles que s'agenouiller, s'accroupir, monter des escaliers et soulever des objets. L'arthroplastie totale du genou (TKA) est un traitement éprouvé avec jusqu'à 20 % d'échec nécessitant probablement une reprise chirurgicale. C’est estimé que le nombre de procédures TKA d'ici 2030, avec 3,5 millions de procédures par an, connaîtra une forte augmentation. Les lésions du ligament croisé antérieur (LCA) sont plus fréquentes chez les jeunes, en particulier chez les athlètes féminines. Les athlètes masculins courent un risque 5 fois plus faible de déchirures du LCA par rapport aux femmes. Même avec une chance de succès relativement élevée pour les chirurgies de reconstruction du LCA, les patients avec un LCA déficient sont sujets à un risque élevé de maladies du genou à long terme, en particulier l'arthrose.

Par rapport à la marche en palier comme l’activité quotidienne la plus populaire, la montée d'escaliers est moins fréquente mais une activité beaucoup plus exigeante avec surtout des forces de contact PF beaucoup plus importantes. La montée d'escaliers est une activité avec des moments et des angles sagittaux de la hanche et du genou plus importants que la marche à niveau. La

quantification précise de la biomécanique de l'articulation du genou dans la montée des escaliers est d'une grande aide non seulement dans la prévention des blessures et de la dégénérescence, mais également dans l'amélioration de la conception des implants, des stratégies de réadaptation et de traitement lors de la gestion des troubles de l'articulation du genou.

Pour étudier la biomécanique des membres inférieurs dans diverses activités, de nombreuses études in vitro, in vivo et de modélisation ont été réalisées. En raison du coût, de la difficulté et des limites des études de mesure in vitro et in vivo, les modèles numériques des membres inférieurs sont largement utilisés. Dans cette étude, nous visons à analyser la biomécanique détaillée de l'articulation du genou pendant la phase d'appui de la montée des escaliers en développant un modèle éléments finis- musculosquelettique (EF-MS) couplé et à comparer les résultats avec ceux de la marche à niveau tout en concentrant sur les forces musculaires, les forces de contact fémorotibiale-fémoropatellaire (FT-FP), les contraintes, et les zones ainsi que les forces dans les ligaments.

Dans ce travail, nous employons un modèle MS validé du membre inférieur couplé à un modèle FE détaillé de l'ensemble de l'articulation du genou tout en étant piloté par la moyenne des mesures cinématiques et cinétiques disponibles. Les insertions musculaires ont été extraites d'OpenSim puis appliquées au modèle EF-MS en ABAQUS. Les ligaments étaient représentés par plusieurs éléments de treillis (précontraints non linéaires,tension uniquement) dont leurs propriétés avaient déjà été étudiés et appliqués au modèle EF par notre groupe. L'articulation de la hanche a été tournée en fonction de la cinématique de la hanche, puis fixée. Les GRF ont été appliqués sur le pied à un endroit pour générer des moments signalés au niveau du genou pendant les simulations. Le poids du bas de la jambe et du pied a été pris en compte. Les forces musculaires ont été estimées de manière itérative à l'aide d'une approche d'optimisation contrainte par 7 équations moment-équilibre. On suppose que, par rapport à la marche en palier et sous la cinématique moyenne, la cinétique et les forces de réaction au sol (GRF) rapportées chez les individus en bonne santé, la montée d'escalier génère des forces de contact beaucoup plus importantes sur l'articulation PF mais des forces plus faibles dans le LCA. Les forces musculaires estimées à chaque étape, à l'aide d'une routine d'optimisation, ont été réappliquées de manière itérative (à leurs insertions et directions mises à jour) sur le modèle EF en tant que forces supplémentaires et l'analyse a été répétée jusqu'à convergence (moments déséquilibrés <0, 8 Nm).

Les activités musculaires estimées se comparent bien aux données électromyographiques enregistrées. Les quadriceps et les ischio-jambiers médiaux étaient les plus activés dans la première moitié de la position tandis que les gastrocnémiens ont atteint leurs forces maximales tardivement en position. Les forces maximales dans le quadriceps (3,87 poids corporel (PC), à 20 % chez notre sujet de 61,9 kg), les ischio-jambiers médiaux (0,77 PC à 20 %) et les gastrocnémiens (1,21 PC à 80 %) sont estimées. En raison d'angles-moments de flexion beaucoup plus importants au niveau des articulations de la hanche et du genou dans la première moitié de la position, on a estimé les forces et contraintes de contact de l'articulation FP dépassent leurs pics de marche en palier de quatre et de deux fois, respectivement. Par rapport à la marche à niveau, les forces du LCA diminuent dans la première moitié de la position mais augmentent considérablement plus tard dans la seconde moitié (pic de 0,76 PC à 75 % de la position). Sous des forces de contact presque similaires à 20 % de la position d'appui, la contrainte de contact dans le plateau médial tibio-fémoral atteint un pic (9,68 MPa) deux fois supérieur à celui de l'articulation FP, suggérant la vulnérabilité des deux articulations. En tant que stratégie efficace (pour réduire les charges internes et la douleur), les forces de contact FP élevées peuvent être atténuées en diminuant l'angle et/ou le moment de flexion du pic du genou. L'identification de l'efficacité relative du moment de flexion plus petit par rapport à l'angle de flexion plus petit nécessite cependant des études futures.

ABSTRACT

The knee is a highly loaded joint in the human body that undergoes large movements in various daily activities. As a result, it is vulnerable to failure and degeneration. About a third of joint disorders originate from the patellofemoral (PF) region that is highly loaded in many activities as squat lifting, kneeling and stair ascent. As one of the most commonly injured joints of the human body, the knee suffers from osteoarthritis (OA) more than any other weight bearing joint. OA is destructive to the knee joint by degrading its lubrication, mechanical properties, composition, and morphology. Obesity, heavy daily tasks (Stair ascent for instance) and existing injuries place the knee at even a higher risk of OA initiation and progression. Results of the 3rd National Health and Nutrition Examination Survey (1988-1994) on 6596 older adults (>60 years) revealed that merely 18.1% of US men and 23.5% of US women suffered from knee pain with the prevalence rising with age. Knee pains are also more common in women than men. A sound and generally accepted hypothesis is that the initiation and progression of OA are associated with both abnormal changes in contact areas and elevated magnitude of contact stresses. There is a clear dose-response correlation between knee OA symptoms and heavy work activities such as kneeling, squatting, stair climbing, and lifting. Total knee arthroplasty (TKA) is a common procedure with up to 20% failure likely requiring revision surgery. It is predicted that the number of TKA procedures rises by 2030 to an estimated 3.5 million procedures per year. Anterior cruciate ligament (ACL) injuries are more common among younger population, especially in female athletes. Male athletes are at a 5 times lower risk of ACL tears in comparison with their female counterparts. Even with a relatively high chance of success for ACL reconstruction surgeries, ACL deficient patients are prone to a high risk of long-term knee diseases especially OA.

Compared to the level walking as the most popular daily activity, stair ascent is less frequent but a much more demanding activity with especially much greater PF contact forces. Stair ascent is an activity with greater hip and knee sagittal moments and angles when compared to the level walking. Accurate quantification of the knee joint biomechanics in stair ascent is of great help not only in the injury and degeneration prevention but also in the improved design of implants, and rehabilitation and treatment strategies when managing knee joint disorders.

To investigate the biomechanics of the lower extremity in various activities, many in vitro, in vivo, and model studies have been carried out. Due to the cost, difficulty, and limitations in in vitro and in vivo measurement studies, lower extremity computational models are widely used. In this study, we aim to analyze the detailed knee joint biomechanics during the stance phase of stair ascent by employing a coupled FE-MS model and compare results with those during level walking while focusing on muscle forces, tibiofemoral-patellofemoral (TF-PF) contact forces, stresses, and areas as well as forces in ligaments.

In this work, we employed a validated MS model of the lower extremity coupled with a detailed FE model of the entire knee joint while being driven by the mean of available kinematics and kinetics recorded in vivo in healthy subjects. The muscle insertions were taken from Opensim and then applied to ABAQUS FE model. Ligaments were represented by multiple (nonlinear pre-strained) truss elements (tension only) with properties taken from the literature and validated earlier by our group. The hip joint was initially rotated from the reference upright standing based on hip kinematics and then fixed thereafter. The GRFs were applied on the foot at a location to generate reported moments at the knee during the simulations. The weight of the lower leg and foot were considered. The knee joint was rotated during the analysis by ABAQUS. Unknown muscle forces were iteratively estimated using an optimization approach constrained by 7 moment-equilibrium equations. It is hypothesized that, in comparison with level walking and under the mean kinematics, kinetics, and ground reaction forces (GRF) reported in healthy individuals, stair ascent generates much greater contact forces-stresses on the PF joint but smaller forces in ACL. Estimated muscle forces at each step, using an optimization routine, were iteratively reapplied (at their updated insertions and directions) onto the FE model as additional forces and the analysis was repeated until convergence (unbalanced moments <0.8 Nm).

Predicted muscle activities compared well to the recorded electromyography data. Quadriceps and medial hamstrings were most activated in the first half of stance whereas gastrocnemii reached their maximum forces late in stance. Peak forces in quadriceps (3.87BW, body weight, at 20% instance in our 61.9 kg subject), medial hamstrings (0.77BW at 20%), and gastrocnemii (1.21BW at 80%) were estimated. Due to much greater flexion angles-moments at the hip and knee joints in the first half of stance, large PF contact forces (peak of 3.1BW at 20% stance) and stresses (peak of 4.83 MPa at 20% stance) were estimated that exceeded their peaks in level walking by four- and

two-fold, respectively. Compared to level walking, ACL forces diminished in the first half of stance but substantially increased later in the second half (peak of 0.76BW at 75% stance). Under nearly similar contact forces at 20% of stance, the contact stress in the tibiofemoral medial plateau reached a peak (9.68 MPa) twice that in the PF joint suggesting the vulnerability of both TF and PF joints. As an effective strategy (to reduce internal loads and pain), high PF contact forces can be mitigated by decreasing the knee peak flexion angle and/or moment. Identification of the relative effectiveness of smaller flexion moment versus smaller flexion angle, however, requires future studies.

TABLE OF CONTENTS

LIST OF TABLES

LIST OF FIGURES

LIST OF SYMBOLS AND ABBREVIATIONS

ACL Anterior cruciate ligament

ADB Adductor brevis

ADL Adductor longus

ADM Adductor magnus

AM Anterior-medial

BFLH Biceps femoris long head

BFSH Biceps femoris short head

GRAC Gracilis

GRF Ground reaction force

GL Gastrocnemius lateral

GM Gastrocnemius medial

GMAX Gluteus max

GMED Gluteus med

GMIN Gluteus min

ILA Iliacus

JCS Joint coordinate system

LCL Lateral collateral ligament

LPFL lateral patellofemoral ligament

MCL Medial collateral ligament

MPFL Medial patellofemoral ligament

MS Musculoskeletal

MVIC Maximum voluntary isometric contraction

OA Osteoarthritis

PCL Posterior cruciate ligament

PCSA Physiological cross-sectional area

PECT Pectineus

PL Posterior-lateral

PF Patellofemoral

PSOAS Iliopsoas

PT Patellar tendon

RF Rectus femoris

SM Semimembranosus

SOL Soleus

SAR Sartorius

SEMIT Semitendinosus

TF Tibiofemoral

TFL Tensor fasciae latae

THR Total hip replacement

TKA Total knee arthroplasty

VI Vastus intermedius

VL Vastus lateralis

VM Vastus medialis

LIST OF APPENDICES

CHAPTER 1 INTRODUCTION

1.1 Epidemiology of knee disorders

The knee is a highly loaded joint in the human body that undergoes large movements in various daily activities. Being the most injury prone joint of the human body, it consists of three articulations (medial and lateral tibiofemoral (TF) and patellofemoral (PF)) and 4 bony structures (tibia, fibula, patella, and femur). The knee joint functions under the activation and control of multiple muscles. The whole structure is passively integrated and controlled with ligaments such as the anterior cruciate ligament (ACL), posterior cruciate ligament (PCL), lateral collateral ligament (LCL), and medial collateral ligament (MCL). Knee PF and TF articular joints carry large contact forces exceeding the entire body weight in daily activities. Consequently, they are regularly prone to large contact stresses. As one of the most commonly injured joints of the human body (Nicholl, Coleman, & Williams, 1991), the knee suffers from osteoarthritis (OA) more than any other weight bearing joint. In fact, with a prevalence of 24%, the human knee joint is the 2nd most frequent anatomical site affected by OA after hand joints (Pereira et al, 2011). OA is destructive to the knee joint by degrading its mechanical properties, composition, and morphology. Obesity, heavy daily tasks (stair ascent for instance), fatigue loading, and existing injuries place the knee at even a higher risk of OA initiation and progression. Results of the 3rd National Health and Nutrition Examination Survey (1988-1994) on 6596 older adults (>60 years) revealed that merely 18.1% of US men and 23.5% of US women suffered from knee pain with the prevalence rising with age (Andersen et al, 1999). Commonly referred to as the knee anterior disorder and pain, PF joint pathologies account for more than a third of all those associated with the knee (Dehaven KE, Lintner DM AJSM 1986; Lankhorst et al, Osteoarth Cart 2017; Taunton et al., BJ Sports Medicine, 2002). Knee pain is also more common in women than men (Boling et al, J Medicine and Science in Sports 2010). A solid and generally accepted hypothesis is that the initiation and progression of OA are associated with both abnormal changes in contact areas and elevated magnitude of contact stresses (Andriacchi et al, ABE 2004; Ward and Powers, 2004). There is a clear dose-response correlation between knee symptoms and heavy work activities such as kneeling, squatting, stair climbing, and lifting (Herquelot et al, 2015; Jones et al, 2007; Mikkelsen et al, 2019; Palmer, 2012; Plotnikoff et al, 2015). Prevention, diagnosis and treatment of knee OA require much improved knowledge of the joint in normal and perturbed conditions. Non-operative treatments including medication, intra articular injection and exercise are not as effective as expected and may mitigate the problem only in the short-term (Van Jonbergen et al., 2010). The operative treatments in the

case of advanced OA vary from joint debridement to arthroplasty. However, joint-preserving procedures, including anterior tibial tubercle transfer or cartilage focal replacements, may not lead to noticeable improvements. Total knee arthroplasty (TKA) is a well-proven surgery with up to 20% failure likely requiring revision surgery (Walker et al., 2012, Argenson et al., 1995). In the US alone, more than 700,000 TKA procedures were performed in 2012 (Kathryn et al. 2014). It is estimated that the number of TKA procedures by 2030 will rise to about 3.5 million procedures per year (Kurtz et al., 2007). Detailed knee joint analysis could be of a great help in prevention and treatment managements of knee disorders.

1.2 Functional anatomy

Three major joints exist in lower limbs. The hip, knee, and ankle joints are actively controlled by muscles and passively by ligaments. The lower limb consists of foot, lower leg (shank) and upper leg (thigh). Pelvis, Femur, Tibia, Fibula, and Patella are the main bony structures of the lower extremity. The schematic of lower extremity is shown in Figure 1.1.

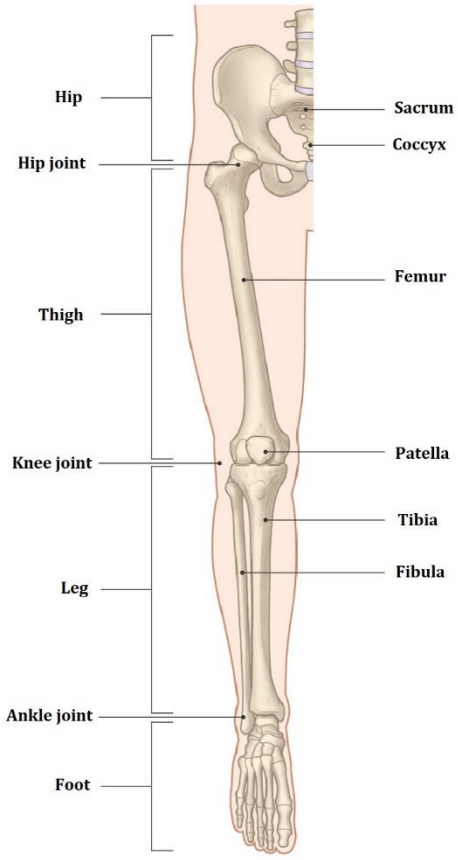

Figure 1.1 Schematic of the lower extremity. (Lower Limb – Earth's Lab (earthslab.com))

1.2.1 Hip joint

Hip joint consists of a ball-shaped head of femur which articulates within a socket-shaped acetabulum located in the pelvis. The surfaces of the femoral head and acetabulum are covered with articular cartilage layers which facilitate the relative movement with little resistance. Hip joint has 3 degrees of freedom. The center of rotation in this joint is commonly considered fixed in the musculoskeletal (MS) models. It is represented as a frictionless spherical joint with no passive resistance. Similar to the knee, OA is also a common disease affecting the hip joint. According to the American Academy of Orthopaedic Surgeons, more than 231,000 total hip replacements were performed each year in the US (Kim et al., 2014) Annually, more than 1 million THR are done worldwide (Organisation for Economic Co-operation and Development OECD health data, 2017).

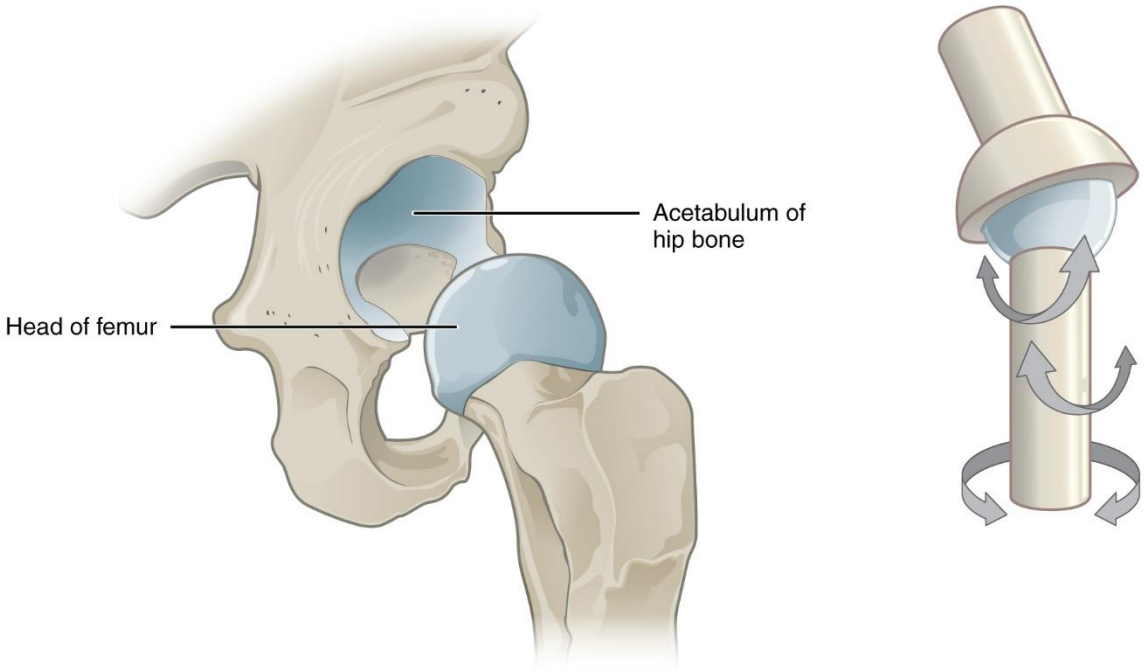

Figure 1.2 Schematic of a hip joint (9.1 Classification of Joints – Anatomy & Physiology (oregonstate.education)).

1.2.2 Knee joint

As a complex structure, knee joint is mechanically one of the most important joints in human body. It connects the leg (shin) to the thigh and plays a crucial role in human movements. The knee joint consists of 3 major TF and PF articulations. The knee joint is surrounded by major muscles of the lower extremity, which help activate, control, and stabilize the joint in various regular and sportive activities. The tibio-femoral articulation is formed by several non-congruent surfaces, the femoral

condyles, and the tibial plateaus. The latter consists of two glenoid cavities: the medial glenoid cavity and the lateral glenoid cavity.

To dampen the impacts and ease articulations between the parts, the articular surfaces of the patella, tibial plateaus and femoral condyles are covered by thick articular cartilage layers. Cartilage layers are made mainly of water, collagen networks, and a matrix of proteoglycans that together facilitate maintaining the function and hydration of the cartilage layers. These layers have usually between 2 to 4 mm thickness and their water content, fibril networks and matrix properties are depth dependent. The superficial fibrils are parallel to the surface while the deeper fibrils are perpendicular to the surface and insert firmly into the calcified cartilage at the junction with the subchondral bone. Due to the lack of blood vessels and nerves, the injured cartilage tissue has a low potential of healing and self repair (Pearle et al., 2005).

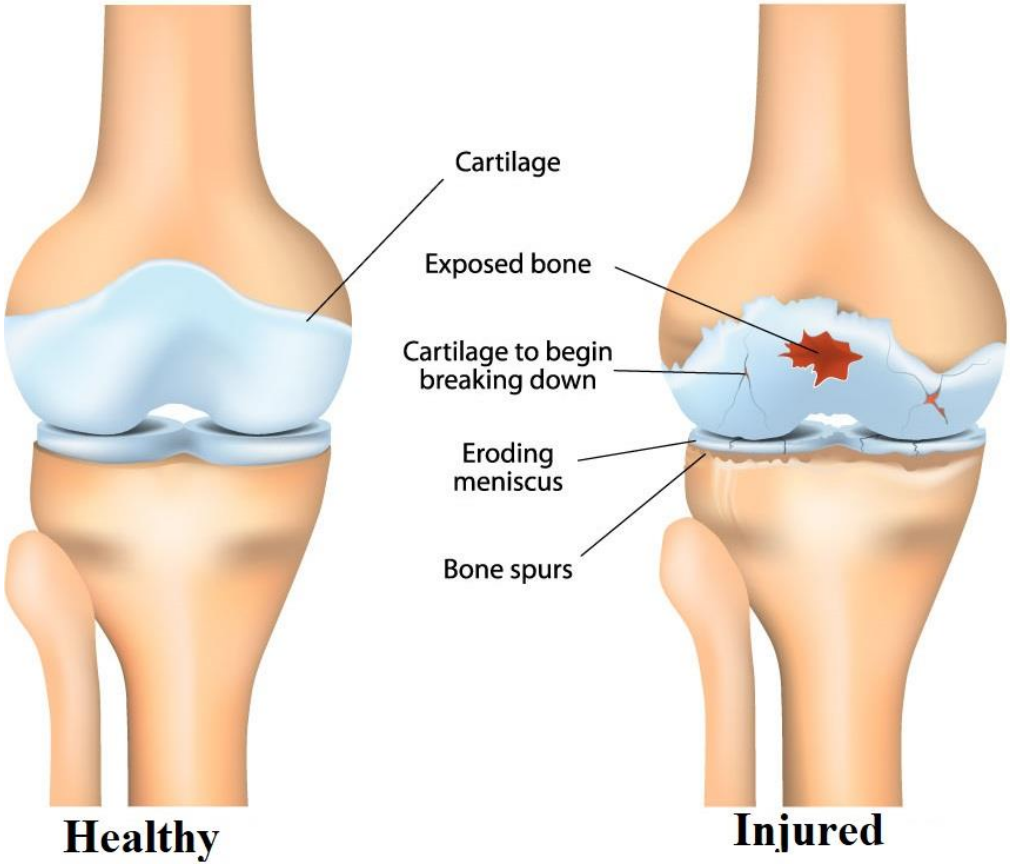

Figure 1.3. Schematic demonstration of a pathologic versus healthy cartilage layers (pathologic versus healthy) (Knee Arthritis | Knee Specialist | Van Nuys, Thousand Oaks, Los Angeles, CA (lasportsorthomd.com)).

The main task of the menisci is to distribute the load on the tibial surface in order to decrease the contact stress. They dampen the fatigue and suddenly applied loads as well. Menisci have medial

and lateral components covering more than half of both lateral and medial tibial plateaus. Similar to the cartilage, menisci are also made of water, collagen fibril networks and an extracellular matrix of proteoglycans. Medial and lateral menisci are almost of the same width (about 27 mm), but medial menisci are much longer (40 to 45 mm) than lateral menisci (32 to 35 mm) (Makris et al., 2011). Sports incidents stand for one of the main reasons of meniscus ruptures. Meniscus tears increase the risk of cartilage destruction and consequently may result in OA in long term. (Persson, Turkiewicz, Bergkvist, Neuman, & Englund, 2018). Almost half of the knee arthroscopic surgeries in the US are performed due to partial meniscus ruptures. (Kim, Bosque, Meehan, Jamali, & Marder, 2011).

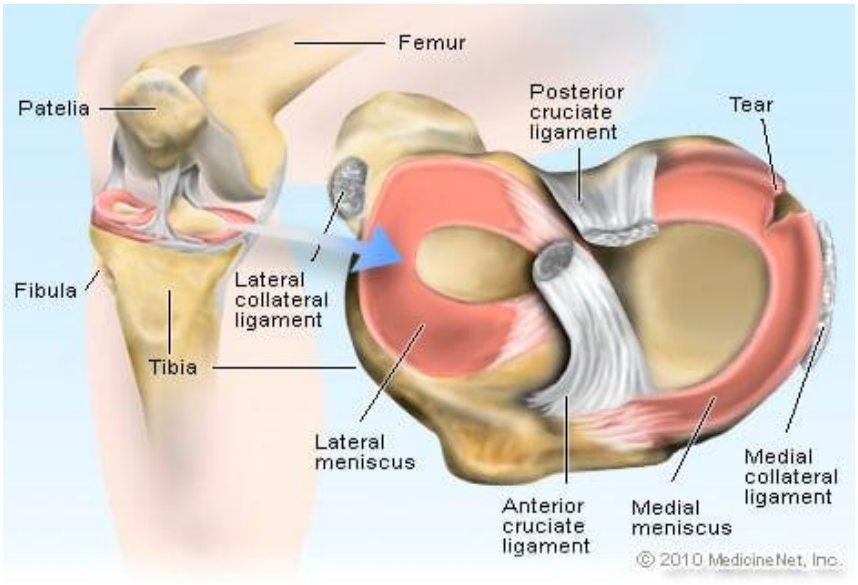

Figure 1.4. Schematic view of the knee components (Torn Meniscus Picture Image on MedicineNet.com).

Ligaments are passive fibrous connective tissues that connect bones together in order to restrict and stabilize the joint movements in various directions. In the human knee joint several major ligaments exist. These ligaments connect patella, tibia and femur and are crucial for the joint stiffness and stability. Anterior cruciate ligament (ACL), posterior cruciate ligament (PCL), lateral collateral ligament (LCL), medial collateral ligament (MCL), lateral patellofemoral ligament (LPFL) and medial patellofemoral ligament (MPFL) are the main ligaments of the knee joint.

Increasing the effective lever arm of the knee extension mechanism (i.e., quadriceps activation) to resist external knee flexion moments and/or generate extensor moments to move and stabilize the knee joint is the primary biomechanical task of the patella. Quadriceps muscles apply their force to the patella through quadriceps tendon and to the tibia through patellar tendon (PT). Therefore,

during demanding tasks like stair ascent and squat that quadriceps muscles are highly activated, PT and PF surfaces carry substantial forces.

The PCL is the main resistor against tibial anterior-to-posterior translation, specially in large knee flexion angles (40 to 120 degrees) (Race & Amis, 1996). PCL injuries occur mostly in accident and sport activities (Swenson et al. 2013). A 2–3% incidence of asymptomatic PCL deficiency has been reported in elite college football players (Parolie and Bergfeld, 1986). Excessive passive sagittal looseness of the medial tibiofemoral compartment increased lateral tibial translation and decreased varus rotation during flexion could be the kinematic consequences of the PCL deficient knee. (Logan et al., 2004, Goyal et al., 2012, Li G et al., 2008).

The MCL connects the medial side of the tibia to the medial side of the femur. At knee small flexions (20 to 30 degrees) it is the primary valgus stabilizer (Grood & Suntay, 1981, Schafer et al., 2016). Primary resistor to varus rotations and the lateral movements is the LCL (Kakarlapudi et al., 2000).

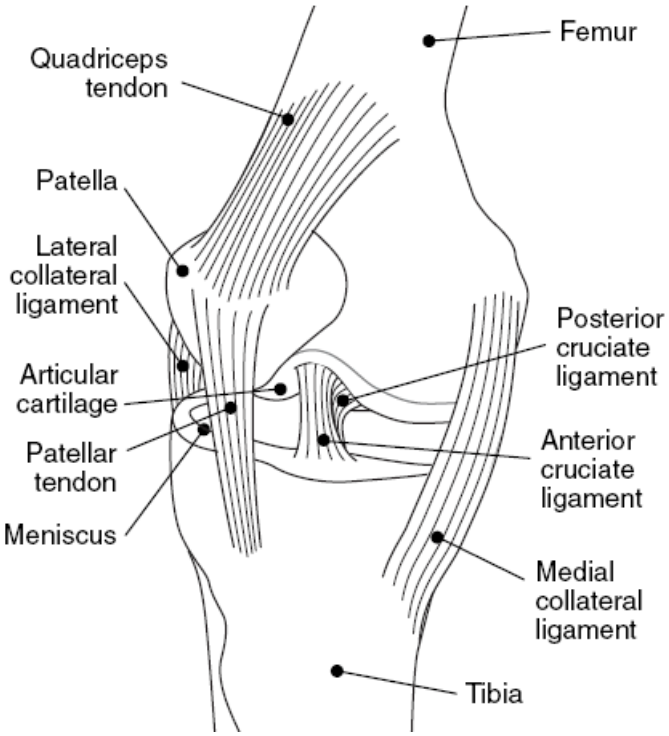

Figure 1.5. Schematic demonstration of knee ligaments (Knee Anatomy – Century City Los Angeles, CA: Millstein Orthopedics).

Limiting the anterior tibial translation (ATT) relative to the femur as well as excessive extension is the main task of the ACL (Kakarlapudi et al., 2000). The ACL consists of two different bundles; anteromedial (AM) bundle is the main resistor to the relative antero-posterior translation of the

knee while the task of posterolateral (PL) bundle is more limiting the rotational movements of the tibia relative to the femur. ACL offers a secondary resistance to varus/valgus and internal\external rotations of the tibia (Kakarlapudi et al., 2000). It has also been reported that during knee joint extension the PL bundle's resistance to the ATT increases while as the knee flexes, the AM bundle carries more load (Gabriel et al., 2004). With about 3.4 billion dollars cost each year for associated rehabilitation following rupture, about 250000 knee ligament injuries happens in the US of which more than two third related to ACL-deficient (ACLD) (Afzali et al., 2018). ACL injuries is more common among younger population, especially in female athletes. Male athletes are at a 5 times lower risk of ACL tears in comparison with female athletes (Hewett et al., 2005).

Even with a relatively high chance of success for ACL reconstruction surgeries (Wright et al., 2008), ACLD patients are prone to a high risk of long-term knee diseases especially OA (Andriacchi, Briant, Bevill, & Koo, 2006).

1.2.3 Ankle joint

It consists of 3 main bones: talus in the foot, tibia, and fibula in the leg. Four ligaments reinforce this joint: deltoid, anterior talofibular, posterior talofibular, and calcaneofibular ligaments. Ankle joint is commonly considered as a spherical joint that allows the foot to only rotate relative to the lower leg. Ankle joint carries a large moment during daily activities like walking and stair ascent. The moment at this joint is usually generated by gastrocnemius and soleus muscles at their insertions through Achille's tendon.

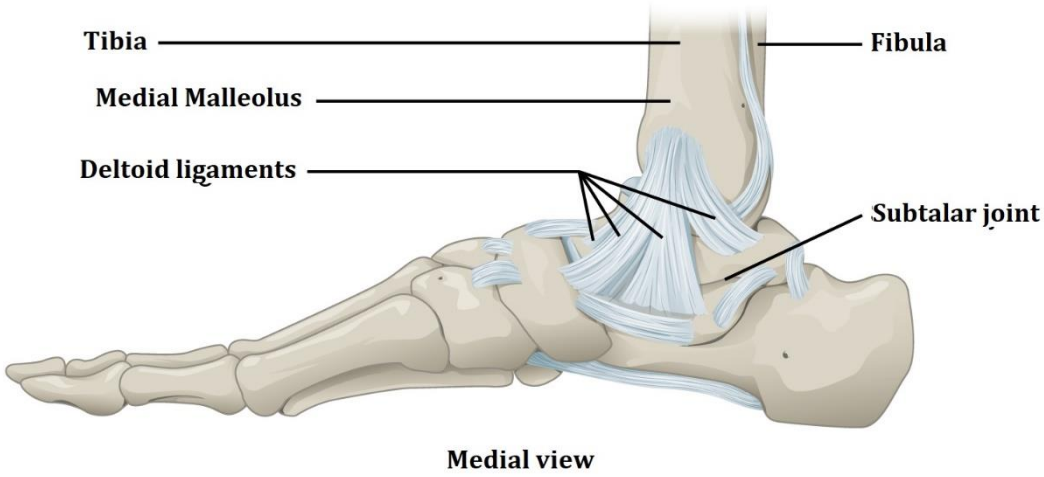

Figure 1.6. Lateral view of the ankle joint (The Ankle Joint – Articulations – Movements – TeachMeAnatomy).

1.2.4 Lower extremity muscles

There are more than 50 muscles in the human lower limb. The main muscles are grouped according to the motion that they cause. Some muscles can cause multiple motions.

Hip flexors: Adductor Brevis, Gracilis, Iliacus, pectoralis, Psoas, Rectus femoris, sartorius and Tensor fasciae latae (TFL).

Hip extensors: Adductor magnus, Biceps femoris, Gluteus maximus, Gluteus medius, Gluteus minimus, Semimembranosus, Semitendinosus.

Hip abductors: Gluteus medius, Gluteus minimus, Piriformis, sartorius and Tensor fasciae latae (TFL).

Hip adductors: Adductor Brevis, Adductor longus, Biceps femoris-long head, Adductor magnus, pectoralis, Gracilis, Semimembranosus, Semitendinosus.

Hip internal rotators: Iliacus, Iliopsoas, Tensor fasciae latae (TFL)

Hip external rotators: Gluteus medius, Gluteus minimus.

Knee flexors: Biceps femoris-long head, Biceps femoris-short head, Gracilis, Gastrocnemius medial, Gastrocnemius lateral, Sartorius, Semimembranosus, Semitendinosus.

Knee extensors: Vastus lateralis, Vastus medialis, Vastus intermedius, Rectus femoris.

Knee abductors: Biceps femoris-long head, Biceps femoris-short head and Vastus lateralis.

Knee adductors: Semimembranosus, Gracilis, Semitendinosus, Sartorius and Vastus medialis.

Knee internal rotators: Semimembranosus, Gracilis, Semitendinosus, Sartorius.

Knee external rotators: Biceps femoris-long head, Biceps femoris-short head.

Ankle dorsi flexors: Peroneus tertius, Anterior tibialis, Extensor hallucis, Extensor digitorum longus.

Ankle plantar flexors: Gastrocnemius medial, Gastrocnemius lateral, Soleus, Posterior tibialis, Peroneus longus, Peroneus brevis, flexor hallucis, Flexor digitorum longus.

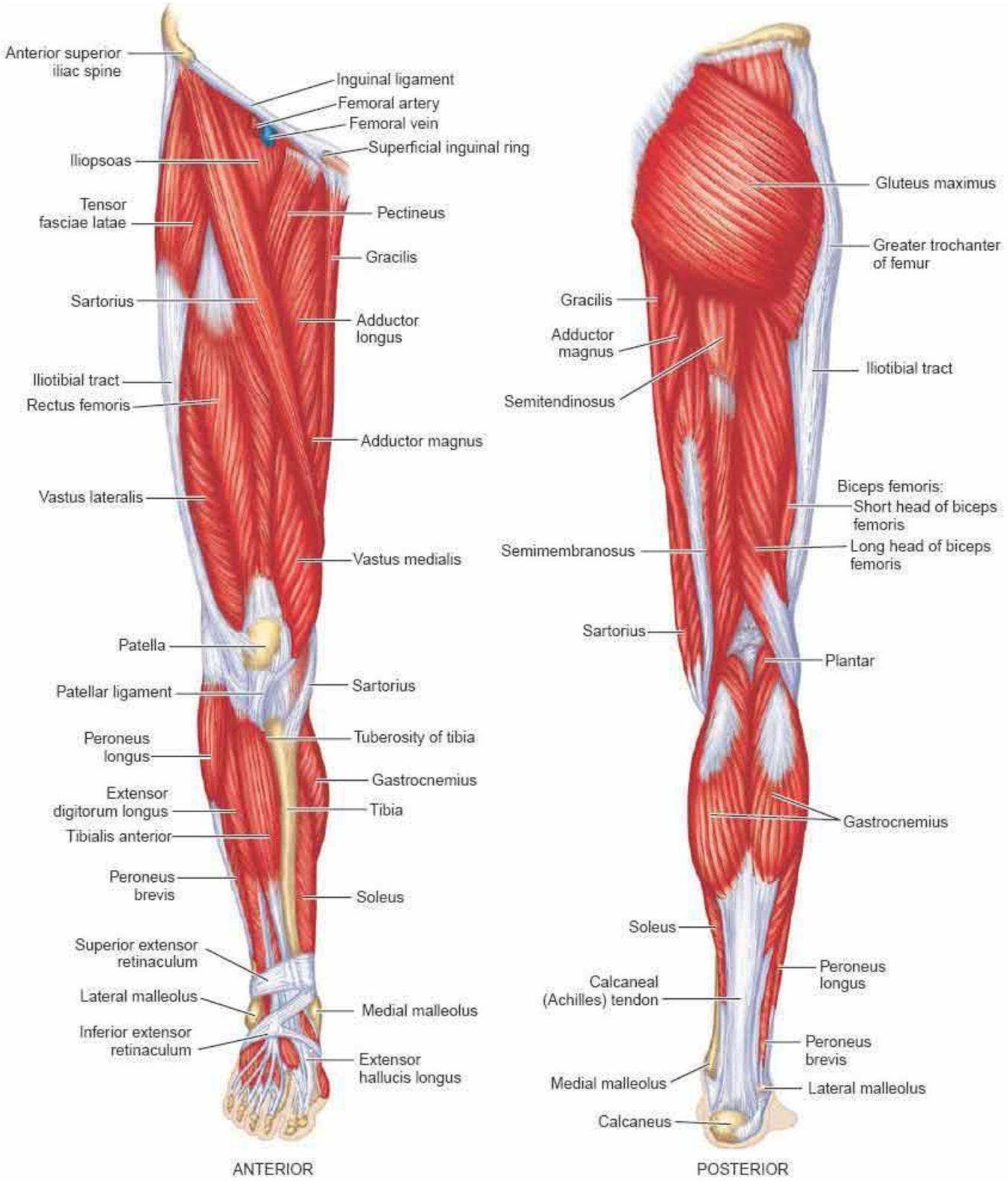

Figure 1.7. Lower extremity muscles (http://anatomyorgan.com/).

1.2.4.1 Muscle wrappings

For lower extremity simulation, it is important to simulate the muscles with forces acting along their trajectory. Some muscles during stair ascent wrap around femur or pelvis or both. Therefore, they can not simply be simulated as a simple straight linear vector connecting two insertion points. For instance, gluteus maximus during stair ascent wraps around hip and femur. Assuming a frictionless contact between muscles and bones, three different force vectors with equal magnitudes can be considered for gluteus maximus. It is important to consider a force vector in a way that moment equilibrium equation has the minimum number of unknown variables.

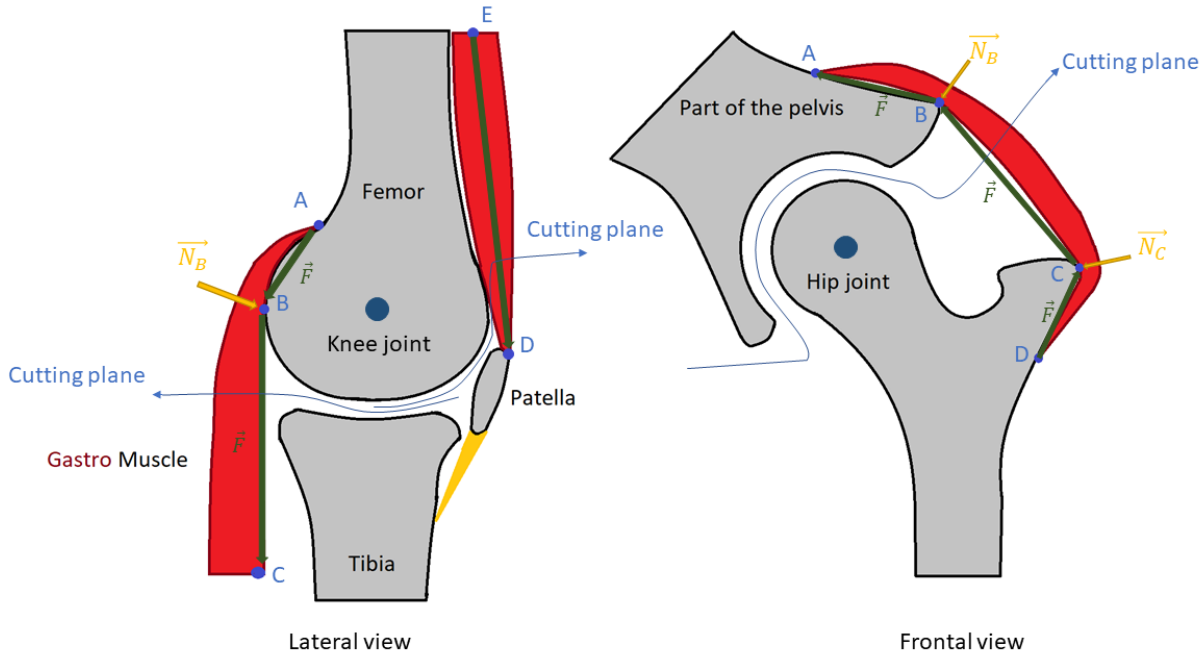

Figure 1.8. Schematic demonstration of muscle wrapping at the knee and the hip joint.

1.3 Anatomical planes and joint motions

Anatomical planes are defined to describe lower extremity kinetics and kinematics.

1.3.1 Anatomical planes

For the MS model, 3 planes have been introduced:

Sagittal plane which separates the body into a left part and right part.

Coronal or frontal plane which divides the body into a posterior and an anterior part.

Transverse plane which separates the body into upper and lower parts.

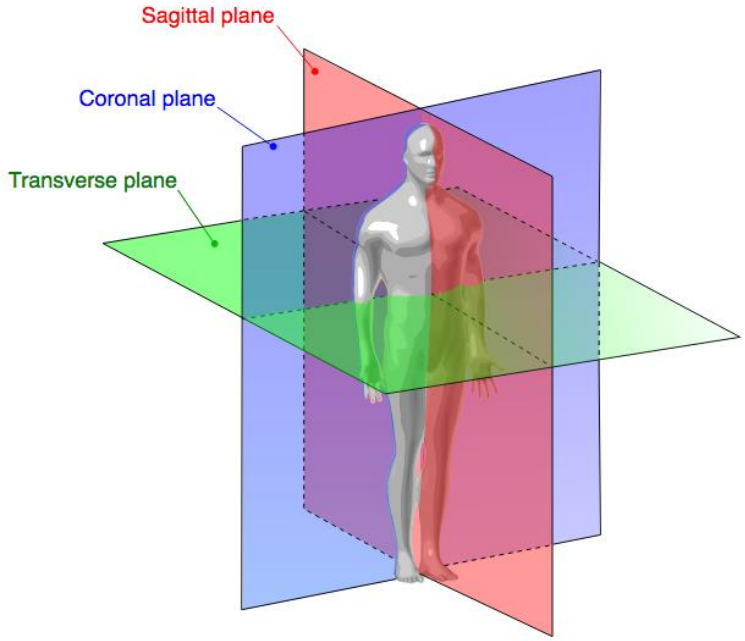

Figure 1.9. Anatomical planes (1.4D: Body Planes and Sections – Medicine LibreTexts).

1.3.2 Joint movements

Having defined the anatomical planes, it is possible to describe the joints movements. For the hip joint and the knee joint, movements in sagittal, coronal, and transverse planes are flexion/extension, abduction/adduction, and internal/external rotations, respectively. For the ankle joint, movements in the sagittal plane are defined as dorsiflexion and plantar flexion (see Figure 1.9).

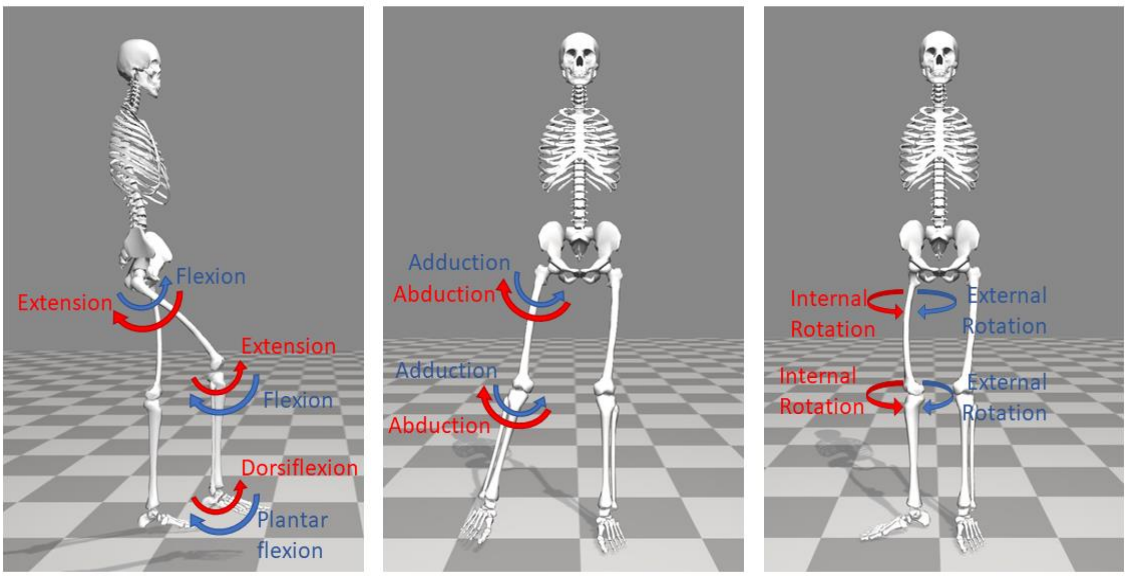

Figure 1.10. Joint movement definitions. (Opensim 4.3)

1.3.3 Grood and Suntay joint coordinate system (JCS)

There are multiple coordinate systems in the literature which are necessary for defining the joint translations and rotations. We use a common coordinate system for lower extremity in our group, which is the coordinate system introduced by (Grood, E. S. & Suntay) in 1983. As a non-orthogonal coordinate system, it uses 3 axes to define the joint rotations. Later on, these 3 axes are used to define the joint moments. These 3 axes are defined based on the topology of bony structures at the particular joint. In the knee joint for instance, the axis which passes through the epicondylar centers of the femur is the X and it is attached to the femur. The axis connecting the center of the ankle and the point which is proximally midway between the two inter-condylar eminences, is the Z and it is attached to the tibia. The third floating axis that is perpendicular to both X and Z axes is Y axis.

In this coordinate system the sequence of rotations is important. In order to determine the axes of the joint coordinate system, first, the extension-flexion angle is applied in a way that the tibia rotates about the X axis. As X axis is attached to the femur and Z axis is attached to the tibia, Y axis is calculated. Then abduction-adduction angle is applied where the tibia rotates about the Y axis. Finally, and at the third step, tibia rotates about the Z axis by the knee external-internal angle. (Grood, E. S. & Suntay, 1983)

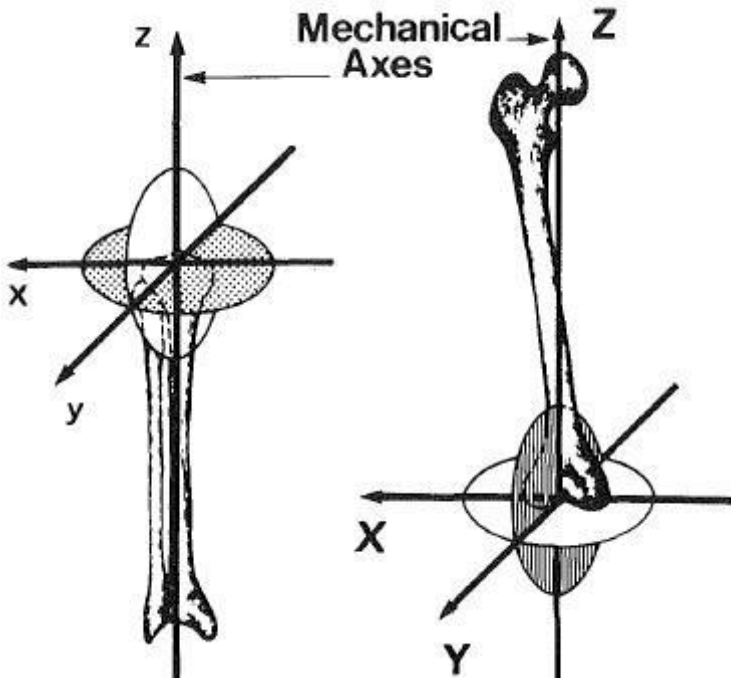

Figure 1.11. Axis definitions (Grood, E. S. & Suntay, 1983)

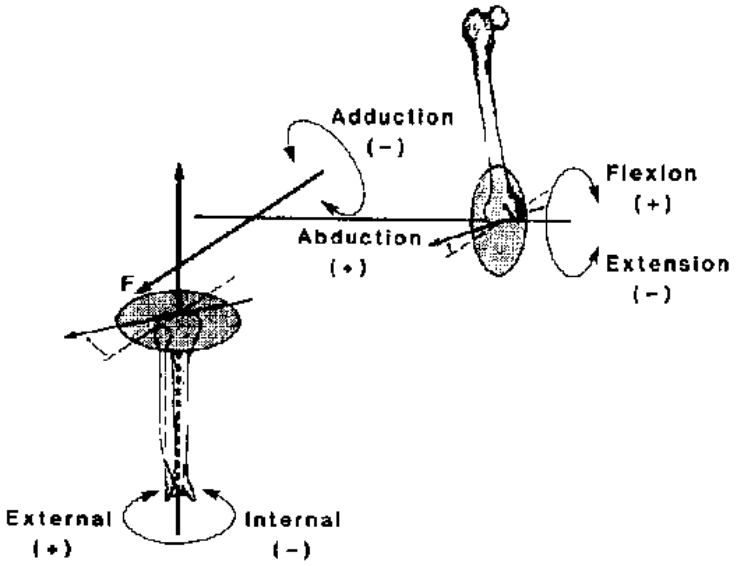

Figure 1.12. Movement definitions (Grood, E. S. & Suntay, 1983)

1.3.4 Joint moments

Joint moments during level walking and stair ascent are commonly reported in Grood and Suntay (1983) coordinate system. At each joint 3 moments exist. For example, at the knee joint, extension-flexion moment is measured and reported about the axis which passes through the epicondylar centers of the femur. Knee internal-external moment is reported about the axis connecting the center of the ankle and the point which is proximally midway between the two inter-condylar eminences. Knee adduction-abduction moment is reported about the floating axis which is perpendicular to the other two already defined for knee extension-flexion and knee internal-external moments.

1.3.4.1 Joint moments transformation

Joint moments are also usually calculated and reported in Grood and Suntay (1983) joint coordinate system which is also suitable for clinical interpretations. For the simulation studies, however, it is necessary to use an orthogonal coordinate system. Therefore, transformation matrices are needed to convert these to joint moments in the ground Cartesian coordinate system which is orthogonal.

For the transformation of the right knee, following matrices T, U_1 and U_2 have been developed (Adouni, 2017, Grood and Suntay, 1983):

$$U_1 = \begin{bmatrix} 1 & 0 & Cos(\theta_2 + {}^{\pi}/_{2}) \\ 0 & Cos(\theta_1) & Sin(\theta_1)Sin(\theta_2 + {}^{\pi}/_{2}) \\ 0 & -Sin(\theta_1) & Cos(\theta_1)Sin(\theta_2 + {}^{\pi}/_{2}) \end{bmatrix} \qquad (1)$$

$$U_2 = \begin{bmatrix} 1 & 0 & Cos(\alpha_2 + {}^{\pi}/_{2}) \\ 0 & Cos(\alpha_1) & Sin(\alpha_1)Sin(\alpha_2 + {}^{\pi}/_{2}) \\ 0 & -Sin(\alpha_1) & Cos(\alpha_1)Sin(\alpha_2 + {}^{\pi}/_{2}) \end{bmatrix} \quad (2)$$

$$T = \begin{bmatrix} Cos(\theta_2)Cos(\theta_3) & -Cos(\theta_2)Sin(\theta_3) & Sin(\theta_2) \\ Sin(\theta_1)Sin(\theta_2)Cos(\theta_3) + Cos(\theta_1)Sin(\theta_3) & -Sin(\theta_1)Sin(\theta_2)Cos(\theta_3) + Cos(\theta_2)Cos(\theta_3) & -Cos(\theta_2)Sin(\theta_1) \\ -Cos(\theta_1)Sin(\theta_2)Cos(\theta_3) + Sin(\theta_1)Sin(\theta_3) & Cos(\theta_1)Sin(\theta_2)Sin(\theta_3) + Sin(\theta_1)Cos(\theta_3) & Cos(\theta_1)Cos(\theta_2) \end{bmatrix} \quad (3)$$

To transform hip moments reported in Grood and Suntay (1983) joint coordinate system to the xyz ground coordinate system:

$$\begin{bmatrix} M_x\, hip \\ M_y\, hip \\ M_z\, hip \end{bmatrix} = [U_1] \begin{bmatrix} M_{ext/flex}\, hip \\ M_{add/abd}\, hip \\ M_{\ ext/int}\, hip \end{bmatrix}$$

θ_1 : Hip extension (-)/flexion (+) angle

θ_2 : Hip abduction (-)/adduction (+) angle

θ_3 : Hip external (-)/internal (+) angle

$M_{ext/flex}\, hip$: Hip extension (-)/flexion (+) moment

$M_{add/abd}\, hip$: Hip abduction (-)/adduction (+) moment

$M_{\ ext/int}\, hip$: Hip external (-)/internal (+) moment

To transform knee moments reported in Grood and Suntay coordinate system to ground coordinate system (xyz), these equations are needed:

$$\begin{bmatrix} M_x\, knee \\ M_y\, knee \\ M_z\, knee \end{bmatrix} = [T][U_2] \begin{bmatrix} M_{ext/flex}\, knee \\ M_{add/abd}\, knee \\ M_{\ ext/int}\, knee \end{bmatrix}$$

α_1 : knee extension (+)/flexion (-) angle

α_2 : knee abduction (-)/adduction (+) angle

α_3 : knee external (-)/internal (+) angle

$M_{ext/flex}\, knee$: knee extension (+)/flexion (-) moment

$M_{add/abd}\, knee$: knee abduction (-)/adduction (+) moment

$M_{\ ext/int}\, knee$: knee external (-)/internal (+) moment

CHAPTER 2 LITERATURE REVIEW

2.1 Stair ascent

Compared to the level walking as the most popular daily activity, stair ascent is less frequent but constitutes a much more demanding activity. Stair ascent is a complex activity with greater hip and knee sagittal moments and angles when compared to the level walking. Every stair ascent gait cycle consists of two distinct phases:

Stance phase: it starts as the foot touches the stair and ends as that same foot lifts off the stair. It accounts for about 65% of the entire stair ascent cycle.

Swing phase: it starts as the foot ceases contact with the stair and ends as the same foot lands again on the stair to start another gait cycle. It also accounts for about 35% of the stair ascent cycle.

Figure shows the schematic of a stair ascent stance phase.

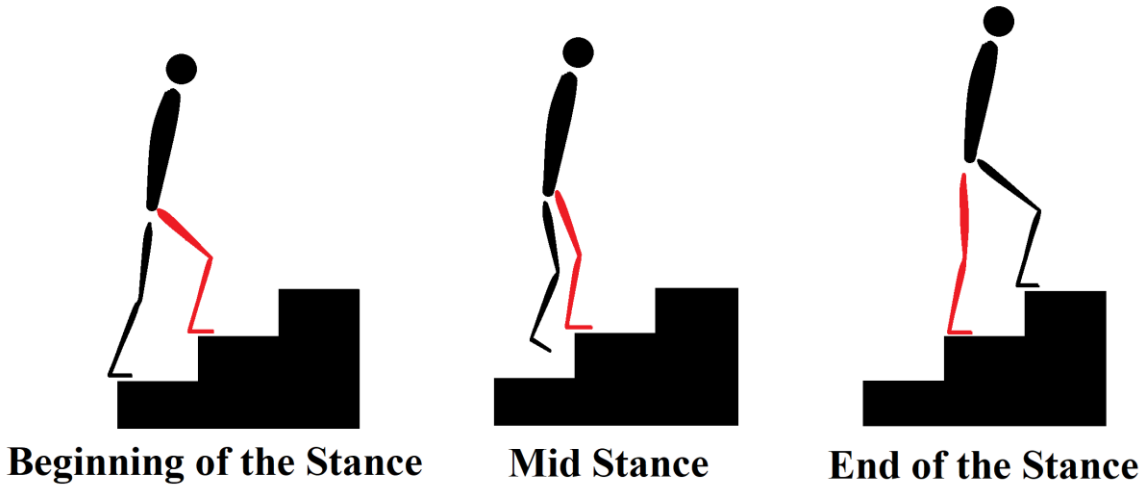

Figure 2.1. Stair ascent during stance phase.

2.2 Lower extremity models

To investigate the biomechanics of the lower extremity in various activities, many in vitro, in vivo, and model studies have been carried out. Due the cost, difficulty, and limitations in in vitro and in vivo measurement studies, lower extremity computational models are widely used. Examples include investigations on the role of muscles, evaluation of surgical interventions, changes in the bone topology, knee total replacements, cartilage damage and degeneration, menisci injuries, ligament ruptures, joint kinematics, and kinetics. Accurate quantification of the knee joint biomechanics in such activities can be of great help not only in the injury and degeneration

prevention applications, but also in the improved design of implants for TKA, rehabilitation and treatment strategies when managing knee joint diseases. Lower extremity modelling can have an important role in understanding the knee joint function and therefore in suggesting solutions to prevent and treat joint disorders and pain. Generally, these models are divided into active and passive models.

2.2.1 Passive computational models

Passive models neglect the role of active components in the level walking or stair ascent. They usually employ finite element models of passive components including bony parts, ligaments, menisci, and cartilages. These models are suitable to investigate stress distributions, strain, and ligaments forces under various load- and displacement-control conditions. For instance, to study the joint response under varus-valgus moments (Bendjaballah, Mzea, Shirazi-Adl, & Zukor, 1997), compression force (Bendjaballah, M. Z., Shirazi-Adl, & Zukor, 1995), drawer force in intact and for ACL-D knee joints (Moglo & Shirazi-Adl, 2003), anterior posterior (AP) drawer force (Bendjaballah, MZ, Shirazi-Adl, & Zukor, 1998), and internal/external moments (Jilani, Shirazi-Adl, & Bendjaballah, 1997). Also, for open kinetic chain flexion-extension movements (Mesfar & Shirazi-Adl, 2008a, 2008b), for the effect of OA, partial meniscectomy and cartilage and menisci stress distribution under different loading conditions (Shirazi & Shirazi-Adl, 2005, 2009a, 2009b; Shirazi, Shirazi-Adl, & Hurtig, 2008), and closed kinetic chain movements (Adouni, M & Shirazi-Adl, 2009). In order to study the knee OA progression, a number of passive FE models have been developed (Mootanah et al., 2014). A passive model using linear elastic and homogeneous material was proposed (Haut Donahue 2002). Single phase linear elastic and isotropic materials was used for cartilage simulations (Pena 2006) and then fibril reinforces poroviscoelastic material properties was then used by Mononen et al., 2012. Due to lack of muscles, these models are not able to simulate accurate in vivo experiments. Therefore, to simulate in vivo experiments, muscles activities should be considered

2.2.2 Musculoskeletal (MS) models

Musculoskeletal models consider the active musculature in the simulation. Therefore, muscle forces calculation are also required. Using kinetics and kinematics of the joints, equilibrium equations at each joint are stablished. Muscle forces are calculated in a way that these equations are satisfied. Due to the large number of muscles with unknown forces in the lower extremity which exceeds the number of available equilibrium equations, 2 different methods are commonly

used to estimate muscle forces and hence joint internal loads: 1-inverse dynamics and 2-forward dynamics. To drive these models required input data are needed for the solution which depends on the approach considered.

2.2.2.1 Inverse dynamics

Inverse dynamics is a rapid and widely used approach to determine joint reaction moments and forces in MS models. In order to estimate net joint loads, recorded joint kinematics and segment inertial properties are used while satisfying the dynamic equations of motion at various joints. In order to subsequently evaluate muscle forces and internal joint loads, however, additional techniques should be employed. Many algorithms exist but the two mains are EMG assisted and optimization approaches.

2.2.2.1.1.1 Electromyography (EMG) assisted approach.

It is possible to use surface electromyography (EMG) to estimate unknown muscle forces in MS models. EMG signals are usually normalized to their maximum values recorded during voluntary isometric contraction tasks. These normalized signals are assumed linearly proportional to the muscle forces (Hall et al., 2015; Hammond et al., 2017).

2.2.2.1.1.2 Optimization approach

The number of equations is less than the number of unknown muscle forces existing in the lower limb resulting in a redundant system. In search of a unique solution, one or multiple cost functions are employed that will be combined with constraint equilibrium equations as well as inequality equations on muscle forces. There are many cost functions proposed in the literature, we use sum of cubed muscles stresses to optimize the muscle forces (Arjmand & Shirazi-Adl, 2006b).

The optimization approach satisfy the equilibrium equations. However, it does not consider the effect of the agonist and antagonist contractions. On the other hand, although EMG assisted approach considers agonist and antagonist muscle synergies, this approach does not necessarily satisfy the equilibrium equations at the Ankle-Knee-Hip joints. To address these missing elements of these two approaches, hybrid approached have been developed which use both EMG signals and optimization tools simultaneously.

2.2.2.2 Forward dynamics

In forward dynamics, muscle forces, external and gravity loads are inputs to be used to estimate the full motion trajectory. In this approach full dynamic equations of motion under given muscle

forces are step by step computed with the known joint kinematics often considered as constraint to adjust applied muscle forces.

2.3 Stair ascent kinematics-kinetics measurements

The data input for this work has been taken from numerous in vivo studies. Only the mean values recorded on healthy individuals have been considered. The weighted (by the number of subjects in each study) mean angles and moments at the hip, knee, and ankle plus the GRF recorded during the stance phase of the stair ascent have been calculated to drive our coupled FE-MS model.

2.3.1 Kinematics

The needed kinematics during stair ascent to run the simulations in this work include the hip and knee flexion-extension, adduction-abduction, and internal-external angles during the stance phase of the stair ascent.

2.3.2 Kinetics

The necessary kinetics during stair ascent to drive the model include the hip and knee flexion-extension, adduction-abduction, and internal-external moments as well as ankle dorsiflexion moments during the stance phase of the stair ascent.

2.3.3 GRF

The necessary ground reaction force during stair ascent to drive the model include Anterior-posterior GRF, medial-lateral GRF and vertical GRF. These ground reaction forces apply to the tow in ground orthogonal coordinate system.

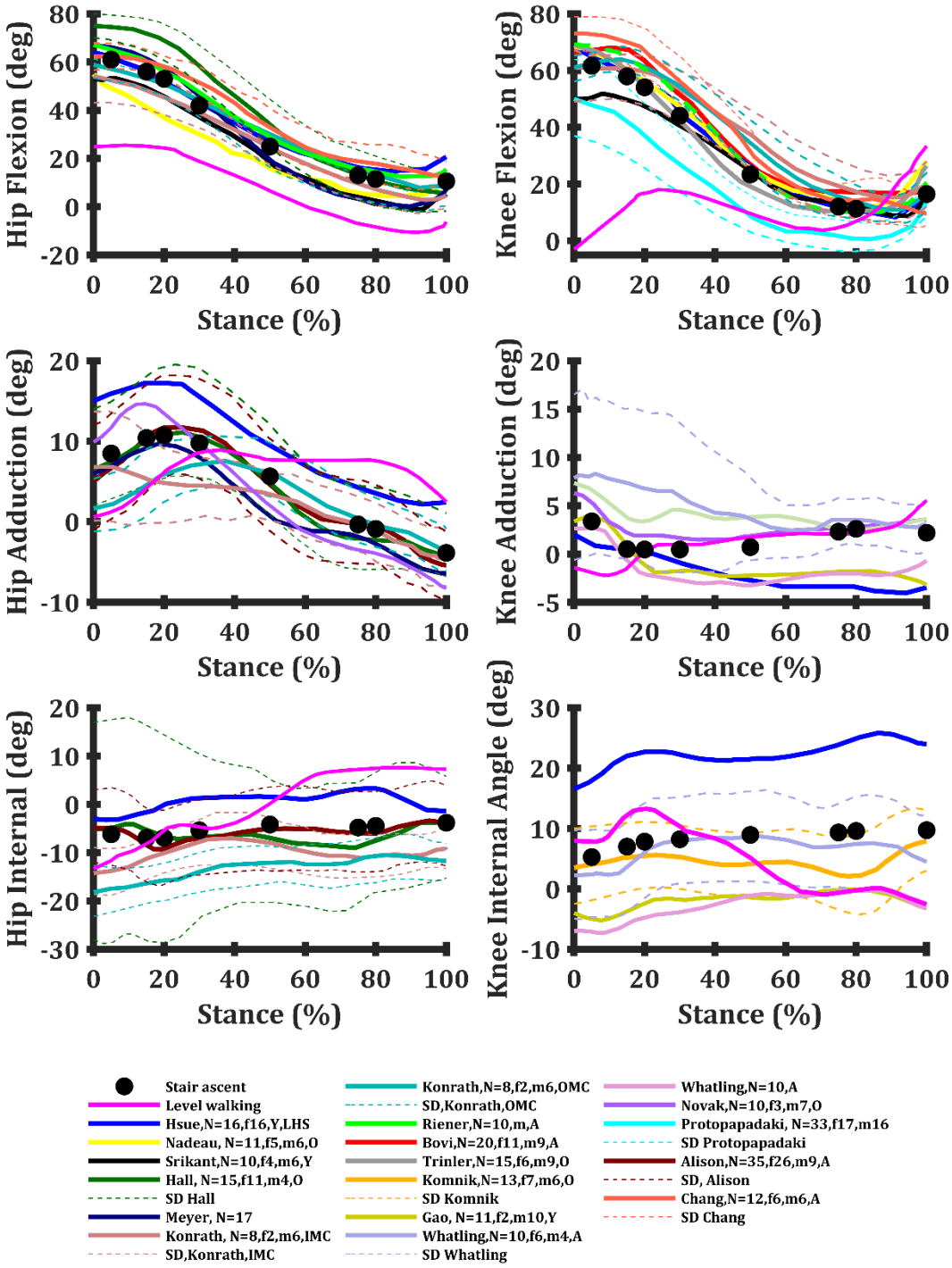

Figure 2.2. The hip and the knee kinematics. Black circles represent the weighted mean values reported in the stair ascent of in vivo studies (Allison et al. 2016; Bovi et al. 2011; Chang et al. 2020; Gao et al. 2012; Hall et al. 2017; Hsue and Su 2009; Komnik et al. 2018; Konrath et al. 2019; Mandeville et al. 2008; Meyer et al. 2016; Nadeau et al. 2003; Novak and Brouwer 2013; Protopapadaki et al. 2007; Riener et al. 2002; Trinler et al. 2016; Vallabhajosula et al. 2015;

Whatling et al. 2010). The solid pink lines represent the input data (Astephen et al. 2008) used in our gait simulations reported in this work for comparison.

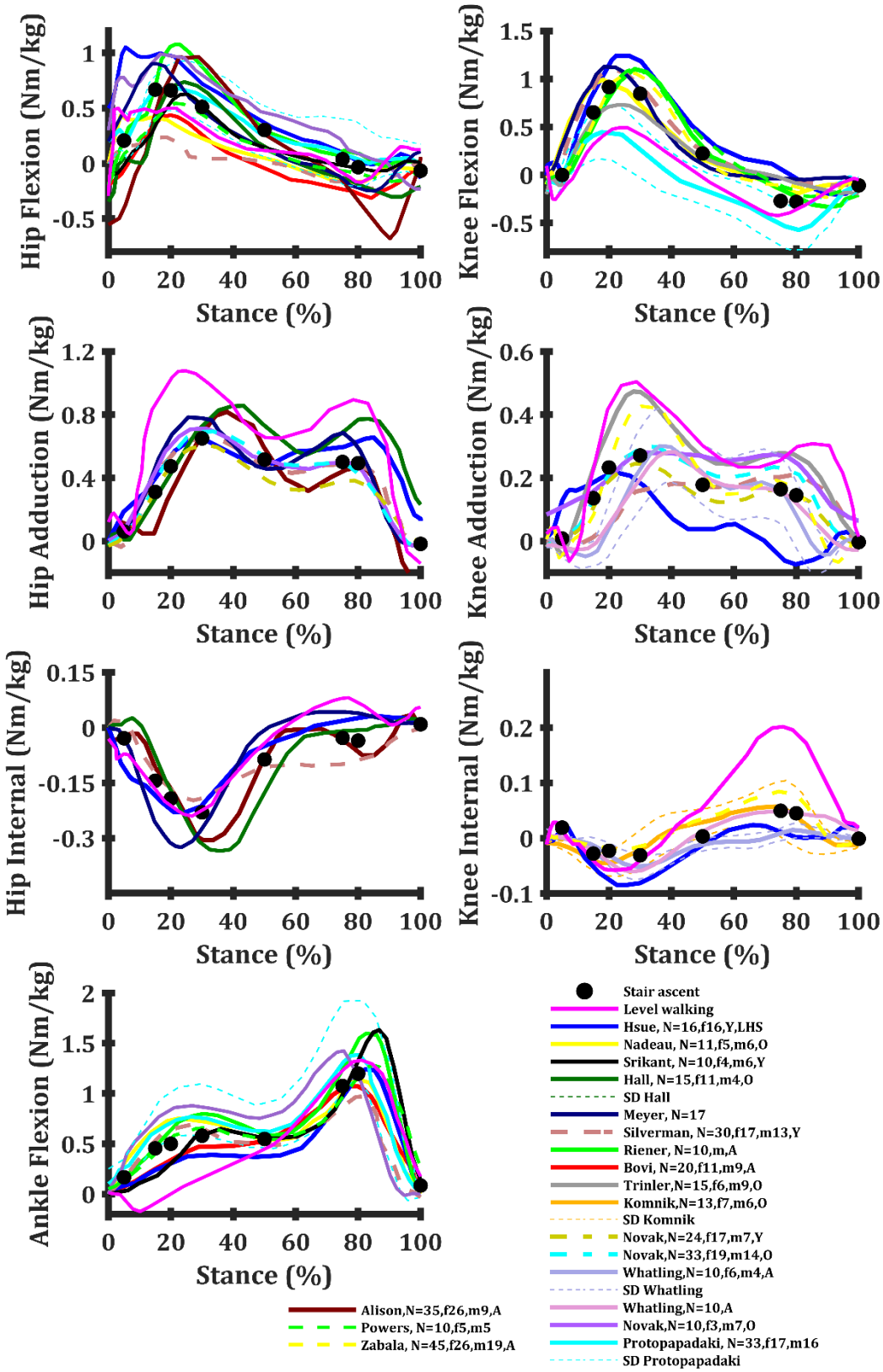

Figure 2.3. Hip, knee, and ankle moments represented normalized to 61.9 kg as our subject's body mass. Black circles are based on the weighted mean values reported in stair ascent measurements (Allison et al. 2016; Bennett et al. 2017; Bovi et al. 2011; Gao et al. 2012; Hall et al. 2017; Hsue and Su 2009; King et al. 2017; Komnik et al. 2018; Meyer et al. 2016; Nadeau et al. 2003; Novak and Brouwer 2013; Protopapadaki et al. 2007; Riener et al. 2002; Salsich et al. 2001; Silverman et al. 2014; Trinler et al. 2016; Vallabhajosula et al. 2015; Whatling et al. 2010; Zabala et al. 2013) that drive along with kinematics (Figure 1.14.) the current simulations. The solid pink lines represent the input data (Astephen et al. 2008) used in our gait simulations reported here for comparison.

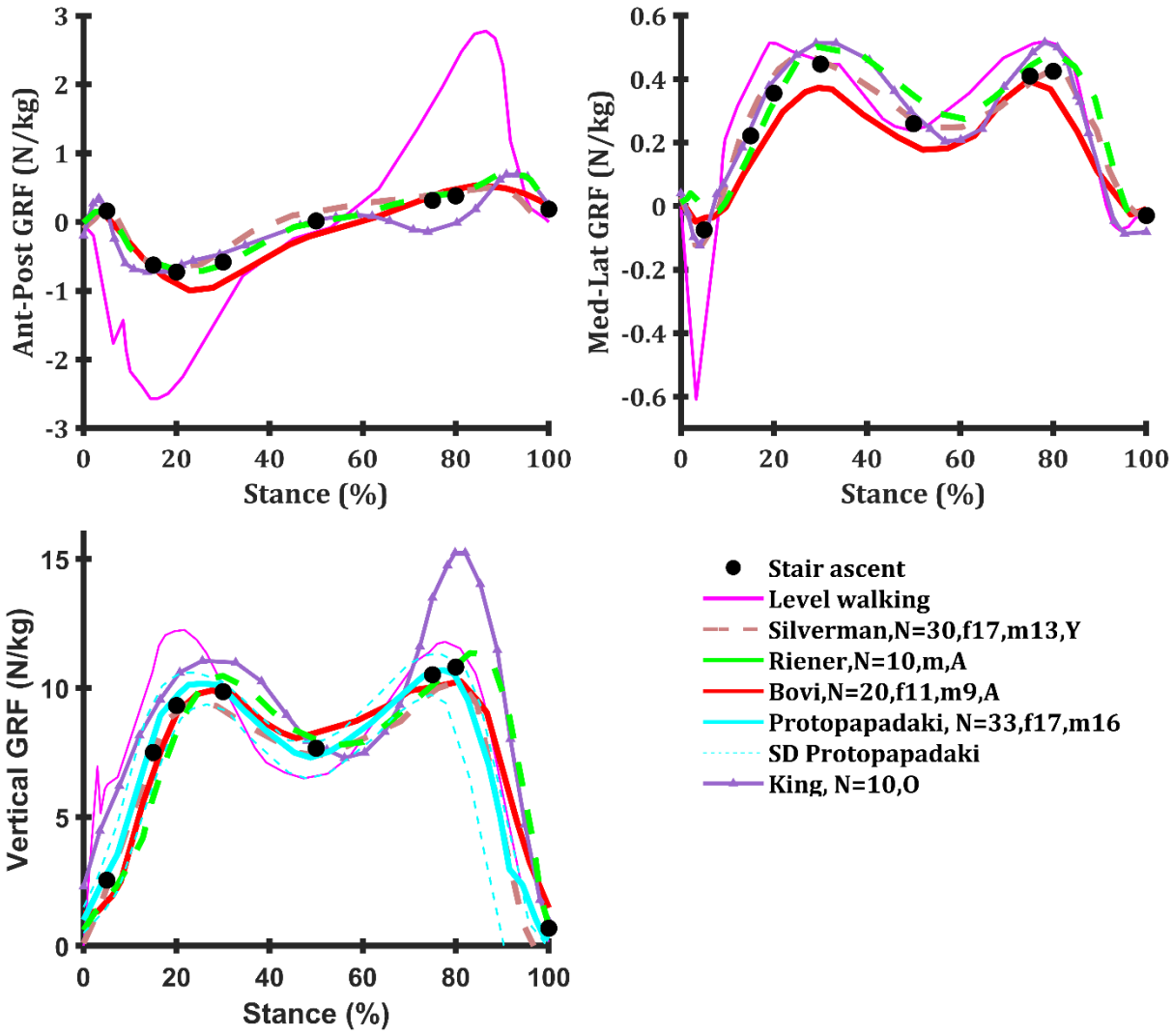

Figure 2.4. GRF are represented normalized to 61.9 kg as our subject's body mass. Black circles are based on the weighted mean values reported in stair ascent measurements that drive along with kinematics (Fig. 1.14) the current simulations (Bovi et al., 2011 King et al., 2017 Protopapadaki et

al., 2007; Riener et al., 2002; Silverman et al., 2014). The solid pink lines represent the input data used in our gait simulations (Astephen et al., 2008) reported here for comparison.

2.4 Joints equilibrium and optimization

For lower extremity simulation during activities like stair ascent and level walking, it is necessary to maintain equilibrium equations when calculating muscle forces. To establish equilibrium equations at each joint, the instantaneous lever arm of muscles crossing the joint in question should be obtained. Considering that a muscle is modelled as a force vector and generates moments around a particular joint, insertion points should be determined to obtain the vector:

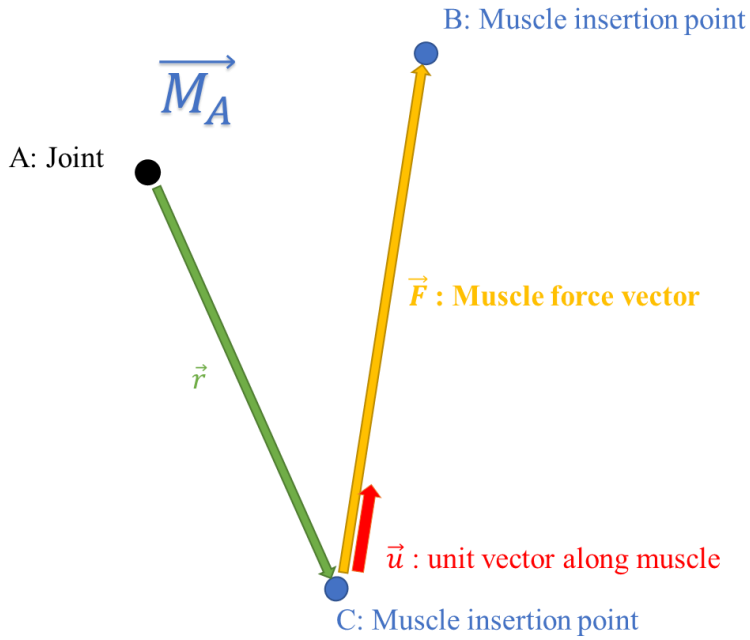

Figure 2.5. Vectors for calculation of level arms.

$$\overrightarrow{M_A} = \vec{r} \times \vec{F} \qquad \overrightarrow{M_A} = \vec{r} \times |F|\vec{u}$$

$$\overrightarrow{m_A} = \vec{r} \times \vec{u} \qquad \overrightarrow{M_A} = |F|\ \overrightarrow{m_A}$$

If we have n as the number of muscles around joint A and consider m_A the lever arm vector for a specific muscle, the sum of moments that muscles generate about the joint A is calculated from the equation bellow:

$$\overrightarrow{M_{Total^A}} = \sum_{1}^{n} \overrightarrow{M_{n^A}} = \sum_{1}^{n} |F_n| \overrightarrow{m_{n^A}}$$

We define a tolerance for muscle force optimizations:

$$\overrightarrow{M_{Total^A}} - \varepsilon < \sum_{1}^{n} |F_n| \overrightarrow{m_{n^A}} < \overrightarrow{M_{Total^A}} + \varepsilon$$

We can re-write the above equation in a matrix form:

$$\begin{bmatrix} M_{x^A} \\ M_{y^A} \\ M_{z^A} \end{bmatrix} - \varepsilon < \begin{bmatrix} m_{1^x} & m_{2^x} & m_{3^x} & \dots & m_{n^x} \\ m_{1^y} & m_{2^y} & m_{3^y} & \dots & m_{n^y} \\ m_{1^z} & m_{2^z} & m_{3^z} & \dots & m_{n^z} \end{bmatrix} \begin{bmatrix} F_1 \\ \vdots \\ F_n \end{bmatrix} < \begin{bmatrix} M_{x^A} \\ M_{y^A} \\ M_{z^A} \end{bmatrix} + \varepsilon$$

Muscle forces are iteratively estimated by minimizing the following cost function f while satisfying the upper and lower bounds inequality equations on muscle forces:

$$f = \sum_{1}^{n} \left(\frac{F_n}{PCSA_n} \right)^3$$

2.5 Objectives

Our objective here is to analyze the detailed knee joint biomechanics during the stance phase of stair ascent and perform a comparison with results obtained during level walking. In continuation of our earlier studies, we use a validated MS model of the lower extremity coupled to a detailed finite element (FE) model of the entire knee joint (Adouni et al, 2012; Mesfar and Shirazi-Adl, 2006; Sharifi and Shirazi-Adl, 2020, 2021). We focus our attention on the estimation of muscle forces, TF and PF joint contact forces and stresses as well as forces in the joint ligaments. It is hypothesized that, in comparison with the level walking and under mean reported kinematics-kinetics-ground reaction forces (GRF), stair ascent generates much greater contact forces-stresses on the PF joint but overall smaller forces in ACL.

2.6 Structure of the dissertation

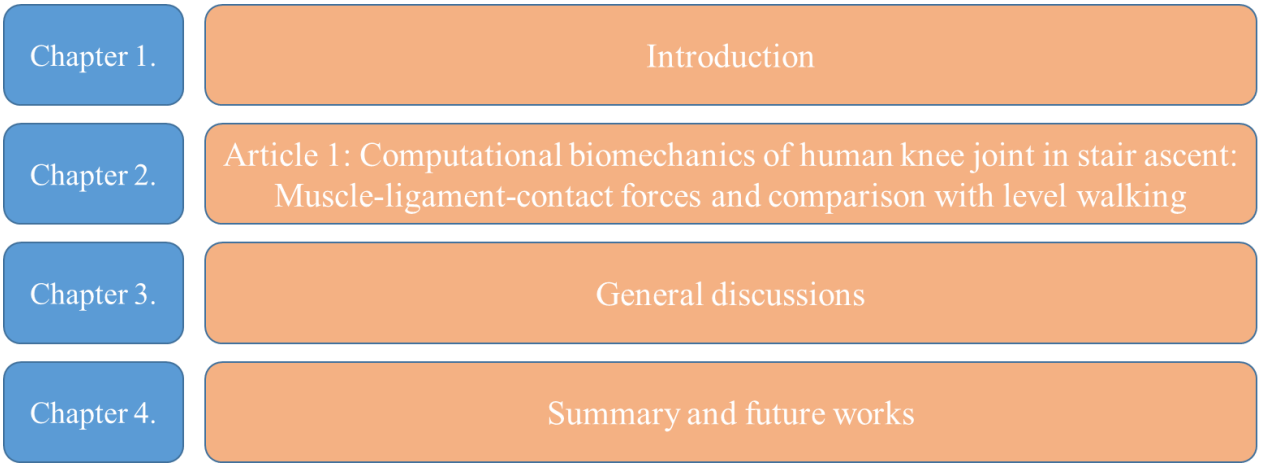

Several FE models have been proposed to simulate the knee joint in various daily activities. Commonly, the knee joint is considered as a planar (2D) joint where the effects of kinetics and kinematics in other planes are neglected.

Compared to the level walking, the stairs ascent is another important activity that, though less common, is nevertheless physically much more demanding especially for those with knee pathologies (Andriacchi et al, JBJS 1980). It involves larger hip-knee-ankle angles and moments with especially much greater (~8 times, Costigan et al, GP 2002) PF contact forces. Stair ascent is also a more demanding biomechanical task when in comparison with the stair descent (Protopaapadaki et al, 2006). Other than limited number of model studies with idealized representations of the knee joint (Taylor et al., 2004; Ghafari et al., 2009), there is no complex and realistic musculoskeletal (MS) analysis of this daily activity.

On the other hand, *in vitro* measurement studies of the extensor mechanism often represent the quadriceps muscle group by a single muscle (rectus femoris, RF) with an overall idealized loading (Mesfar and Shirazi-Adl, 2006) which could adversely affect PF kinematics and contact pressures.

CHAPTER 3 ARTICLE 1 COMPUTATIONAL BIOMECHANICS OF HUMAN KNEE JOINT IN STAIR ASCENT: MUSCLE-LIGAMENT-CONTACT FORCES AND COMPARISON WITH LEVEL WALKING

Submitted to *International Journal for Numerical Methods in Biomedical Engineering*

March 2022

A.Makani, A. Shirazi-Adl, F. Ghezelbash

Abstract

About a third of knee joint disorders originate from the patellofemoral (PF) site that makes stair ascent a difficult activity for patients. A detailed finite element model of the knee joint is coupled to a lower extremity musculoskeletal model to simulate the stance phase of stair ascent. It is driven by the mean of measurements on the hip-knee-ankle moments-angles as well as ground reaction forces reported in healthy individuals. Predicted muscle activities compare well to the recorded electromyography data. Peak forces in quadriceps (3.87BW, body weight, at 20% instance in our 61.9 kg subject), medial hamstrings (0.77BW at 20%), and gastrocnemii (1.21BW at 80%) are estimated. Due to much greater flexion angles-moments at the hip and knee joints in the first half of stance, large PF contact forces (peak of 3.1BW at 20% stance) and stresses (peak of 4.83 Mpa at 20% stance) are estimated that exceed their peaks in level walking by four- and two-fold, respectively. Compared to level walking, ACL forces diminish in the first half of stance but substantially increase later in the second half (peak of 0.76BW at 75% stance). Under nearly similar contact forces at 20% of stance, the contact stress on the tibiofemoral (TF) medial plateau reaches a peak (9.68 Mpa) twice that on the PF joint suggesting the vulnerability of both joints. Compared to walking, stair ascent increases peak ACL force and both TF and PF contact stresses. Reductions in the knee flexion moment and/or angle appear as a viable strategy to mitigate internal loads and pain.

Keywords: Knee joint; Stair ascent; Muscle forces; Finite element; Anterior cruciate ligament; Contact forces; Patellofemoral joint; Contact stress

3.1 INTRODUCTION

In daily activities, knee patellofemoral (PF) and tibiofemoral (TF) articular joints experience large contact forces exceeding the entire body weight and consequently large contact stresses. With a prevalence of 24%, the human knee joint is the 2nd most frequent anatomical site affected by OA after hand joints (Pereira et al., 2011). Knee OA prevalence increases in presence of a number of personal (being overweight, obese, of older age, and female and/or having previous injuries) (Blagojevic et al., 2010; Reid et al., 2010) and occupational (kneeling/squatting, stair climbing, lifting/carrying heavy loads) (Klussmann et al., 2010; Reid et al., 2010) risk factors. Results of the third National Health and Nutrition Examination Survey (1988-1994) on 6596 older adults (>60 years) revealed overall that 18.1% of US men and 23.5% of US women suffered from knee pain with the prevalence rising with age (Andersen et al., 1999). Commonly referred to as the knee anterior disorder and pain, PF joint pathologies account for more than a third of all those associated with the knee (DeHaven and Lintner, 1986; Lankhorst et al., 2017; Taunton et al., 2002). They are also more prevalent in women than men (Boling et al., 2010). A sound hypothesis is that the initiation and progression of OA are associated with both abnormal changes in contact areas and elevated contact stresses (Andriacchi et al., 2004; Ward and Powers, 2004). There is a dose-response correlation between knee symptoms and heavy work activities such as kneeling, squatting, stair climbing, and lifting (Herquelot et al., 2015; Jones et al., 2007; Mikkelsen et al., 2019; Palmer, 2012; Plotnikoff et al., 2015).

The primary biomechanical function of patella is to increase the effective lever arm of the knee extension mechanism. As a result, the PF joint is the origin of the knee anterior pain related to disturbances in normal tracking, instability, and excessive pressure syndrome. In level walking as the most common daily activity, however, the PF joint is not loaded as high as the TF joint is (Adouni et al., 2012; Sharifi et al., 2020; Thomeer et al., 2020). In contrast, however, the PF joint experiences much greater forces in activities with large quadriceps exertion and knee flexion angles; e.g., squat lifts, stair ascent, and extension exercises (Adouni and Shirazi-Adl, 2009; Bischoff et al., 2009; Chen et al., 2010; Cohen et al., 2001; Farrokhi et al., 2011; Goudakos et al., 2009; Mesfar and Shirazi-Adl, 2005 and 2008). Accurate quantification of the knee joint biomechanics in such activities is of great help not only in the injury and degeneration prevention but also in the improved design of implants, rehabilitation and treatment strategies when managing

knee joint disorders.

Compared to the level walking, the stair negotiation is a daily activity that, though less common, is nevertheless physically more demanding especially for those with knee pathologies (Andriacchi et al., 1980). It involves larger hip and knee angles and moments with especially much greater (Chen et al., 2010; Costigan et al., 2002; Farrokhi et al., 2011; Price et al., 2017) PF contact forces. Stair ascent is also a more demanding biomechanical task than the stair descent (Protopapadaki et al., 2007). Earlier model studies of stair ascent considered either an idealized knee without PF joint (Bennett et al., 2018; Ghafari et al., 2009; Lin et al., 2015; Taylor et al., 2004; Valente et al., 2015) or PF joint alone (Chen et al., 2010 ; de Oliveira Silva et al., 2020 ; Farrokhi et al., 2011). There is no realistic coupled finite element (FE)-musculoskeletal (MS) analysis of this activity. On the other hand, *in vitro* measurement studies of the extensor mechanism often represent the quadriceps by a single muscle (Ahmed et al., 1987; Goodfellow et al., 1976; Heegaard et al., 1995; Hirokawa, 1991; Huberti et al., 1984; Huberti and Hayes, 1984; Huberti and Hayes, 1988) which could adversely affect PF kinematics and kinetics (Powers et al., 1998; Sakai et al., 1996). Besides, to counterbalance the extensor moment of quadriceps forces, measurement studies often restrain the motion of the tibia at a distal point away from the joint (Draganich et al., 1987; Farahmand et al., 1998; Farahmand et al., 2004; Goudakos et al., 2009; Hsich and Draganich, 1997; Jurist and Otis, 1985; Li et al., 1999; Pandy and Shelburne, 1997; Senavongse et al., 2003). This constraint on the movement causes a posterior shear force on the tibia whose magnitude varies with the knee flexion angle, location of restraint, and quadriceps forces. It, therefore, influences to different extents the magnitudes of the tibial anterior translation and anterior cruciate ligament (ACL) force (Jurist and Otis, 1985; Mesfar and Shirazi-Adl, 2006a; Pandy and Shelburne, 1997).

In this study, we aim to analyze the detailed knee joint biomechanics during the stance phase of stair ascent and compare results with those during level walking while focusing on muscle forces, TF-PF contact forces, stresses, and areas as well as forces in ligaments. In continuation of our earlier studies, we use a validated MS model of the lower extremity coupled with a detailed FE model of the entire knee joint (Adouni and Shirazi-Adl, 2009; Mesfar and Shirazi-Adl, 2006b; Sharifi and Shirazi-Adl, 2021b; Sharifi et al., 2020). It is hypothesized that, in comparison with level walking and under the mean kinematics, kinetics, and ground reaction forces (GRF) reported in healthy individuals, stair ascent generates much greater contact forces and stresses on PF joint

but smaller ACL forces and TF medial-lateral contact forces and stresses.

3.2 METHODS

3.2.1 Coupled FE-MS Model:

The coupled finite element-musculoskeletal (FE-MS) model of the lower extremity includes 34 distinct muscles along with the hip and ankle taken as frictionless spherical joints while the knee joint is simulated in details by a validated complex elastostatic FE model (reconstructed from a female cadaver specimen (Bendjaballah et al., 1995)) (see supplementary Figs S2 and S3). The knee FE model is made of 3 bony structures (tibia, femur, and patella), their articular cartilage layers, menisci, TF ligaments (including ACL by 2 bundles, posterior cruciate ligament (PCL) by 2 bundles, lateral collateral ligament (LCL), medial collateral ligament (MCL), PF ligaments (MPFL and LPFL), and patellar tendon (PT)). The model was driven by mean 3D angles and moments (3 of each at the knee and hip whereas one at the ankle joint) and GRF reported in the literature for healthy individuals (Figs 3.1 and 3.2).

Bony structures are simulated as rigid bodies while the articular cartilage layers and menisci as nonlinear depth-dependent composites of collagen fibril networks and hyperelastic matrices (see (Shirazi and Shirazi-Adl, 2008) for more details). Ligaments are each represented by multiple (nonlinear pre-strained) truss elements (tension only) (Mesfar and Shirazi-Adl, 2006a). In addition to this model with a refined mesh (~1 mm size), another model with a coarser mesh was used in preliminary analyses (see (Sharifi et al., 2020)). Further details are available elsewhere (Adouni and Shirazi-Adl, 2013; Sharifi et al., 2018; Shirazi et al., 2008).

To simulate each instance of stair ascent, the femur was initially rotated about the hip joint by reported kinematics (i.e., 3 angles; Fig. 3.1). It was then kept fixed, pre-strains in the knee joint ligaments applied, and knee angles in the joint coordinates system (Grood and Suntay, 1983) prescribed (Fig. 2.1). The GRFs were applied on the foot at a location to generate reported moments at the knee. The weight of the lower leg and foot were considered (29.78 N and 7.98 N, respectively). With 3 TF translations and 6 PF displacements free, muscle forces were iteratively estimated using an optimization approach (Eq. 1) constrained by 7 moment-equilibrium equations (Eq. 2a) as well as inequality equations (Eq. 2b):

$$\text{Cost function:}\quad \min \sum_{i=1}^{34}(F_i/PCSA_i)^3 \qquad (1)$$

subject to (at each joint):

$$\vec{M} = \sum \vec{r_i} \times \vec{F_i} \tag{2a}$$

$$F_{pi} \leq F_i \leq (F_{pi} + \sigma_{i\,max}\, PCSA_i) \tag{2b}$$

where F_i, F_{pi}, $PCSA_i$, $\sigma_{i\,max}$, r_i, and M are respectively the unknown force in the ith muscle, its passive force (Davis et al., 2003), physiological cross-sectional area, maximum active stress (taken as 0.6 MPa), moment arm as well as the reaction moment in different directions at the hip (3 moments), knee (3 moments) and ankle (one moment) joints. Estimated muscle forces at each step were reapplied (at their updated insertions and directions) onto the FE model as additional forces and the analysis was repeated until convergence (unbalanced moments <0.8 Nm). Nonlinear FE analyses employed ABAQUS (version 6.18, Simulia, Inc., Providence, RI, USA) while the optimization algorithm was performed in Matlab (R2019a Optimization Toolbox, genetic algorithms-fmincon).

3.2.2 Prescribed Kinematics and Kinetics:

The weighted (by the number of subjects in each study) mean angles and moments at the hip, knee and ankle plus GRFs recorded during the stance phase of stair ascent were taken from multiple available in vivo measurements of healthy adults (see Figs 2.1 and 2.2 captions). For moments and GRFs, the mean reported normalized (to body mass) values were scaled back using the body mass of 61.9 kg (De Leva, 1996) in accordance with our knee model reconstructed from a female cadaver (Bendjaballah et al., 1995).

3.2.3 Comparison with Measurements:

To perform qualitative comparison with measurements, estimated muscle forces were normalized to their maximum force calculated as 0.6 PCSA. This was then compared with the recorded electromyography (EMG) that was normalized to its peak collected during maximum voluntary isometric contractions. Comparison in trends was carried out using the standard correlation coefficient r that measures the strength of a linear relationship. Due to multiple reasons indicated later in Discussion, the use of Bland-Altman analysis that is more suitable for comparison of

magnitudes was not considered.

3.3 RESULTS

Quadriceps and medial hamstrings were most activated in the first half of stance (15-50%) whereas gastrocnemii reached their maximum forces late in stance (Fig. 3.3). Forces in quadriceps peaked at 3.87BW (body weight) at 20%. In medial hamstrings, semimembranosus and tripod muscles reached their maximums at 20% (0.73BW) and 30% (0.12BW), respectively. In contrast to medial hamstrings, lateral hamstrings (i.e., biceps) remained nearly inactive (<0.03 BW). Medial and lateral gastrocnemii reached, respectively, peaks of 0.81BW and 0.40BW at 80% of stance. The gluteus medius and maximus showed higher activities at 20-80% instances with no activity at extreme periods (see Fig. 3.7).

Vector sum of forces in various muscle groups (Fig. 3.4) demonstrated overall a greater activity in the early stance of stair climbing. At these periods, forces in quadriceps, medial hamstrings (Fig. 3.3) and PT (2.66BW) as well as the PF contact force (3.1BW) reached their maximum. In contrast, forces in ACL (0.76BW) and gastrocnemii peaked later in the stance (at 75% and 80% of stance, respectively). Small forces were computed in other ligaments (<0.01 BW).

Maximum contact force on the TF lateral plateau occurred at the first half of stance (1.29BW at 30%) which was much smaller than that in level walking (2.65BW at 5% (Marouane et al., 2017)), Fig. 3.5. The medial contact force peaked once at the first half (3.04 BW at 30%) and then again at the second half (2.97BW at 80%) of stance. Nearly similar peak medial contact forces (3.19BW at 25%) were also estimated in walking (Marouane et al., 2017). The peak total TF contact force in level walking (4.06 BW at 25%) was slightly higher than that in stair ascent (3.89 BW at 30%) though they both followed a similar pattern throughout. With the exception of the terminal periods of stance, the total PF contact force during stair ascent was substantially higher than that in level walking; at 20% stance (3.10BW) it was almost 4 times greater than that in level walking (0.78BW at 25%).

Contact stress distributions, especially on the PF surface, showed much greater peaks in stair ascent than in walking (Fig. 3.6). The PF contact stresses were markedly higher at 20% of the stair ascent and reached twice that in the level walking (with its peak at 25% stance). In stair ascent, the peak contact stress was on the TF medial side at 80% stance and on the PF surface at 20% stance. As

the knee extended (from 20% to 80%), the contact area shifted anteriorly on the TF joint and distally on the PF joint (Fig. 3.6). The total PF and TF (medial/lateral) contact areas were found much larger at 20% than at 80% (7.4 and 6.94/4.6 cm^2, respectively, versus 1.24 and 5.21/1.7 cm^2).

3.4 DISCUSSION

A coupled FE-MS model was employed to investigate the detailed biomechanics of the knee joint during the stance phase of stair ascent. A detailed FE model of the knee joint was integrated within a lower extremity MS model and driven by the mean of in vivo measured GRFs and angles-moments at hip, knee and ankle joints collected on healthy individuals (Figs 3.1 and 3.2). Constrained by prescribed kinematics and kinetics as well as equilibrium equations at various joints, muscle forces were iteratively estimated while minimizing the sum of cubed muscle stresses. Computed results confirmed the hypothesis that the PF joint is loaded much more in stair ascent than in level walking. In contrast, however, peak ACL force and TF contact stresses were found also greater in stair ascent.

Overall, very good agreements with high correlation coefficients (r) are found between the estimated muscle activities (normalized to 0.6 PCSA) and reported normalized EMGs (Fig. 3.7). Trends are similar particularly for quadriceps and gastrocnemii muscles where peak activities occur in the first and second halves of stance, respectively. The correlation is poor in bicep femoris-long head (BF-LH) which is due likely to the small estimated forces and rather low measured EMGs. Computed muscle forces are also in good agreement with others reporting EMG during stair ascent either in absolute values with no normalization to their peaks at maximum voluntary contractions (Bovi et al., 2011; Camargo et al., 2021; Reeves et al., 2009; Valente et al., 2015) or in combination for multiple muscles and locations (Lin et al., 2015). It is crucial that these qualitative comparisons be made in the light of concerns on EMG collection and manipulations (e.g., cross-talk, susceptibility to contamination, filtering, normalization, maximum values) especially in the larger and deeper muscles. Substantial differences have been noted in surface EMGs along a single muscle at different locations (Ghezelbash et al., 2020). Besides, the EMG-force relation in both timing and magnitude, maximum muscle force used for normalization of computed forces, and limitations in the FE-MS model (see below) are additional issues to be aware of. For example, in our model studies, alterations in the maximum muscle stress or the consideration of some minimum

contraction threshold in muscles would directly affect estimated values.

In comparison to level walking, stair ascent is distinguished by overall much larger flexion moments and angles at the knee, hip and ankle joints during the first half of stance (Figs 3.1 and 3.2). Despite similar trends, hip and knee adduction moments are smaller in stair ascent while GRFs are nearly the same (Fig. 3.2). As a direct consequence of much greater flexion moments, large activity in quadriceps is estimated; 3.87BW at 20% that is more than twice 1.79BW at 25% in walking (Marouane et al., 2017). Together with the large knee flexion angle, they generate very large PT and PF contact forces that peak at 20% stance (Fig. 3.4). For example, PF contact force reaches the peak of 3.1BW at 20% stance that is about 4 times larger than that in level walking (0.78BW at 25% stance). Compared to TF contact forces, this PF contact force is even slightly larger than 3.04BW computed on the medial plateau at 30% but smaller than 3.89BW as the peak total TF contact force. In contrast to PF contact forces, total TF contact forces were slightly larger in level walking (4.06BW at 25% in walking versus 3.89BW at 30% in stair ascent) with nearly similar medial TF contact forces in both activities. In addition, contrary to level walking with larger lateral TF contact forces early in stance, the medial compartment carried a larger portion of total TF load throughout the stance in stair ascent. During 20-80% periods of stance in stair ascent, our total TF contact forces are larger than those measured in patients with instrumented knees (Fig. 3.5). It is important to note that patients in these studies were old and mainly males with much higher body masses of 90-100 kg (5 patients aged 63-70 years in Kutzner et al., 2010) and 69-109 kg (9 patients aged 62-76 years in Bergmann et al., 2014). Apart from the likely nonlinearity in BW-TF contact force relation, likely changes in their kinematics-kinetics along with implanted knee joints versus the intact one in our study require particular attention. The in vivo-based subject-specific stair ascent simulations of Bennett et al (2018) and Valente et al (2015) (both with a 1-D knee and no PF joint), Taylor et al (2004) (with a 3-D hinge knee joint and no PF joint), and Price et al (2017) (with a 3D link-segment model with ligaments and patella) estimated greater (mean) peak TF resultant forces in the range of 4 to 6BW.

It is important to recognize that foregoing predictions on PF contact forces depend on the prescribed maximal knee flexion moment of 0.92 Nm/kg (at 20% stance, Fig. 3.2) which is within the range of reported peak moments of 0.76 to 1.46 Nm/kg (Costigan et al., 2002). Greater knee flexion moments in our model could further increase forces in quadriceps and PT and hence PF

contact forces. Using a larger flexion moment of 1.16±0.23 Nm/kg and a simple knee model, Costigan et al. (2002) estimated a peak PF contact force 8 times greater in stair ascent than in level walking. Our computed increase in the peak PF contact force from 7.7 N/kg in walking to 30.4 N/kg in stair ascent (Fig. 3.4) also agrees very well with respective subject-specific predictions of 10.1 N/kg and 33.9 N/kg reported as means of 10 male and 10 female healthy volunteers (Chen et al., 2010). Smaller increases of about two-fold were reported in another study (Price et al., 2017). Our results support the strategy to reduce knee flexion moments (i.e., quadriceps avoidance) reported in patients with PF pain (Salsich et al., 2001; Zabala et al., 2013). The reported significant decrease in the knee flexion angle during stair ascent in such patients (de Oliveira Silva et al., 2015), however and if not accompanied with similar decreases in the knee flexion moment, markedly increases forces in ACL and on TF joint (Mesfar and Shirazi-Adl, 2005). It is also interesting to note that, in contrast to hamstrings, the moment-generating capacity of quadriceps increases at lower knee flexion angles (Mesfar and Shirazi-Adl, 2006b). Due to the concurrent decreases in PF contact force and contact area as the knee flexion moment or the knee flexion angle decreases (Mesfar and Shirazi-Adl, 2005), quantification of the relative effects of alterations in the knee flexion moment versus angle on PF contact stresses require separate studies. It is also to be noted that earlier personalized PF model studies during static squats report higher PF contact stresses in patients with PF pain when compared to healthy subjects under the same knee angle (Farrokhi et al., 2011). Moreover, kinesiophobia has been reported to be more associated with the self-reported pain and disability in PF pain patients than PF contact forces (de Oliveira Silva et al. 2020).

As a result of important PF and TF contact forces, large contact stresses are computed (Fig. 3.6). In stair ascent, despite slightly smaller peak TF contact force compared to level walking, moderately greater medial TF contact stress (10.49 MPa at 80% stance) is predicted. The contact areas shift anteriorly on TF compartments and distally on PF contact areas when the knee extends from 20% to 80% instances in stair ascent (Fig. 3.6). Due to much greater PF contact forces in stair ascent, much larger (4.83 MPa at 20% stance in stair ascent versus 2.46 MPa at 25% stance in walking) maximal contact stresses are estimated on both medial and lateral facets of the PF articular areas. It is interesting that, in stair ascent, under nearly equal contact forces on the PF (at 20% stance) and medial TF (at 20-30% stance) joints and due to the larger PF contact area, the

peak contact stress is nearly twice greater on the medial TF than on the PF surface.

Peak PF contact pressure (4.83 MPa) and area (7.4 cm^2) are computed (Fig. 3.6) at 20% of stance in stair ascent (at the knee flexion angle of 54^o) under 3.87BW (2350 N) quadriceps, 0.73BW (443.3 N) medial hamstrings and 3.1BW PF contact (1882 N) forces. While simulating stair ascent, Goudakos et al. (2009) measured, though at 30^o knee flexion, PF peak pressures and areas in the ranges of 6.98-12.95 MPa and 222-600 mm^2, respectively, under 1657 N PF joint force. Peak contact areas of 400 mm^2 under 2200 N (Quintelier et al., 2008) and about 460 mm^2 under 1468 N (Ahmed et al., 1983) quadriceps forces were also measured. Bearing in mind that the PF contact area markedly increases with the knee flexion angle and quadriceps force magnitude, these measurements corroborate our predicted values. The substantial increase in PF contact area under greater knee flexion angles and quadriceps forces, found here (7.4 cm^2 at 20% and 1.24 cm^2 at 80%) and reported elsewhere (Ahmed et al., 1983; Goudakos et al., 2009; Mesfar and Shirazi-Adl, 2005) is beneficial in mitigating the large PF contact forces in stair ascent. Indeed, higher flexion angles have opposing effects on PF contact stresses in increasing PF contact forces and areas alike (Mesfar and Shirazi-Adl, 2005). It is to be noted that i*n vitro* studies commonly simulate quadriceps by a single muscle (Ahmed et al., 1987; Heegaard et al., 1995; Mesfar and Shirazi-Adl, 2006b) which influences PF kinematics and kinetics (Ahmed et al., 1983; Powers et al., 1998; Sakai et al., 1996). In addition, they often apply small quadriceps forces and restrain the tibia at an arbitrary distal point while resisting the moment of muscle forces (Ahmed et al., 1983; Farahmand et al., 1998; Goudakos et al., 2009; Hsieh and Draganich, 1998; Li et al., 1999; Li et al., 2004; Pandy and Shelburne, 1997). This constraint generates additional forces on the tibia whose magnitude varies with the knee flexion, location of the restraint, and quadriceps forces (Mesfar and Shirazi-Adl, 2006b; Pandy and Shelburne, 1997).

During the first half of stance and despite a much larger activity in quadriceps in stair ascent compared to level walking, much smaller forces are computed in ACL; they increase from nil at or before 15% of stance to 0.22BW at 30% of stance (Fig. 2.4) compared to 0.39BW at the heel strike to 0.58BW at 25% stance in level walking (Marouane et al., 2017). This is a direct consequence of concomitant much larger knee flexion angles that markedly diminish ACL forces (Mesfar and Shirazi-Adl, 2005). As the knee flexion angle increases, the direction of PT force on the tibia

reverses from an anterior pull to a posterior one that as a result influences ACL force (DeFrate et al., 2007; Mesfar and Shirazi-Adl, 2005; Thomeer et al., 2020). Nevertheless at the second half of stance under much smaller flexion angles, ACL force peaks at 0.76BW (75% of stance) that exceeds its maximum of 0.58BW evaluated at 25% in walking (Marouane et al., 2017). High activity in gastrocnemii that, similar to quadriceps, are ACL antagonist (Adouni et al., 2016; Sharifi and Shirazi-Adl, 2021a) plays a role here. These findings point to a greater vulnerability of ACL in stair ascent when compared to level walking.

Interpretations of predictions should be made in the light of some limitations. We used a single knee geometry reconstructed from a female cadaveric specimen (Bendjaballah et al., 1995). Though input data into the model are taken from the literature, we have extensively validated this model with available in vitro and in vivo data (Bendjaballah et al., 1997; Marouane and Shirazi-Adl, 2019; Mesfar and Shirazi-Adl, 2006a, b; Moglo and Shirazi-Adl, 2005). The lower extremity musculature as well as input kinematics-kinetics-GRFs were taken from the mean of data on asymptomatic subjects available in the literature (see captions of Figs 3.1 and 3.2). Due to the large scatter and absence of a unique study of stair ascent with all required data, this approach of taking the mean of available data appears justified. Determination of the extent of changes in predicted outputs as a result of scatter in the input kinematics and kinetics should however await future statistical analyses (see (Sharifi et al., 2020) in walking). The assumption of the bony structures as rigid bodies, though time consuming in the current nonlinear FE-MS model, may affect results especially of stresses and strains in the deeper cartilage layers. Finally, a non-zero minimum muscle activity threshold to enhance cocontraction was not considered in this optimization-based model.

In summary, a detailed FE model of the knee joint within a lower extremity MS model was employed to simulate the stair ascent while being driven by the mean of available kinematics and kinetics measurements. Results are also compared with earlier predictions of the same model during walking. Quadriceps and medial hamstrings are activated mainly in the first half while gastrocnemii contribute in the second half of stance. Due to the much greater flexion angles and moments at the hip and knee joints in the first half of stance, large PF contact forces and stresses are estimated that exceed (four-fold and two-fold, respectively) those in level walking. Compared

to level walking, forces in ACL diminish in the first half of stance but increase later in the second half. These ACL forces in both stair ascent and level walking are primarily controlled by the changes in the knee flexion angle and muscle recruitments at different instances. Under nearly similar total contact forces at 20% of stance in the stair ascent, the medial TF articular contact stress reaches a peak more than twice that in PF joint suggesting that both joints are highly solicited and are hence vulnerable during stair ascent. Findings highlight that large PF contact stresses and forces can be mitigated by reducing the peak knee joint flexion angle and moment. Finally and compared to the level walking, stair ascent increases peak ACL force, PF contact force, and TF and PF contact stresses.

ACKNOWLEDGEMENTS: The financial support of the Natural Science and Engineering Research Council of Canada (RGPIN5595) are acknowledged.

3.5 REFERENCES

Adouni, M., Shirazi-Adl, A., 2009. Knee joint biomechanics in closed-kinetic-chain exercises. Computer Methods in Biomechanics Biomedical Engineering 12, 661-670.

Adouni, M., Shirazi-Adl, A., 2013. Consideration of equilibrium equations at the hip joint alongside those at the knee and ankle joints has mixed effects on knee joint response during gait. Journal of Biomechanics 46, 619-624.

Adouni, M., Shirazi-Adl, A., Marouane, H., 2016. Role of gastrocnemius activation in knee joint biomechanics: gastrocnemius acts as an ACL antagonist. Computer Methods in Biomechanics and Biomedical Engineering 19, 376-385.

Adouni, M., Shirazi-Adl, A., Shirazi, R., 2012. Computational biodynamics of human knee joint in gait: from muscle forces to cartilage stresses. Journal of Biomechanics 45, 2149-2156.

Ahmed, A., Burke, D., Hyder, A., 1987. Force analysis of the patellar mechanism. Journal of Orthopaedic Research 5, 69-85.

Ahmed, A., Burke, D., Yu, A., 1983. In-vitro measurement of static pressure distribution in synovial joints—Part II: retropatellar surface. Journal of Biomechanical Engineering 105, 226-236.

Allison, K., Bennell, K.L., Grimaldi, A., Vicenzino, B., Wrigley, T.V., Hodges, P.W., 2016. Single leg stance control in individuals with symptomatic gluteal tendinopathy. Gait & Posture 49, 108-113.

Andersen, R.E., Crespo, C.J., Ling, S.M., Bathon, J.M., Bartlett, S.J., 1999. Prevalence of significant knee pain among older Americans: results from the Third National Health and Nutrition Examination Survey. Journal of the American Geriatrics Society 47, 1435-1438.

Andriacchi, T., Andersson, G., Fermier, R., Stern, D., Galante, J., 1980. A study of lower-limb mechanics during stair-climbing. Journal of Bone Joint Surgery 62, 749-757.

Andriacchi, T.P., Mündermann, A., Smith, R.L., Alexander, E.J., Dyrby, C.O., Koo, S., 2004. A framework for the in vivo pathomechanics of osteoarthritis at the knee. Annals of Biomedical Engineering 32, 447-457.

Astephen, J.L., Deluzio, K.J., Caldwell, G.E., Dunbar, M.J., 2008. Biomechanical changes at the hip, knee, and ankle joints during gait are associated with knee osteoarthritis severity. Journal of Orthopaedic Research 26, 332-341.

Bendjaballah, M., Shirazi-Adl, A., Zukor, D., 1995. Biomechanics of the human knee joint in compression: reconstruction, mesh generation and finite element analysis. Knee 2, 69-79.

Bendjaballah, M., Shirazi-Adl, A., Zukor, D., 1997. Finite element analysis of human knee joint in varus-valgus. Clinical Biomechanics 12, 139-148.

Bergmann, G., Bender, A., Graichen, F., Dymke, J., Rohlmann, A., Trepczynski, A., Heller, M.O., Kutzner, I., 2014. Standardized loads acting in knee implants. PloS one 9, e86035.

Bischoff, J.E., Hertzler, J.S., Mason, J.J., 2009. Patellofemoral interactions in walking, stair ascent, and stair descent using a virtual patella model. Journal of Biomechanics 42, 1678-1684.

Blagojevic, M., Jinks, C., Jeffery, A., Jordan, K., 2010. Risk factors for onset of osteoarthritis of the knee in older adults: a systematic review and meta-analysis. Osteoarthritis and Cartilage 18, 24-33.

Boling, M., Padua, D., Marshall, S., Guskiewicz, K., Pyne, S., Beutler, A., 2010. Gender differences in the incidence and prevalence of patellofemoral pain syndrome. Scandinavian Journal of Medicine & Science in Sports 20, 725-730.

Bovi, G., Rabuffetti, M., Mazzoleni, P., Ferrarin, M., 2011. A multiple-task gait analysis approach: Kinematic, kinetic and EMG reference data for healthy young and adult subjects. Gait & Posture 33, 6-13.

Camargo, J., Ramanathan, A., Flanagan, W., Young, A., 2021. A comprehensive, open-source dataset of lower limb biomechanics in multiple conditions of stairs, ramps, and level-ground ambulation and transitions. Journal of Biomechanics 119, 110320.

Chang, B.-C., Khan, M.I., Prado, A., Yang, N., Ou, J., Agrawal, S.K., 2020. Biomechanical differences during ascent on regular stairs and on a stairmill. Journal of Biomechanics 104, 109758.

Cohen, Z.A., Roglic, H., Grelsamer, R.P., Henry, J.H., Levine, W.N., Van Mow, C., Ateshian,

G.A., 2001. Patellofemoral stresses during open and closed kinetic chain exercises: an analysis using computer simulation. The American Journal of Sports Medicine 29, 480-487.

Costigan, P.A., Deluzio, K.J., Wyss, U.P., 2002. Knee and hip kinetics during normal stair climbing. Gait & Posture 16, 31-37.

Davis, J., Kaufman, K.R., Lieber, R.L., 2003. Correlation between active and passive isometric force and intramuscular pressure in the isolated rabbit tibialis anterior muscle. Journal of Biomechanics 36, 505-512.

De Leva, P., 1996. Adjustments to Zatsiorsky-Seluyanov's segment inertia parameters. Journal of Biomechanics 29, 1223-1230.

de Oliveira Silva, D., Briani, R.V., Pazzinatto, M.F., Ferrari, D., Aragão, F.A., de Azevedo, F.M., 2015. Reduced knee flexion is a possible cause of increased loading rates in individuals with patellofemoral pain. Clinical Biomechanics 30, 971-975.

DeFrate, L.E., Nha, K.W., Papannagari, R., Moses, J.M., Gill, T.J., Li, G., 2007. The biomechanical function of the patellar tendon during in-vivo weight-bearing flexion. Journal of Biomechanics 40, 1716-1722.

DeHaven, K.E., Lintner, D.M., 1986. Athletic injuries: comparison by age, sport, and gender. The American Journal of Sports Medicine 14, 218-224.

Draganich, L., Andriacchi, T., Andersson, G., 1987. Interaction between intrinsic knee mechanics and the knee extensor mechanism. Journal of Orthopaedic Research 5, 539-547.

Farahmand, F., Tahmasbi, M., Amis, A., 1998. Lateral force–displacement behaviour of the human patella and its variation with knee flexion—a biomechanical study in vitro. Journal of Biomechanics 31, 1147-1152.

Farahmand, F., Tahmasbi, M.N., Amis, A., 2004. The contribution of the medial retinaculum and quadriceps muscles to patellar lateral stability—an in-vitro study. Knee 11, 89-94.

Gao, B., Cordova, M.L., Zheng, N., 2012. Three-dimensional joint kinematics of ACL-deficient and ACL-reconstructed knees during stair ascent and descent. Human Movement Science 31, 222-235.

Ghafari, A.S., Meghdari, A., Vossoughi, G., 2009. Muscle-driven forward dynamics simulation for the study of differences in muscle function during stair ascent and descent. Proceedings of the Institution of Mechanical Engineers, Part H: Journal of Engineering in Medicine 223, 863-874.

Ghezelbash, F., Shirazi-Adl, A., El Ouaaid, Z., Plamondon, A., Arjmand, N., 2020. Subject-specific regression equations to estimate lower spinal loads during symmetric and asymmetric static lifting. J Biomech 102, 109550.

Goodfellow, J., Hungerford, D., Zindel, M., 1976. Patello-femoral joint mechanics and pathology.

1. Functional anatomy of the patello-femoral joint. The Journal of Bone Joint Surgery 58, 287-290.

Goudakos, I.G., König, C., Schöttle, P.B., Taylor, W.R., Singh, N.B., Roberts, I., Streitparth, F., Duda, G.N., Heller, M.O., 2009. Stair climbing results in more challenging patellofemoral contact mechanics and kinematics than walking at early knee flexion under physiological-like quadriceps loading. Journal of Biomechanics 42, 2590-2596.

Grood, E.S., Suntay, W.J.J.J.o.b.e., 1983. A joint coordinate system for the clinical description of three-dimensional motions: application to the knee. Journal of biomechanical engineering 105, 136-144.

Hall, M., Stevermer, C.A., Gillette, J.C., 2015. Muscle activity amplitudes and co-contraction during stair ambulation following anterior cruciate ligament reconstruction. Journal of Electromyography and Kinesiology 25, 298-304.

Hall, M., Wrigley, T.V., Kean, C.O., Metcalf, B.R., Bennell, K.L., 2017. Hip biomechanics during stair ascent and descent in people with and without hip osteoarthritis. Journal of Orthopaedic Research 35, 1505-1514.

Hammond, C.A., Hatfield, G.L., Gilbart, M.K., Garland, S.J., Hunt, M.A., 2017. Trunk and lower limb biomechanics during stair climbing in people with and without symptomatic femoroacetabular impingement. Clinical Biomechanics 42, 108-114.

Heegaard, J., Leyvraz, P., Curnier, A., Rakotomanana, L., Huiskes, R., 1995. The biomechanics of the human patella during passive knee flexion. Journal of Biomechanics 28, 1265-1279.

Herquelot, E., Bodin, J., Petit, A., Ha, C., Leclerc, A., Goldberg, M., Zins, M., Roquelaure, Y., Descatha, A., 2015. Incidence of chronic and other knee pain in relation to occupational risk factors in a large working population. Annals of Occupational Hygiene 59, 797-811.

Hirokawa, S., 1991. Three-dimensional mathematical model analysis of the patellofemoral joint. Journal of Biomechanics 24, 659-671.

Hsich, Y.-F., Draganich, L., 1997. Knee kinematics and ligament lengths during physiologic levels of isometric quadriceps loads. Knee 4, 145-154.

Hsieh, Y.-F., Draganich, L.F., 1998. Increasing Quadriceps Loads Affect the Lengths of the Ligaments and the Kinematics of the Knee. Journal of Biomechanical Engineering 120, 750-756.

Hsue, B.-J., Su, F.-C., 2009. Kinematics and kinetics of the lower extremities of young and elder women during stairs ascent while wearing low and high-heeled shoes. Journal of Electromyography Kinesiology 19, 1071-1078.

Huberti, H., Hayes, W., Stone, J., Shybut, G., 1984. Force ratios in the quadriceps tendon and ligamentum patellae. Journal of Orthopaedic Research 2, 49-54.

Huberti, H.H., Hayes, W., 1984. Patellofemoral contact pressures. The influence of q-angle and

tendofemoral contact. The Journal of Bone Joint Surgery 66, 715-724.

Huberti, H.H., Hayes, W.C., 1988. Contact pressures in chondromalacia patellae and the effects of capsular reconstructive procedures. Journal of Orthopaedic Research 6, 499-508.

Jones, G.T., Harkness, E.F., Nahit, E.S., McBeth, J., Silman, A.J., Macfarlane, G., 2007. Predicting the onset of knee pain: results from a 2-year prospective study of new workers. Annals of the Rheumatic Diseases 66, 400-406.

Jurist, K.A., Otis, J.C., 1985. Anteroposterior tibiofemoral displacements during isometric extension efforts: the roles of external load and knee flexion angle. American Journal of Sports Medicine 13, 254-258.

King, S.L., Vanicek, N., O'Brien, T.D., 2017. Sagittal plane joint kinetics during stair ascent in patients with peripheral arterial disease and intermittent claudication. Gait & Posture 55, 81-86.

Klussmann, A., Gebhardt, H., Nübling, M., Liebers, F., Perea, E.Q., Cordier, W., von Engelhardt, L.V., Schubert, M., Dávid, A., Bouillon, B., 2010. Individual and occupational risk factors for knee osteoarthritis: results of a case-control study in Germany. Arthritis Research Therapy 12, 1-15.

Komnik, I., David, S., Funken, J., Haberer, C., Potthast, W., Weiss, S., 2018. Compromised knee internal rotation in total knee arthroplasty patients during stair climbing. PloS one 13, e0205492.

Konrath, J.M., Karatsidis, A., Schepers, H.M., Bellusci, G., de Zee, M., Andersen, M.S., 2019. Estimation of the knee adduction moment and joint contact force during daily living activities using inertial motion capture. Sensors 19, 1681.

Kutzner, I., Heinlein, B., Graichen, F., Bender, A., Rohlmann, A., Halder, A., Beier, A., Bergmann, G., 2010. Loading of the knee joint during activities of daily living measured in vivo in five subjects. Journal of Biomechanics 43, 2164-2173.

Lankhorst, N., Damen, J., Oei, E., Verhaar, J., Kloppenburg, M., Bierma-Zeinstra, S., van Middelkoop, M., 2017. Incidence, prevalence, natural course and prognosis of patellofemoral osteoarthritis: the Cohort Hip and Cohort Knee study. Osteoarthritis and Cartilage 25, 647-653.

Li, G., Rudy, T., Sakane, M., Kanamori, A., Ma, C., Woo, S., 1999. The importance of quadriceps and hamstring muscle loading on knee kinematics and in-situ forces in the ACL. Journal of Biomechanics 32, 395-400.

Li, G., Zayontz, S., DeFrate, L.E., Most, E., Suggs, J.F., Rubash, H.E., 2004. Kinematics of the knee at high flexion angles: an in vitro investigation. Journal of Orthopaedic Research 22, 90-95.

Mandeville, D., Osternig, L.R., Lantz, B.A., Mohler, C.G., Chou, L.-S., 2008. The effect of total knee replacement on the knee varus angle and moment during walking and stair ascent. Clinical Biomechanics 23, 1053-1058.

Marouane, H., Shirazi-Adl, A., 2019. Sensitivity of medial-lateral load sharing to changes in

adduction moments or angles in an asymptomatic knee joint model during gait. Gait & Posture 70, 39-47.

Marouane, H., Shirazi-Adl, A., Adouni, M., 2017. 3D active-passive response of human knee joint in gait is markedly altered when simulated as a planar 2D joint. Biomechanics modeling in mechanobiology 16, 693-703.

Mesfar, W., Shirazi-Adl, A., 2005. Biomechanics of the knee joint in flexion under various quadriceps forces. Knee 12, 424-434.

Mesfar, W., Shirazi-Adl, A., 2006a. Biomechanics of changes in ACL and PCL material properties or prestrains in flexion under muscle force-implications in ligament reconstruction. Computer Methods in Biomechanics Biomedical Engineering 9, 201-209.

Mesfar, W., Shirazi-Adl, A., 2006b. Knee joint mechanics under quadriceps–hamstrings muscle forces are influenced by tibial restraint. Clinical Biomechanics 21, 841-848.

Mesfar, W., Shirazi-Adl, A., 2008. Knee joint biomechanics in open-kinetic-chain flexion exercises. Clinical Biomechanics 23, 477-482.

Meyer, C.A.G., Corten, K., Fieuws, S., Deschamps, K., Monari, D., Wesseling, M., Simon, J.-P., Desloovere, K., 2016. Evaluation of stair motion contributes to new insights into hip osteoarthritis-related motion pathomechanics. Journal of Orthopaedic Research 34, 187-196.

Mikkelsen, S., Pedersen, E.B., Brauer, C., Møller, K.L., Alkjær, T., Koblauch, H., Simonsen, E.B., Thygesen, L.C., 2019. Knee osteoarthritis among airport baggage handlers: A prospective cohort study. American Journal of Industrial Medicine 62, 951-960.

Moglo, K.E., Shirazi-Adl, A., 2005. Cruciate coupling and screw-home mechanism in passive knee joint during extension–flexion. Journal of Biomechanics 38, 1075-1083.

Nadeau, S., McFadyen, B.J., Malouin, F., 2003. Frontal and sagittal plane analyses of the stair climbing task in healthy adults aged over 40 years: what are the challenges compared to level walking? Clinical biomechanics 18, 950-959.

Novak, A.C., Brouwer, B., 2013. Kinematic and kinetic evaluation of the stance phase of stair ambulation in persons with stroke and healthy adults: a pilot study. Journal of Applied Biomechanics 29, 443-452.

Palmer, K.T., 2012. Occupational activities and osteoarthritis of the knee. British Medical Bulletin 102, 147-170.

Pandy, M.G., Shelburne, K.B., 1997. Dependence of cruciate-ligament loading on muscle forces and external load. Journal of Biomechanics 30, 1015-1024.

Pereira, D., Peleteiro, B., Araujo, J., Branco, J., Santos, R., Ramos, E., 2011. The effect of osteoarthritis definition on prevalence and incidence estimates: a systematic review. Osteoarthritis

and Cartilage 19, 1270-1285.

Plotnikoff, R.C., Costigan, S.A., Williams, R.L., Hutchesson, M.J., Kennedy, S.G., Robards, S.L., Allen, J., Collins, C.E., Callister, R., Germov, J., 2015. Effectiveness of interventions targeting physical activity, nutrition and healthy weight for university and college students: a systematic review and meta-analysis. International Journal of Behavioral Nutrition Physical Activity 12, 1-10.

Powers, C.M., Lilley, J.C., Lee, T.Q., 1998. The effects of axial and multi-plane loading of the extensor mechanism on the patellofemoral joint. Clinical Biomechanics 13, 616-624.

Protopapadaki, A., Drechsler, W.I., Cramp, M.C., Coutts, F.J., Scott, O.M., 2007. Hip, knee, ankle kinematics and kinetics during stair ascent and descent in healthy young individuals. Clinical Biomechanics 22, 203-210.

Quintelier, J., Lobbestael, F., Verdonk, P., De Baets, P., Almqvist, F., 2008. Patellofemoral contact pressures. Acta of Bioengineering Biomechanics 10, 23-28.

Reeves, N.D., Spanjaard, M., Mohagheghi, A.A., Baltzopoulos, V., Maganaris, C.N., 2009. Older adults employ alternative strategies to operate within their maximum capabilities when ascending stairs. Journal of Electromyography Kinesiology 19, e57-e68.

Reid, C.R., Bush, P.M., Cummings, N.H., McMullin, D.L., Durrani, S.K., 2010. A review of occupational knee disorders. Journal of Occupational Rehabilitation 20, 489-501.

Riener, R., Rabuffetti, M., Frigo, C., 2002. Stair ascent and descent at different inclinations. Gait & Posture 15, 32-44.

Sakai, N., Luo, Z.-P., Rand, J.A., An, K.-N., 1996. Quadriceps forces and patellar motion in the anatomical model of the patellofemoral joint. Knee 3, 1-7.

Salsich, G.B., Brechter, J.H., Powers, C.M., 2001. Lower extremity kinetics during stair ambulation in patients with and without patellofemoral pain. Clinical Biomechanics 16, 906-912.

Senavongse, W., Farahmand, F., Jones, J., Andersen, H., Bull, A., Amis, A., 2003. Quantitative measurement of patellofemoral joint stability: force–displacement behavior of the human patella in vitro. Journal of Orthopaedic Research 21, 780-786.

Sharifi, M., Shirazi-Adl, A., 2021a. Changes in gastrocnemii activation at mid-to-late stance markedly affects the intact and anterior cruciate ligament deficient knee biomechanics and stability in gait. Knee 29, 530-540.

Sharifi, M., Shirazi-Adl, A., 2021b. Knee flexion angle and muscle activations control the stability of an anterior cruciate ligament deficient joint in gait. Journal of Biomechanics 117, 110258.

Sharifi, M., Shirazi-Adl, A., Marouane, H., 2018. Computation of the role of kinetics, kinematics, posterior tibial slope and muscle cocontraction on the stability of ACL-deficient knee joint at heel

strike–Towards identification of copers from non-copers. Journal of Biomechanics 77, 171-182.

Sharifi, M., Shirazi-Adl, A., Marouane, H., 2020. Sensitivity of the knee joint response, muscle forces and stability to variations in gait kinematics-kinetics. Journal of Biomechanics 99, 109472.

Shirazi, R., Shirazi-Adl, A., Hurtig, M., 2008. Role of cartilage collagen fibrils networks in knee joint biomechanics under compression. Journal of Biomechanics 41, 3340-3348.

Shirazi, R., Shirazi-Adl, A., 2008. Deep vertical collagen fibrils play a significant role in mechanics of articular cartilage. Journal of Orthopaedic Research 26, 608-615.

Silverman, A.K., Neptune, R.R., Sinitski, E.H., Wilken, J.M., 2014. Whole-body angular momentum during stair ascent and descent. Gait & Posture 39, 1109-1114.

Taunton, J.E., Ryan, M.B., Clement, D., McKenzie, D.C., Lloyd-Smith, D., Zumbo, B., 2002. A retrospective case-control analysis of 2002 running injuries. British Journal of Sports Medicine 36, 95-101.

Taylor, W.R., Heller, M.O., Bergmann, G., Duda, G.N., 2004. Tibio-femoral loading during human gait and stair climbing. Journal of Orthopaedic Research 22, 625-632.

Thomeer, L.T., Lin, Y.-C., Pandy, M.G., 2020. Load Distribution at the Patellofemoral Joint During Walking. Annals of Biomedical Engineering 48, 2821-2835.

Trinler, U.K., Baty, F., Mündermann, A., Fenner, V., Behrend, H., Jost, B., Wegener, R., 2016. Stair dimension affects knee kinematics and kinetics in patients with good outcome after TKA similarly as in healthy subjects. Journal of Orthopaedic Research 34, 1753-1761.

Vallabhajosula, S., Tan, C.W., Mukherjee, M., Davidson, A.J., Stergiou, N., 2015. Biomechanical analyses of stair-climbing while dual-tasking. Journal of Biomechanics 48, 921-929.

Ward, S.R., Powers, C.M., 2004. The influence of patella alta on patellofemoral joint stress during normal and fast walking. Clinical Biomechanics 19, 1040-1047.

Whatling, G.M., Evans, S.L., Holt, C.A., 2010. Introducing a new staircase design to quantify healthy knee function during stair ascent and descent. Computer Methods in Biomechanics Biomedical Engineering 13, 371-378.

Zabala, M.E., Favre, J., Scanlan, S.F., Donahue, J., Andriacchi, T.P., 2013. Three-dimensional knee moments of ACL reconstructed and control subjects during gait, stair ascent, and stair descent. Journal of Biomechanics 46, 515-520.

Figure Captions

Figure 3.1. The hip and the knee kinematics. Black circles represent the weighted mean values reported in

the stair ascent of in vivo studies (Allison et al., 2016; Bovi et al., 2011; Chang et al., 2020; Gao et al., 2012; Hall et al., 2017; Hsue and Su, 2009; Komnik et al., 2018; Konrath et al., 2019; Mandeville et al., 2008; Meyer et al., 2016; Nadeau et al., 2003; Novak and Brouwer, 2013; Protopapadaki et al., 2007; Riener et al., 2002; Trinler et al., 2016; Vallabhajosula et al., 2015; Whatling et al., 2010). The solid pink lines represent the input data used in our gait simulations (Astephen et al., 2008) reported in this work for comparison.

Figure 3.2. GRF as well as hip, knee, and ankle moments represented normalized to 61.9 kg as our subject's body mass. Black circles are based on the weighted mean values reported in stair ascent measurements that drive along with kinematics (Fig. 1) the current simulations (Allison et al., 2016; Bennett et al., 2017; Bovi et al., 2011; Gao et al., 2012; Hall et al., 2017; Hsue and Su, 2009; King et al., 2017; Komnik et al., 2018; Meyer et al., 2016; Nadeau et al., 2003; Novak and Brouwer, 2013; Protopapadaki et al., 2007; Riener et al., 2002; Salsich et al., 2001; Silverman et al., 2014; Trinler et al., 2016; Vallabhajosula et al., 2015; Whatling et al., 2010; Zabala et al., 2013). The solid pink lines represent the input data used in our gait simulations (Astephen et al., 2008) reported here for comparison.

Figure 3.3. Normalized (to 61.9 kg as the body mass of our model) computed forces in muscles crossing the knee joint at different instances of the stance phase during stair ascent. Estimated forces in a number of muscles are also shown and compared with reported electromyography (EMG) activity in Fig. 7. VM: vastus medialis obliqus; VL: vastus lateralis; VI: vastus intermedius medialis; RF: rectus femoris; SM: semimembranous; TRIPOD: made of sartorius (SR), gracilis (GA) and semitendinosus (ST); GM: Gastrecnemius medial; GL: gastrocnemius lateral.

Figure 3.4. The norm of vector sum of normalized (to body mass of 61.9 kg) forces in different muscle groups, ACL and PT as well as PF total contact force during the stance phase of stair ascent. PT: patellar tendon; ACL: anterior sruciate ligament; PF: patellofemoral ligament; QUAD: quadriceps; HAM: hamstring; GAS: gastrocnemii.

Figure 3.5. Estimated normalized (to body mass of 61.9 kg) contact forces on the tibial and patellar articular surfaces during both stair ascent and level walking (Marouane et al., 2017). Measured contact forces during stair ascent by instrumented implants are also shown for comparison (Bergmann et al., 2014; Kutzner et al., 2010).

Figure 3.6. Contact pressure distribution on patellar and tibial articular surfaces at critical instances of stance during stair ascent (top two rows) and level walking (bottom row).

Figure 3.7. Comparison of predicted muscle activities (muscle forces normalized to $\sigma_{max} \times PCSA$) versus measured EMG values (normalized to their peaks recorded at maximum voluntary isometric contractions) (Hall et al., 2015; Hammond et al., 2017) during the stance phase of stair ascent. The correlation coefficients

r) between estimated and measured data are also given.

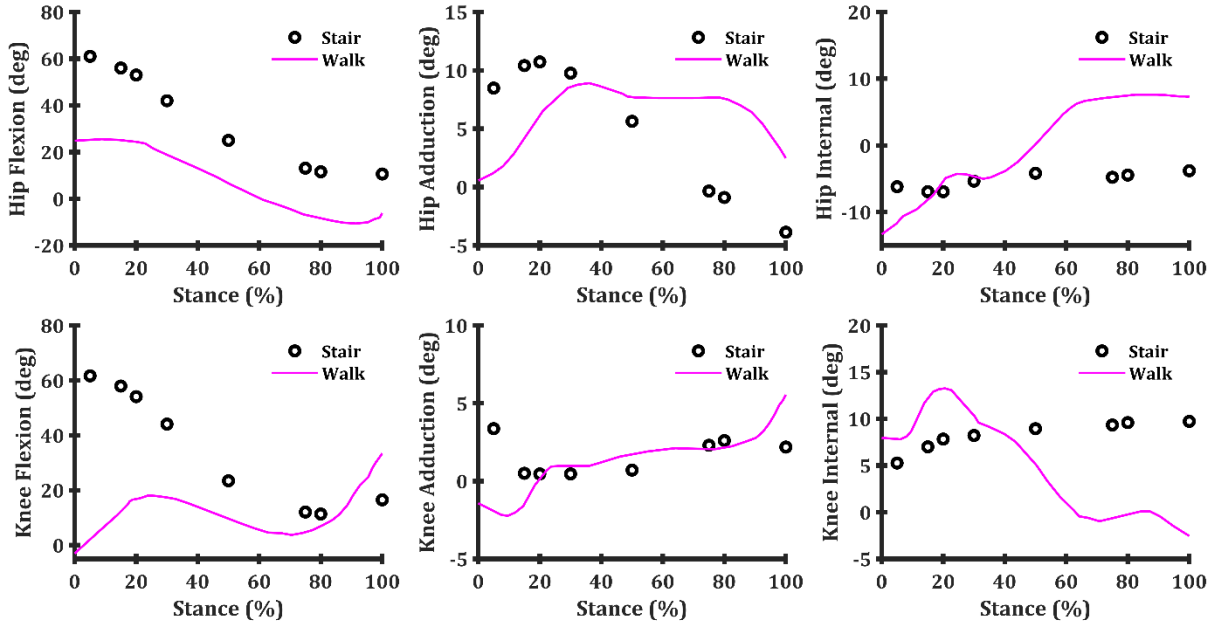

Figure 3.1. The hip and the knee kinematics. Black circles represent the weighted mean values reported in the stair ascent of in vivo studies (Allison et al. 2016; Bovi et al. 2011; Chang et al. 2020; Gao et al. 2012; Hall et al. 2017; Hsue and Su 2009; Komnik et al. 2018; Konrath et al. 2019; Mandeville et al. 2008; Meyer et al. 2016; Nadeau et al. 2003; Novak and Brouwer 2013; Protopapadaki et al. 2007; Riener et al. 2002; Trinler et al. 2016; Vallabhajosula et al. 2015; Whatling et al. 2010). The solid pink lines represent the input data (Astephen et al. 2008) used in our gait simulations reported in this work for comparison.

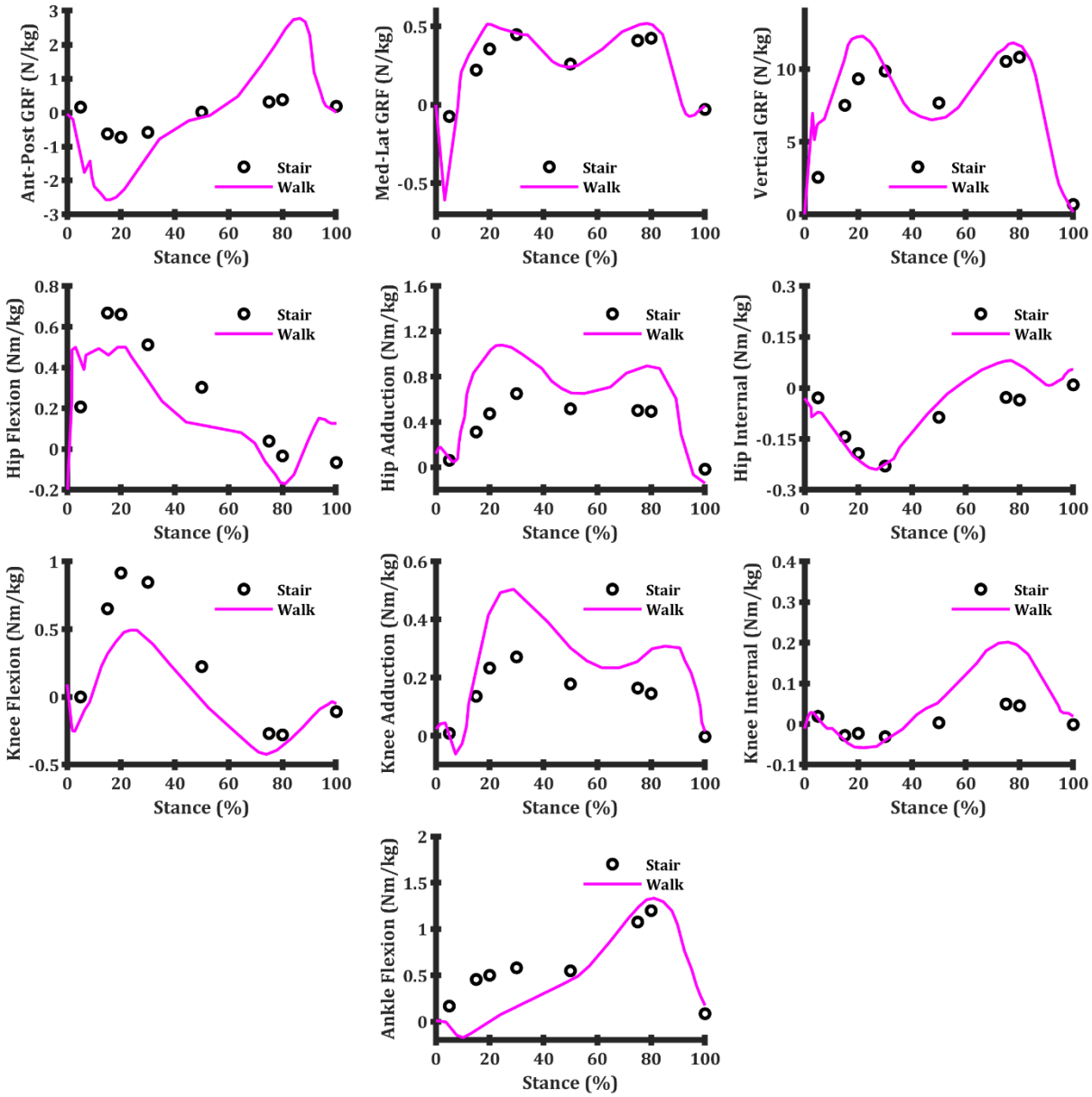

Figure 3.2. GRF as well as hip, knee, and ankle moments represented normalized to 61.9 kg as our subject's body mass. Black circles are based on the weighted mean values reported in stair ascent measurements (Allison et al. 2016; Bennett et al. 2017; Bovi et al. 2011; Gao et al. 2012; Hall et al. 2017; Hsue and Su 2009; King et al. 2017; Komnik et al. 2018; Meyer et al. 2016; Nadeau et al. 2003; Novak and Brouwer 2013; Protopapadaki et al. 2007; Riener et al. 2002; Salsich et al. 2001; Silverman et al. 2014; Trinler et al.

2016; Vallabhajosula et al. 2015; Whatling et al. 2010; Zabala et al. 2013) that drive along with kinematics (Fig. 1) the current simulations. The solid pink lines represent the input data (Astephen et al. 2008) used in our gait simulations reported here for comparison.

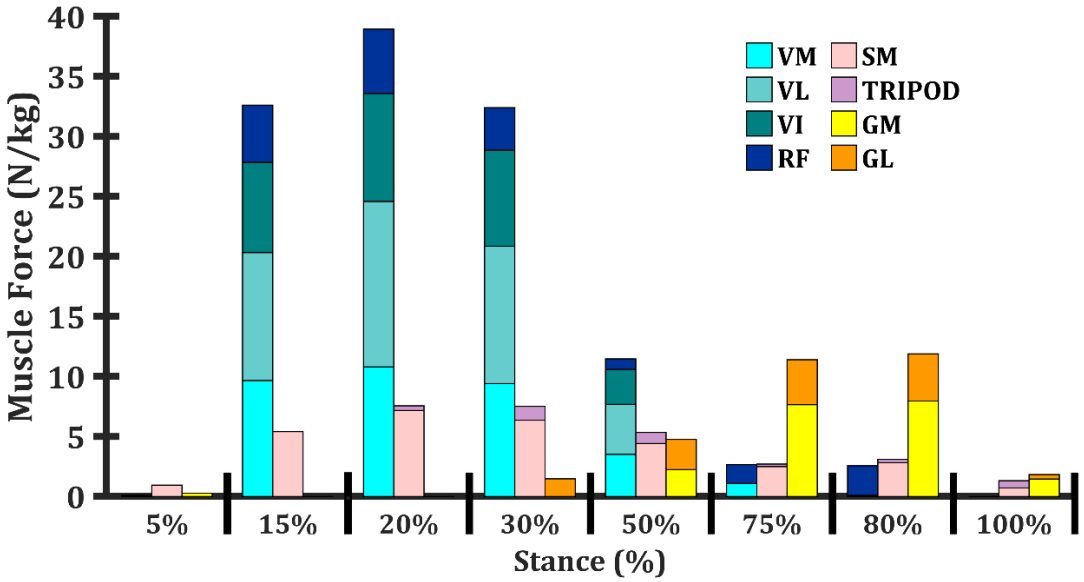

Figure 3.3. Normalized (to 61.9 kg as the body mass of our model) computed forces in muscles crossing the knee joint at different instances of the stance phase during stair ascent. Estimated forces in a number of muscles are also shown and compared with reported electromyography (EMG) activity in Fig. 7. VM: vastus medialis obliqus; VL: vastus lateralis; VI: vastus intermedius medialis; RF: rectus femoris; SM: semimembranous; TRIPOD: made of sartorius (SR), gracilis (GA) and semitendinosus (ST); GM: gastrecnemius medial; GL: gastrocnemius lateral.

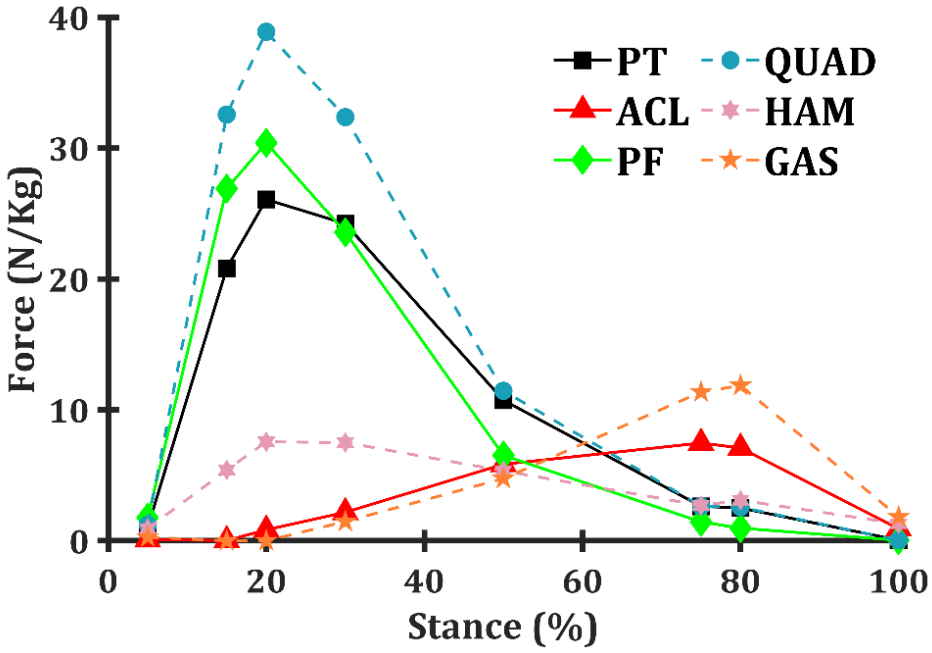

Figure 3.4. The norm of vector sum of normalized (to body mass of 61.9 kg) forces in different muscle groups, ACL and PT as well as PF total contact force during the stance phase of stair ascent. PT: patellar tendon; ACL: anterior cruciate ligament; PF: patellofemoral ligament; QUAD: quadriceps; HAM: hamstrings; GAS: gastrocnemii.

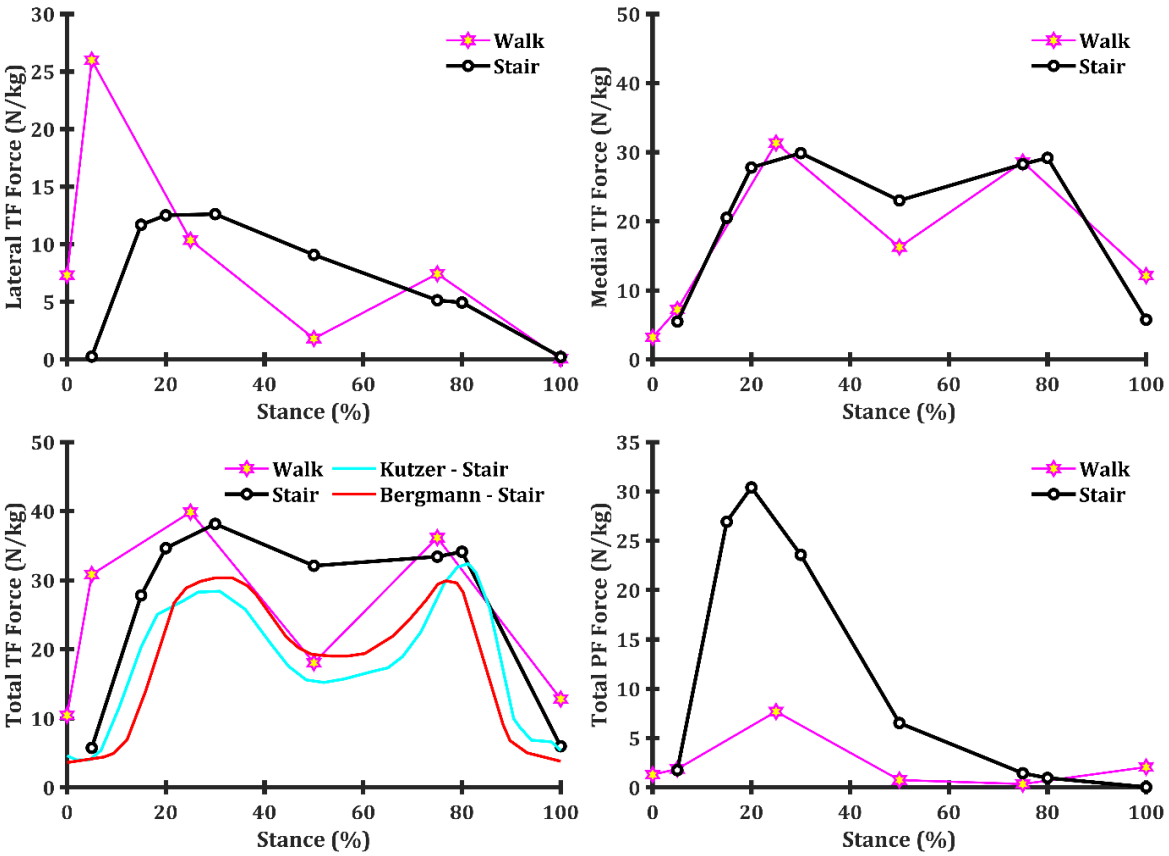

Figure 3.5. Estimated normalized (to body mass of 61.9 kg) contact forces on the tibial and patellar articular surfaces during both stair ascent and level walking (Marouane et al. 2017). Measured contact forces during stair ascent by instrumented implants are also shown for comparison (Bergmann et al. 2014; Kutzner et al. 2010).

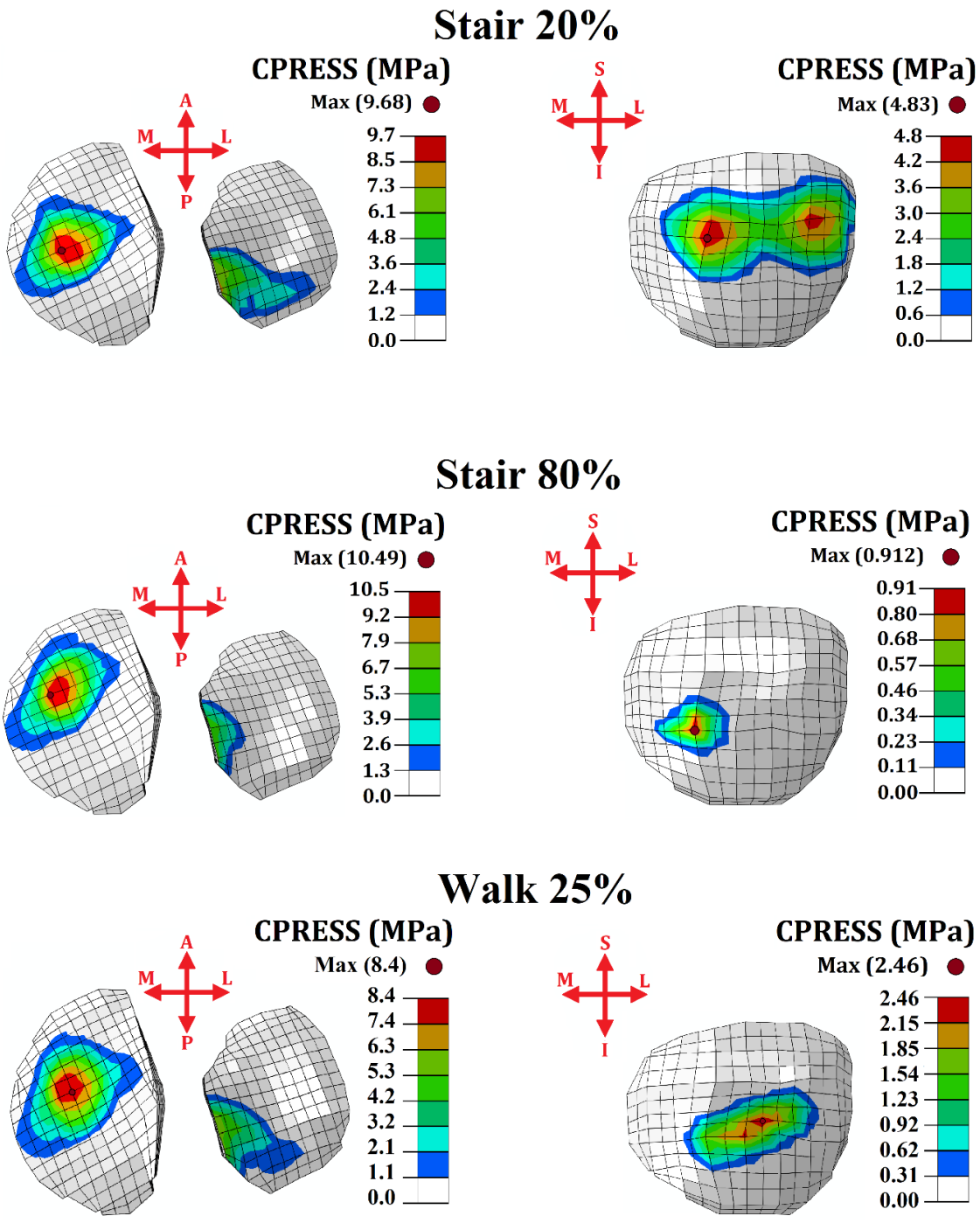

Figure 3.6. Contact pressure distribution on patellar and tibial articular surfaces at critical instances of stance during stair ascent (top two rows) and level walking (bottom row).

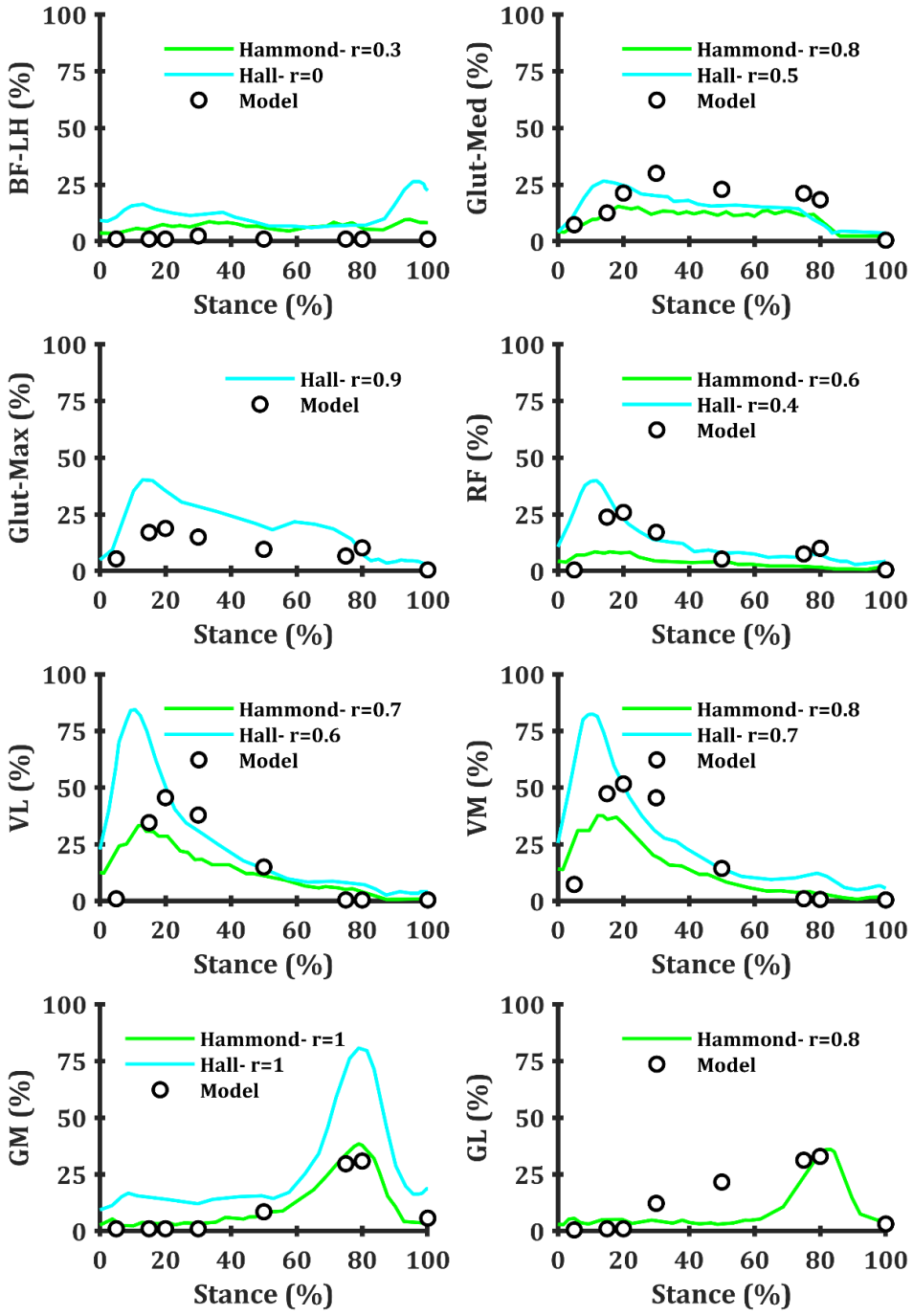

Figure 3.7. Comparison of predicted muscle activities (muscle forces normalized to $\sigma_{max} \times PCSA$) versus measured EMG values (normalized to their peaks recorded at maximum voluntary isometric contractions) (Hall et al. 2015; Hammond et al. 2017) during the stance phase of stair ascent. The correlation coefficients (r) between estimated and measured data are also given.

No conflict of interest to declare.

CHAPTER 4 GENERAL DISCUSSION

We used a coupled MS-FE model to simulate the knee joint during the stance phase of the stair ascent. The detailed FE model of the knee joint was reconstructed from a female cadaveric specimen (Bendjaballah et al., 1995) and integrated within a lower extremity MS model. The mean of in vivo measured GRFs and angles-moments at hip, knee and ankle joints collected on healthy individuals (Figs 2.1 and 2.2) were used to drive the integrated model. With prescribed kinematics-kinetics applied and equilibrium equations maintained at various joints, muscle forces were iteratively estimated while minimizing the sum of cubed muscle stresses. The hypothesis that the PF joint carries much more load in stair ascent in comparison with level walking, was confirmed. Forces in ACL were lower however only in the first half of stance during stair ascent compared to walking.

Overall, high correlation coefficients (r) are found between the estimated muscle activities (normalized to 0.6 PCSA) and reported normalized EMGs (Fig. 2.7). The trend of estimated muscle activities are similar in comparison with the reported MVIC-normalized EMGs. Particularly, for quadriceps and gastrocnemii muscles where peak activities occur in the first and second halves of stance, respectively, very good agreements were observed. Computed muscle forces are also in good agreement with others reporting EMG during stair ascent either in absolute values with no normalization to their peaks at maximum voluntary contractions (Bovi et al., 2011; Camargo et al., 2021; Reeves et al., 2009) or in combination for multiple muscles and locations (Lin et al., 2015).

Overall, much larger flexion moments and angles at the knee, hip and ankle joints during the first half of stance, set stair ascent apart from level walking (Figs 2.1 and 2.2). Following similar trends, hip and knee adduction moments are smaller in stair ascent whereas GRFs are nearly the same (Fig. 2.2). Large knee flexion moment greatly activates quadriceps muscles. Together with the large knee flexion angle, they generate very large PT forces and PF contact forces.

Another subtle issue is that, in contrast to hamstrings, quadriceps muscles ability to generate moments under large knee flexion angles decreases (Mesfar and Shirazi-Adl, 2006b). Results also support the strategy to reduce knee flexion angles-moments (i.e., quadriceps avoidance) observed in patients with PF pain (de Oliveira Silva et al., 2015; Salsich et al., 2001; Zabala et al., 2013).

As a consequence of important PF and TF contact forces, large contact stresses are computed (Fig. 2.6). In stair ascent, despite slightly smaller peak TF contact force compared to level walking, moderately greater medial TF contact stress is predicted. The contact areas shift anteriorly on TF compartments and distally on PF contact areas when the knee extends from 20% to 80% instances in stair ascent (Fig. 2.6). Due to much greater PF contact forces in stair ascent, much larger, maximal contact stresses are estimated on both medial and lateral facets of the PF articular areas. It is interesting that, in stair ascent, under nearly equal contact forces on the PF (at 20% stance) and medial TF (at 20-30% stance) joints and due to the larger PF contact area, the peak contact stress is nearly twice greater on the medial TF than on the PF surface.

Concomitant much larger knee flexion angles markedly diminish ACL forces and consequently, during the first half of stance and despite a much larger activity in quadriceps in stair ascent compared to level walking, much smaller forces are computed in ACL (Mesfar and Shirazi-Adl, 2005). As the knee flexion angle increases, the direction of PT force on the tibia reverses from an anterior pull to a posterior one that as a result influences ACL force (DeFrate et al., 2007; Mesfar and Shirazi-Adl, 2005; Thomeer et al., 2020). High activity in gastrocnemii that, similar to quadriceps, are ACL antagonist (Adouni et al., 2016; Sharifi and Shirazi-Adl, 2021a) also has an effect here.

Interpretations of predictions should be made in the light of some limitations. We used a single knee geometry reconstructed from a female cadaveric specimen (Bendjaballah et al., 1995). Although input data into the model are taken from the literature, we have extensively validated this model with available in vitro and in vivo data (Bendjaballah et al., 1997; Marouane and Shirazi-Adl, 2019; Mesfar and Shirazi-Adl, 2006a, b; Moglo and Shirazi-Adl, 2005). The lower extremity musculature as well as input kinematics-kinetics-GRFs were taken from the mean of data on asymptomatic subjects available in the literature (Figs 2.1 and 2.2). Due to the large scatter and absence of a unique study of stair ascent with all required data, this approach of taking the mean of available data appears justified. Determination of the extent of changes in predicted outputs as a result of scatter in the input kinematics-kinetics should however await future statistical analyses (see (Sharifi et al., 2020) in walking).

CHAPTER 5 CONCLUSION AND RECOMMENDATIONS

During this study a detailed FE model of the knee joint coupled with a lower extremity MS model was developed to simulate stair ascent. In vivo mean measurements including kinematics, kinetics and GRF from earlier studies were considered and rescaled to the body mass of our female subject (61.9 kg). The point at which GRF applies and generates the measured moments was calculated and the masses of the leg and the foot were accounted for. An optimization tool was employed in order to minimize the sum of cubed muscle stresses and a unique optimum set of muscle forces were calculated. ABAQUS software was employed to calculate the stress distributions at the articular surfaces, ligaments forces and contact forces. The muscle forces were compared with the valid studies and a good agreement observed. For comparison purposes, the previous studies of our group on level walking were shown. The PF contact force during stair ascent was much larger in comparison with level walking (almost 4 times larger). Large activity in quadriceps muscles during the first half of the stair ascent stance phase was estimated. Results confirm the correlation between knee flexion angle and ACL force (Mesfar and Shirazi-Adl, 2005); much smaller ACL force observed during stair ascent in comparison with level walking during the first half of the stance. These results help understand the biomechanics of the intact knee joint during the stair ascent cycle and could be of a great for prevention and treatments of the knee disorders.

5.1 Limitations and errors

Interpretations of predictions should be made in the light of some limitations. We used a single knee geometry reconstructed from a female cadaveric specimen (Bendjaballah et al., 1995). Though input data into the model are taken from the literature, we have extensively validated this model with available in vitro and in vivo data (Bendjaballah et al., 1997; Marouane and Shirazi-Adl, 2019; Mesfar and Shirazi-Adl, 2006a, b; Moglo and Shirazi-Adl, 2005). The lower extremity musculature as well as input kinematics-kinetics-GRFs were taken from the mean of data on asymptomatic subjects available in the literature (see captions of Figs 2.1 and 2.2). Due to the large scatter and absence of a unique study of stair ascent with all required data, this approach of taking the mean of available data appears justified. Determination of the extent of changes in predicted outputs as a result of scatter in the input kinematics and kinetics should however await future

statistical analyses (see (Sharifi et al., 2020) in walking). The assumption of the bony structures as rigid bodies, though time consuming in the current nonlinear FE-MS model, may affect results especially of stresses and strains in the deeper cartilage layers. Finally, a non-zero minimum muscle activity threshold to enhance cocontraction was not considered in this optimization-based model.

5.2 Future works

1- Using computed tomography scanning or MRI to develop subject specific FE models with specific geometry including the muscle insertions and bone topology.

2- Using in vivo measurements for a specific individual to accurately simulate the joints biomechanics during daily tasks while considering subject-specific parameters such as sex, weight, and height.

3- Developing a FE model which considers the bony parts as a deformable body. Thus, studying cartilage stresses-strain in deeper zones, bone remodeling and osteoporosis.

REFERENCES

Adouni, M., Shirazi-Adl, A., 2009. Knee joint biomechanics in closed-kinetic-chain exercises. Computer Methods in Biomechanics Biomedical Engineering 12, 661-670.

Adouni, M., Shirazi-Adl, A., 2013. Consideration of equilibrium equations at the hip joint alongside those at the knee and ankle joints has mixed effects on knee joint response during gait. Journal of Biomechanics 46, 619-624.

Adouni, M., Shirazi-Adl, A., Marouane, H., 2016. Role of gastrocnemius activation in knee joint biomechanics: gastrocnemius acts as an ACL antagonist. Computer Methods in Biomechanics and Biomedical Engineering 19, 376-385.

Adouni, M., Shirazi-Adl, A., Shirazi, R., 2012. Computational biodynamics of human knee joint in gait: from muscle forces to cartilage stresses. Journal of Biomechanics 45, 2149-2156.

Afzali, T., Fangel, M. V., Vestergaard, A. S., Rathleff, M. S., Ehlers, L. H., & Jensen, M. B., 2018. Cost-effectiveness of treatments for non-osteoarthritic knee pain conditions: A systematic review. PloS one, 13(12), e0209240.

Ahmed, A., Burke, D., Hyder, A., 1987. Force analysis of the patellar mechanism. Journal of Orthopaedic Research 5, 69-85.

Ahmed, A., Burke, D., Yu, A., 1983. In-vitro measurement of static pressure distribution in synovial joints—Part II: retropatellar surface. Journal of Biomechanical Engineering 105, 226-236.

Allison, K., Bennell, K.L., Grimaldi, A., Vicenzino, B., Wrigley, T.V., Hodges, P.W., 2016. Single leg stance control in individuals with symptomatic gluteal tendinopathy. Gait & Posture 49, 108-113.

Amis, A., & Dawkins, G. ,1991. Functional anatomy of the anterior cruciate ligament. Fibre bundle actions related to ligament replacements and injuries. The Journal of bone and joint surgery. British volume, 73(2), 260-267.

Andersen, R.E., Crespo, C.J., Ling, S.M., Bathon, J.M., Bartlett, S.J., 1999. Prevalence of significant knee pain among older Americans: results from the Third National Health and Nutrition Examination Survey. Journal of the American Geriatrics Society 47, 1435-1438.

Andriacchi, T., Andersson, G., Fermier, R., Stern, D., Galante, J., 1980. A study of lower-limb mechanics during stair-climbing. Journal of Bone Joint Surgery 62, 749-757.

Andriacchi, T.P., Mündermann, A., Smith, R.L., Alexander, E.J., Dyrby, C.O., Koo, S., 2004. A framework for the in vivo pathomechanics of osteoarthritis at the knee. Annals of Biomedical Engineering 32, 447-457.

Andriacchi, T. P., Briant, P. L., Bevill, S. L., & Koo, S., 2006. Rotational changes at the knee after ACL injury cause cartilage thinning. Clinical Orthopaedics and Related Research, 442 39-44.

Argenson JN, Guillaume JM, Aubaniac JM. 1995. Is there a place for patellofemoral arthroplasty? Clinical Orthopaedics and Related Research. (321):162-167. PMID: 7497663.

Astephen, J.L., Deluzio, K.J., Caldwell, G.E., Dunbar, M.J., 2008. Biomechanical changes at the hip, knee, and ankle joints during gait are associated with knee osteoarthritis severity. Journal of Orthopaedic Research 26, 332-341.

Bendjaballah, M., Shirazi-Adl, A., Zukor, D., 1995. Biomechanics of the human knee joint in compression: reconstruction, mesh generation and finite element analysis. Knee 2, 69-79.

Bendjaballah, M., Shirazi-Adl, A., Zukor, D., 1997. Finite element analysis of human knee joint in varus-valgus. Clinical Biomechanics 12, 139-148.

Bergmann, G., Bender, A., Graichen, F., Dymke, J., Rohlmann, A., Trepczynski, A., Heller, M.O., Kutzner, I., 2014. Standardized loads acting in knee implants. PloS one 9, e86035.

Bischoff, J.E., Hertzler, J.S., Mason, J.J., 2009. Patellofemoral interactions in walking, stair ascent, and stair descent using a virtual patella model. Journal of Biomechanics 42, 1678-1684.

Blagojevic, M., Jinks, C., Jeffery, A., Jordan, K., 2010. Risk factors for onset of osteoarthritis of the knee in older adults: a systematic review and meta-analysis. Osteoarthritis and Cartilage 18, 24-33.

Boling, M., Padua, D., Marshall, S., Guskiewicz, K., Pyne, S., Beutler, A., 2010. Gender differences in the incidence and prevalence of patellofemoral pain syndrome. Scandinavian Journal of Medicine & Science in Sports 20, 725-730.

Bovi, G., Rabuffetti, M., Mazzoleni, P., Ferrarin, M., 2011. A multiple-task gait analysis approach: Kinematic, kinetic and EMG reference data for healthy young and adult subjects. Gait & Posture 33, 6-13.

Camargo, J., Ramanathan, A., Flanagan, W., Young, A., 2021. A comprehensive, open-source dataset of lower limb biomechanics in multiple conditions of stairs, ramps, and level-ground ambulation and transitions. Journal of Biomechanics 119, 110320.

Chang, B.-C., Khan, M.I., Prado, A., Yang, N., Ou, J., Agrawal, S.K., 2020. Biomechanical differences during ascent on regular stairs and on a stairmill. Journal of Biomechanics 104, 109758.

Cohen, Z.A., Roglic, H., Grelsamer, R.P., Henry, J.H., Levine, W.N., Van Mow, C., Ateshian, G.A., 2001. Patellofemoral stresses during open and closed kinetic chain exercises: an analysis using computer simulation. The American Journal of Sports Medicine 29, 480-487.

Costigan, P.A., Deluzio, K.J., Wyss, U.P., 2002. Knee and hip kinetics during normal stair climbing. Gait & Posture 16, 31-37.

Davis, J., Kaufman, K.R., Lieber, R.L., 2003. Correlation between active and passive isometric force and intramuscular pressure in the isolated rabbit tibialis anterior muscle. Journal of Biomechanics 36, 505-512.

De Leva, P., 1996. Adjustments to Zatsiorsky-Seluyanov's segment inertia parameters. Journal of Biomechanics 29, 1223-1230.

de Oliveira Silva, D., Briani, R.V., Pazzinatto, M.F., Ferrari, D., Aragão, F.A., de Azevedo, F.M., 2015. Reduced knee flexion is a possible cause of increased loading rates in individuals with patellofemoral pain. Clinical Biomechanics 30, 971-975.

DeFrate, L.E., Nha, K.W., Papannagari, R., Moses, J.M., Gill, T.J., Li, G., 2007. The biomechanical function of the patellar tendon during in-vivo weight-bearing flexion. Journal of Biomechanics 40, 1716-1722.

DeHaven, K.E., Lintner, D.M., 1986. Athletic injuries: comparison by age, sport, and gender. The American Journal of Sports Medicine 14, 218-224.

Draganich, L., Andriacchi, T., Andersson, G., 1987. Interaction between intrinsic knee mechanics and the knee extensor mechanism. Journal of Orthopaedic Research 5, 539-547.

Farahmand, F., Tahmasbi, M., Amis, A., 1998. Lateral force–displacement behaviour of the human patella and its variation with knee flexion—a biomechanical study in vitro. Journal of Biomechanics 31, 1147-1152.

Farahmand, F., Tahmasbi, M.N., Amis, A., 2004. The contribution of the medial retinaculum and quadriceps muscles to patellar lateral stability—an in-vitro study. Knee 11, 89-94.

Gabriel, M. T., Wong, E. K., Woo, S. L. Y., Yagi, M., & Debski, R. E. ,2004. Distribution of in situ forces in the anterior cruciate ligament in response to rotatory loads. Journal of orthopaedic research, 22(1), 85-89.

Gao, B., Cordova, M.L., Zheng, N., 2012. Three-dimensional joint kinematics of ACL-deficient and ACL-reconstructed knees during stair ascent and descent. Human Movement Science 31, 222-235.

Ghafari, A.S., Meghdari, A., Vossoughi, G., 2009. Muscle-driven forward dynamics simulation for the study of differences in muscle function during stair ascent and descent. Proceedings of the Institution of Mechanical Engineers, Part H: Journal of Engineering in Medicine 223, 863-874.

Ghezelbash, F., Shirazi-Adl, A., El Ouaaid, Z., Plamondon, A., Arjmand, N., 2020. Subject-specific regression equations to estimate lower spinal loads during symmetric and asymmetric static lifting. J Biomech 102, 109550.

Goodfellow, J., Hungerford, D., Zindel, M., 1976. Patello-femoral joint mechanics and pathology. 1. Functional anatomy of the patello-femoral joint. The Journal of Bone Joint Surgery 58, 287-290.

Goudakos, I.G., König, C., Schöttle, P.B., Taylor, W.R., Singh, N.B., Roberts, I., Streitparth, F.,

Duda, G.N., Heller, M.O., 2009. Stair climbing results in more challenging patellofemoral contact mechanics and kinematics than walking at early knee flexion under physiological-like quadriceps loading. Journal of Biomechanics 42, 2590-2596.

Goyal, Kanu, et al., 2012. In Vivo Analysis of the Isolated Posterior Cruciate Ligament–Deficient Knee During Functional Activities. The American journal of sports medicine 40.4: 777-785.

Grood, E.S., Suntay, W.J.J.J.o.b.e., 1983. A joint coordinate system for the clinical description of three-dimensional motions: application to the knee. Journal of biomechanical engineering 105, 136-144.

Grood, E., Noyes, F., Butler, D., & Suntay, W., 1981. Ligamentous and capsular restraints preventing straight medial and lateral laxity in intact human cadaver knees. JBJS, 63(8), 1257-1269.

Hall, M., Stevermer, C.A., Gillette, J.C., 2015. Muscle activity amplitudes and co-contraction during stair ambulation following anterior cruciate ligament reconstruction. Journal of Electromyography and Kinesiology 25, 298-304.

Hall, M., Wrigley, T.V., Kean, C.O., Metcalf, B.R., Bennell, K.L., 2017. Hip biomechanics during stair ascent and descent in people with and without hip osteoarthritis. Journal of Orthopaedic Research 35, 1505-1514.

Hammond, C.A., Hatfield, G.L., Gilbart, M.K., Garland, S.J., Hunt, M.A., 2017. Trunk and lower limb biomechanics during stair climbing in people with and without symptomatic femoroacetabular impingement. Clinical Biomechanics 42, 108-114.

Hans-Peter W. van Jonbergen, Dirk M. Werkman, Lex F. Barnaart, Albert van Kampen, 2010. Long-Term Outcomes of Patellofemoral Arthroplasty, The Journal of Arthroplasty,Volume 25, Issue 7,Pages 1066-1071, ISSN 0883-5403, https://doi.org/10.1016/j.arth.2009.08.023.

Heegaard, J., Leyvraz, P., Curnier, A., Rakotomanana, L., Huiskes, R., 1995. The biomechanics of the human patella during passive knee flexion. Journal of Biomechanics 28, 1265-1279.

Herquelot, E., Bodin, J., Petit, A., Ha, C., Leclerc, A., Goldberg, M., Zins, M., Roquelaure, Y., Descatha, A., 2015. Incidence of chronic and other knee pain in relation to occupational risk factors in a large working population. Annals of Occupational Hygiene 59, 797-811.

Haut Donahue, Tammy L., et al., 2002. A finite element model of the human knee joint for the study of tibio-femoral contact." Journal of biomechanical engineering 124.3: 273-280.

Hewett, T. E., Myer, G. D., Ford, K. R., Heidt Jr, R. S., Colosimo, A. J., McLean, S. G., Succop, P., 2005. Biomechanical measures of neuromuscular control and valgus loading of the knee predict

anterior cruciate ligament injury risk in female athletes: a prospective study. The American journal of sports medicine, 33(4), 492-501.

Hirokawa, S., 1991. Three-dimensional mathematical model analysis of the patellofemoral joint. Journal of Biomechanics 24, 659-671.

Hsich, Y.-F., Draganich, L., 1997. Knee kinematics and ligament lengths during physiologic levels of isometric quadriceps loads. Knee 4, 145-154.

Hsieh, Y.-F., Draganich, L.F., 1998. Increasing Quadriceps Loads Affect the Lengths of the Ligaments and the Kinematics of the Knee. Journal of Biomechanical Engineering 120, 750-756.

Hsue, B.-J., Su, F.-C., 2009. Kinematics and kinetics of the lower extremities of young and elder women during stairs ascent while wearing low and high-heeled shoes. Journal of Electromyography Kinesiology 19, 1071-1078.

Huberti, H., Hayes, W., Stone, J., Shybut, G., 1984. Force ratios in the quadriceps tendon and ligamentum patellae. Journal of Orthopaedic Research 2, 49-54.

Huberti, H.H., Hayes, W., 1984. Patellofemoral contact pressures. The influence of q-angle and tendofemoral contact. The Journal of Bone Joint Surgery 66, 715-724.

Huberti, H.H., Hayes, W.C., 1988. Contact pressures in chondromalacia patellae and the effects of capsular reconstructive procedures. Journal of Orthopaedic Research 6, 499-508.

Jones, G.T., Harkness, E.F., Nahit, E.S., McBeth, J., Silman, A.J., Macfarlane, G., 2007. Predicting the onset of knee pain: results from a 2-year prospective study of new workers. Annals of the Rheumatic Diseases 66, 400-406.

Jurist, K.A., Otis, J.C., 1985. Anteroposterior tibiofemoral displacements during isometric extension efforts: the roles of external load and knee flexion angle. American Journal of Sports Medicine 13, 254-258.

Kakarlapudi, T., & Bickerstaff, D. ,2000. Knee instability: isolated and complex. British journal of sports medicine, 34(5), 395-400.

Kathryn R. Fingar, Ph.D., M.P.H., Carol Stocks, Ph.D., R.N., Audrey J. Weiss, Ph.D., and Claudia A. Steiner, M.D., M.P.H., 2014. Healthcare Cost and Utilization Project (HCUP). Nationwide Inpatient Sample (NIS). Statistical Brief # 1862

Kim, Sunny, Bosque, Jose, Meehan, John P. Jamali, Amir, Marder, Richard., 2011. Increase in Outpatient Knee Arthroscopy in the United States: A Comparison of National Surveys of Ambulatory Surgery, 1996 and 2006, The Journal of Bone & Joint Surgery: Volume 93 - Issue 11 - p 994-1000. doi: 10.2106/JBJS.I.01618.

Kim, C., Linsenmeyer, K.D., Vlad, S.C., Guermazi, A., Clancy, M.M., Niu, J. and Felson, D.T., 2014. Prevalence of Radiographic and Symptomatic Hip Osteoarthritis in an Urban United States Community: The Framingham Osteoarthritis Study. Arthritis & Rheumatology, 66: 3013-3017. https://doi.org/10.1002/art.38795

King, S.L., Vanicek, N., O'Brien, T.D., 2017. Sagittal plane joint kinetics during stair ascent in patients with peripheral arterial disease and intermittent claudication. Gait & Posture 55, 81-86.

Klussmann, A., Gebhardt, H., Nübling, M., Liebers, F., Perea, E.Q., Cordier, W., von Engelhardt, L.V., Schubert, M., Dávid, A., Bouillon, B., 2010. Individual and occupational risk factors for knee osteoarthritis: results of a case-control study in Germany. Arthritis Research Therapy 12, 1-15.

Komnik, I., David, S., Funken, J., Haberer, C., Potthast, W., Weiss, S., 2018. Compromised knee internal rotation in total knee arthroplasty patients during stair climbing. PloS one 13, e0205492.

Konrath, J.M., Karatsidis, A., Schepers, H.M., Bellusci, G., de Zee, M., Andersen, M.S., 2019. Estimation of the knee adduction moment and joint contact force during daily living activities using inertial motion capture. Sensors 19, 1681.

Kurtz SM, Ong KL, Lau E, Widmer M, Maravic M, Gomez-Barrena E, et al., 2011. International survey of primary and revision total knee replacement. Int Orthop. 35(12):1783–9.

Kutzner, I., Heinlein, B., Graichen, F., Bender, A., Rohlmann, A., Halder, A., Beier, A., Bergmann, G., 2010. Loading of the knee joint during activities of daily living measured in vivo in five subjects. Journal of Biomechanics 43, 2164-2173.

Lankhorst, N., Damen, J., Oei, E., Verhaar, J., Kloppenburg, M., Bierma-Zeinstra, S., van Middelkoop, M., 2017. Incidence, prevalence, natural course and prognosis of patellofemoral osteoarthritis: the Cohort Hip and Cohort Knee study. Osteoarthritis and Cartilage 25, 647-653.

Li, G., Rudy, T., Sakane, M., Kanamori, A., Ma, C., Woo, S., 1999. The importance of quadriceps and hamstring muscle loading on knee kinematics and in-situ forces in the ACL. Journal of Biomechanics 32, 395-400.

Li, G., Zayontz, S., DeFrate, L.E., Most, E., Suggs, J.F., Rubash, H.E., 2004. Kinematics of the knee at high flexion angles: an in vitro investigation. Journal of Orthopaedic Research 22, 90-95.

Li Guoan, et al., 2008. Effect of posterior cruciate ligament deficiency on in vivo translation and rotation of the knee during weightbearing flexion. The American journal of sports medicine 36.3 : 474-479.

Logan, Martin, et al., 2004. The effect of posterior cruciate ligament deficiency on knee kinematics. The American journal of sports medicine 32.8:1915-1992.

Mandeville, D., Osternig, L.R., Lantz, B.A., Mohler, C.G., Chou, L.-S., 2008. The effect of total knee replacement on the knee varus angle and moment during walking and stair ascent. Clinical Biomechanics 23, 1053-1058.

Marouane, H., Shirazi-Adl, A., 2019. Sensitivity of medial-lateral load sharing to changes in adduction moments or angles in an asymptomatic knee joint model during gait. Gait & Posture 70, 39-47.

Marouane, H., Shirazi-Adl, A., Adouni, M., 2017. 3D active-passive response of human knee joint in gait is markedly altered when simulated as a planar 2D joint. Biomechanics modeling in mechanobiology 16, 693-703.

Mesfar, W., Shirazi-Adl, A., 2005. Biomechanics of the knee joint in flexion under various quadriceps forces. Knee 12, 424-434.

Mesfar, W., Shirazi-Adl, A., 2006a. Biomechanics of changes in ACL and PCL material properties or prestrains in flexion under muscle force-implications in ligament reconstruction. Computer Methods in Biomechanics Biomedical Engineering 9, 201-209.

Mesfar, W., Shirazi-Adl, A., 2006b. Knee joint mechanics under quadriceps–hamstrings muscle forces are influenced by tibial restraint. Clinical Biomechanics 21, 841-848.

Mesfar, W., Shirazi-Adl, A., 2008. Knee joint biomechanics in open-kinetic-chain flexion exercises. Clinical Biomechanics 23, 477-482.

Meyer, C.A.G., Corten, K., Fieuws, S., Deschamps, K., Monari, D., Wesseling, M., Simon, J.-P., Desloovere, K., 2016. Evaluation of stair motion contributes to new insights into hip osteoarthritis-related motion pathomechanics. Journal of Orthopaedic Research 34, 187-196.

Mikkelsen, S., Pedersen, E.B., Brauer, C., Møller, K.L., Alkjær, T., Koblauch, H., Simonsen, E.B., Thygesen, L.C., 2019. Knee osteoarthritis among airport baggage handlers: A prospective cohort study. American Journal of Industrial Medicine 62, 951-960.

Moglo, K.E., Shirazi-Adl, A., 2005. Cruciate coupling and screw-home mechanism in passive knee joint during extension–flexion. Journal of Biomechanics 38, 1075-1083.

Mononen, M.E., Mikkola, M.T., Julkunen, P., Ojala, R., Nieminen, M.T., Jurvelin, J.S. and Korhonen, R.K., 2012. Effect of superficial collagen patterns and fibrillation of femoral articular cartilage on knee joint mechanics—A 3D finite element analysis. Journal of biomechanics, 45(3), pp.579-587.

Mootanah, R., Imhauser, C. W., Reisse, F., Carpanen, D., Walker, R. W., Koff, M. F., Dewan, Z., 2014. Development and validation of a computational model of the knee joint for the evaluation of surgical treatments for osteoarthritis. Computer methods in biomechanics and biomedical engineering, 17(13), 1502-1517.

Nadeau, S., McFadyen, B.J., Malouin, F., 2003. Frontal and sagittal plane analyses of the stair climbing task in healthy adults aged over 40 years: what are the challenges compared to level walking? Clinical biomechanics 18, 950-959.

Nicholl JP, Coleman P, Williams., 1991. BTPilot study of the epidemiology of sports injuries and exercise-related morbidity. British Journal of Sports Medicine 25:61-66.

Novak, A.C., Brouwer, B., 2013. Kinematic and kinetic evaluation of the stance phase of stair ambulation in persons with stroke and healthy adults: a pilot study. Journal of Applied Biomechanics 29, 443-452.

Organisation for Economic Co-operation and Development **OECD health data** http://dx.doi.org/10.1787/health-data-en ,2017. Accessed 1st Oct 2018 Google Scholar

Palmer, K.T., 2012. Occupational activities and osteoarthritis of the knee. British Medical Bulletin 102, 147-170.

Pandy, M.G., Shelburne, K.B., 1997. Dependence of cruciate-ligament loading on muscle forces and external load. Journal of Biomechanics 30, 1015-1024.

Parolie, James M., and John A. Bergfeld., 1986. Long-term results of nonoperative treatment of isolated posterior cruciate ligament injuries in the athlete." The American journal of sports medicine 14.1: 35-38.

Pena, E., Calvo, B., Martinez, M.A. and Doblare, M., 2006. A three-dimensional finite element analysis of the combined behavior of ligaments and menisci in the healthy human knee joint. Journal of biomechanics, 39(9), pp.1686-1701.

Pereira, D., Peleteiro, B., Araujo, J., Branco, J., Santos, R., Ramos, E., 2011. The effect of osteoarthritis definition on prevalence and incidence estimates: a systematic review. Osteoarthritis and Cartilage 19, 1270-1285.

Plotnikoff, R.C., Costigan, S.A., Williams, R.L., Hutchesson, M.J., Kennedy, S.G., Robards, S.L., Allen, J., Collins, C.E., Callister, R., Germov, J., 2015. Effectiveness of interventions targeting physical activity, nutrition and healthy weight for university and college students: a systematic review and meta-analysis. International Journal of Behavioral Nutrition Physical Activity 12, 1-10.

Pearle AD, Russell F. Warren, Scott A. Rodeo, 2005. Basic Science of Articular Cartilage and Osteoarthritis, Clinics in Sports Medicine, Volume 24, Issue 1,2005,Pages 1-12, ISSN 0278-5919, https://doi.org/10.1016/j.csm.2004.08.007.

Persson F, A. Turkiewicz, D. Bergkvist, P. Neuman, M. Englund, 2018.The risk of symptomatic knee osteoarthritis after arthroscopic meniscus repair vs partial meniscectomy vs the general population, Osteoarthritis and Cartilage, Volume 26, Issue 2, 2018, Pages 195-201, ISSN 1063-4584, https://doi.org/10.1016/j.joca.2017.08.020.

Powers, C.M., Lilley, J.C., Lee, T.Q., 1998. The effects of axial and multi-plane loading of the extensor mechanism on the patellofemoral joint. Clinical Biomechanics 13, 616-624.

Protopapadaki, A., Drechsler, W.I., Cramp, M.C., Coutts, F.J., Scott, O.M., 2007. Hip, knee, ankle kinematics and kinetics during stair ascent and descent in healthy young individuals. Clinical Biomechanics 22, 203-210.

Quintelier, J., Lobbestael, F., Verdonk, P., De Baets, P., Almqvist, F., 2008. Patellofemoral contact pressures. Acta of Bioengineering Biomechanics 10, 23-28.

Race, A., & Amis, A. A. ,1996. Loading of the two bundles of the posterior cruciate ligament: an analysis of bundle function in aP drawer. Journal of biomechanics, 29(7), 873-879.

Reeves, N.D., Spanjaard, M., Mohagheghi, A.A., Baltzopoulos, V., Maganaris, C.N., 2009. Older adults employ alternative strategies to operate within their maximum capabilities when ascending stairs. Journal of Electromyography Kinesiology 19, e57-e68.

Reid, C.R., Bush, P.M., Cummings, N.H., McMullin, D.L., Durrani, S.K., 2010. A review of occupational knee disorders. Journal of Occupational Rehabilitation 20, 489-501.

Riener, R., Rabuffetti, M., Frigo, C., 2002. Stair ascent and descent at different inclinations. Gait & Posture 15, 32-44.

Sakai, N., Luo, Z.-P., Rand, J.A., An, K.-N., 1996. Quadriceps forces and patellar motion in the anatomical model of the patellofemoral joint. Knee 3, 1-7.

Salsich, G.B., Brechter, J.H., Powers, C.M., 2001. Lower extremity kinetics during stair ambulation in patients with and without patellofemoral pain. Clinical Biomechanics 16, 906-912.

Senavongse, W., Farahmand, F., Jones, J., Andersen, H., Bull, A., Amis, A., 2003. Quantitative measurement of patellofemoral joint stability: force–displacement behavior of the human patella in vitro. Journal of Orthopaedic Research 21, 780-786.

Sharifi, M., Shirazi-Adl, A., 2021a. Changes in gastrocnemii activation at mid-to-late stance markedly affects the intact and anterior cruciate ligament deficient knee biomechanics and stability in gait. Knee 29, 530-540.

Sharifi, M., Shirazi-Adl, A., 2021b. Knee flexion angle and muscle activations control the stability of an anterior cruciate ligament deficient joint in gait. Journal of Biomechanics 117, 110258.

Sharifi, M., Shirazi-Adl, A., Marouane, H., 2018. Computation of the role of kinetics, kinematics,

posterior tibial slope and muscle cocontraction on the stability of ACL-deficient knee joint at heel strike–Towards identification of copers from non-copers. Journal of Biomechanics 77, 171-182.

Sharifi, M., Shirazi-Adl, A., Marouane, H., 2020. Sensitivity of the knee joint response, muscle forces and stability to variations in gait kinematics-kinetics. Journal of Biomechanics 99, 109472.

Shirazi, R., Shirazi-Adl, A., Hurtig, M., 2008. Role of cartilage collagen fibrils networks in knee joint biomechanics under compression. Journal of Biomechanics 41, 3340-3348.

Shirazi, R., Shirazi-Adl, A., 2008. Deep vertical collagen fibrils play a significant role in mechanics of articular cartilage. Journal of Orthopaedic Research 26, 608-615.

Silverman, A.K., Neptune, R.R., Sinitski, E.H., Wilken, J.M., 2014. Whole-body angular momentum during stair ascent and descent. Gait & Posture 39, 1109-1114.

Swenson DM, Collins CL, Best TM, Flanigan DC, Fields SK, 2013. Comstock RD. Epidemiology of knee injuries among U.S. high school athletes, 2005/2006-2010/2011. Med Sci Sports Exerc. 45(3):462-469. doi:10.1249/MSS.0b013e318277acca

Taunton, J.E., Ryan, M.B., Clement, D., McKenzie, D.C., Lloyd-Smith, D., Zumbo, B., 2002. A retrospective case-control analysis of 2002 running injuries. British Journal of Sports Medicine 36, 95-101.

Taylor, W.R., Heller, M.O., Bergmann, G., Duda, G.N., 2004. Tibio-femoral loading during human gait and stair climbing. Journal of Orthopaedic Research 22, 625-632.

Thomeer, L.T., Lin, Y.-C., Pandy, M.G., 2020. Load Distribution at the Patellofemoral Joint During Walking. Annals of Biomedical Engineering 48, 2821-2835.

Trinler, U.K., Baty, F., Mündermann, A., Fenner, V., Behrend, H., Jost, B., Wegener, R., 2016. Stair dimension affects knee kinematics and kinetics in patients with good outcome after TKA similarly as in healthy subjects. Journal of Orthopaedic Research 34, 1753-1761.

Vallabhajosula, S., Tan, C.W., Mukherjee, M., Davidson, A.J., Stergiou, N., 2015. Biomechanical analyses of stair-climbing while dual-tasking. Journal of Biomechanics 48, 921-929.

Walker, P., Bali, K., Van der Wall, H. et al., 2012. Evaluation of echogenic emboli during total knee arthroplasty using transthoracic echocardiography. Knee Surg Sports Traumatol Arthrosc 20, 2480–2486. https://doi.org/10.1007/s00167-012-1927-4.

Ward, S.R., Powers, C.M., 2004. The influence of patella alta on patellofemoral joint stress during normal and fast walking. Clinical Biomechanics 19, 1040-1047.

Whatling, G.M., Evans, S.L., Holt, C.A., 2010. Introducing a new staircase design to quantify healthy knee function during stair ascent and descent. Computer Methods in Biomechanics Biomedical Engineering 13, 371-378.

Wright, R. W., Preston, E., Fleming, B. C., Amendola, A., Andrish, J. T., Bergfeld, J. A., Marx, R. G., 2008. A Systematic Review of Anterior Cruciate Ligament Reconstruction Rehabilitation–Part II: Open Versus Closed Kinetic Chain Exercises, Neuromuscular Electrical Stimulation, Accelerated Rehabilitation, and Miscellaneous Topics. The journal of knee surgery, 21(03), 225-234.

Zabala, M.E., Favre, J., Scanlan, S.F., Donahue, J., Andriacchi, T.P., 2013. Three-dimensional knee moments of ACL reconstructed and control subjects during gait, stair ascent, and stair descent. Journal of Biomechanics 46, 515-520.

APPENDIX A SUPPLEMENTARY RESULTS

In chapter two, the muscle force predictions have been shown as well as reported EMG, the magnitude of which were normalized to MVIC (refs to be added). These reported EMGs allow to verify both the magnitude and the trend of predicted muscle forces during stair ascent. Nevertheless, other studies have been performed reporting EMG of muscles during stair ascend, but they are not normalized to MVIC (Bovi et al., 2011; Camargo et al., 2021; Reeves et al., 2009). These studies can be beneficial for verifying the trend of muscle forces during stair ascent. In figure 3.1. the muscle activities with the recorded EMG have been shown.

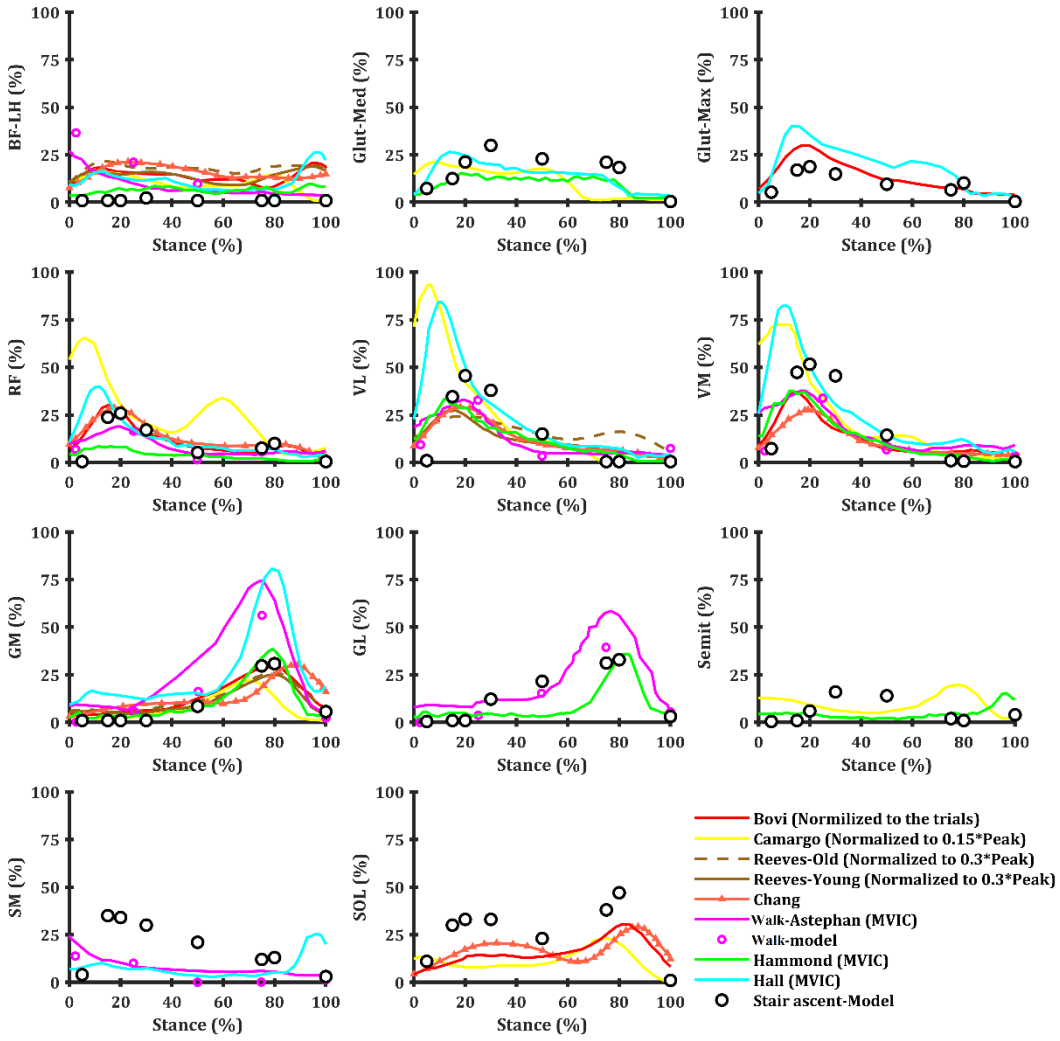

Figure S1. Comparison of predicted muscle activities (muscle forces normalized to $\sigma_{max} \times PCSA$) versus measured EMG values (normalized to their peaks recorded at maximum voluntary isometric

contractions) (Hall et al., 2015; Hammond et al., 2017) during the stance phase of stair ascent. Other studies that are not normalized to MVIC are also given for the purpose of trend comparison. (Bovi et al., 2011; Camargo et al., 2021; Reeves et al., 2009)

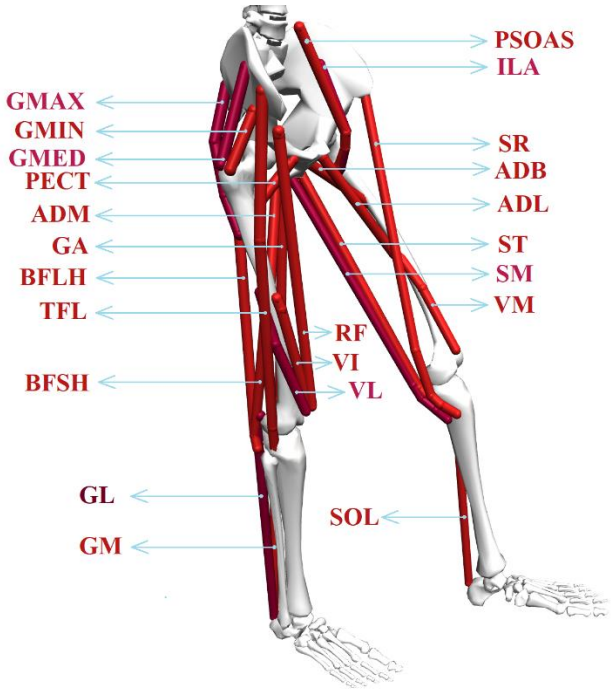

Figure S2- Schematic diagram showing the 34 muscles incorporated into the lower extremity model (OpenSim; Delp et al. (2007)). Quadriceps components are vastus medialis obliqus (VM), rectus femoris (RF), vastus intermidus medialis (VI) and vastus lateralis (VL). Hamstrings components include biceps femoris long head (BFLH), biceps femoris short head (BFSH), semi membranous (SM) and TRIPOD made of sartorius (SR), gracilis (GA) and semitendinosus (ST). Gastrocnemius components are gastrocnemius medial (GM) and gastrocnemius lateral (GL). Soleus (SOL) muscle is uni-articular ankle muscle. Hip joint muscles (not all shown) include adductor, long (ADL), mag (3 components ADM) and brev (ADB); gluteus max (3 components GMAX), med (3 components GMED) and min (3 components GMIN), iliacus (ILA), iliopsoas (PSOAS), quadriceps femoris; pectineus (PECT), tensor facia lata (TFL), periformis. OpenSim is used to define muscle insertions and wrappings (via points) before transferring the model to Abaqus for FE analyses (BH = 169 cm; BM= 61.9 kg).

Delp, S.L., Anderson, F.C., Arnold, A.S., Loan, P., Habib, A., John, C.T., Guendelman, E., Thelen, D.G., 2007. OpenSim: open-source software to create and analyze dynamic simulations of movement. IEEE Transactions on Biomedical Engineering 54, 1940-1950.

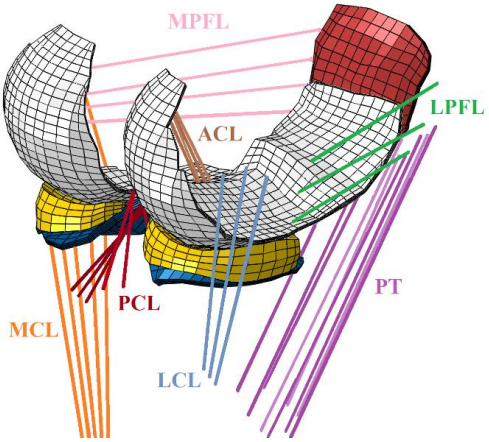

Figure S3- Detailed knee FE model; tibiofemoral (TF) and patellofemoral (PF) articular cartilage layers, menisci, and patellar tendon (PT). Joint ligaments include lateral patellofemoral (LPFL), medial patellofemoral (MPFL), anterior cruciate (ACL), posterior cruciate (PCL), lateral collateral (LCL) and medial collateral (MCL). The rigid bony structures are not shown.

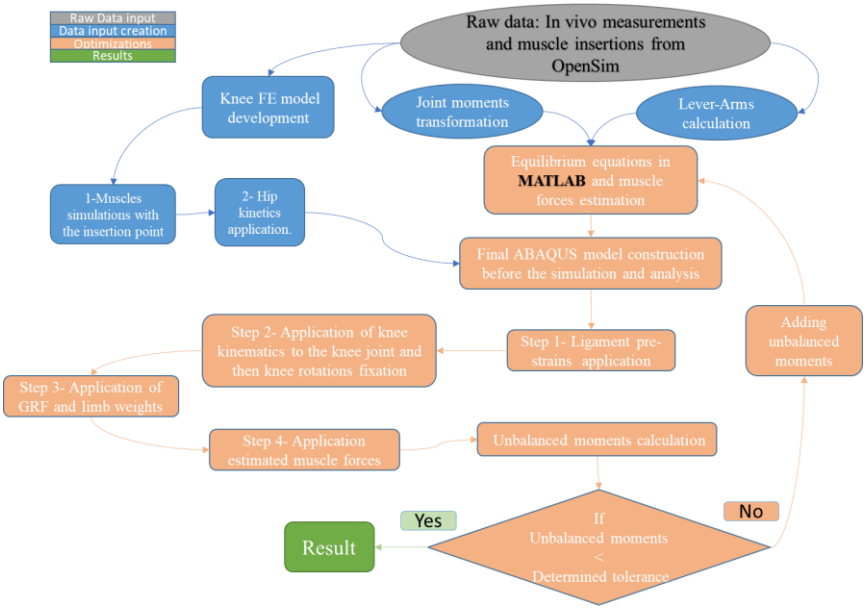

Figure S4- Step by step flow-chart of the simulation.

Muscles	PCSA (mm^2)
ADB	907
ADL	1326
ADM 1	805
ADM 2	725
ADM 3	1032
BF-lh	1894
GEM	347
GMAX 1	1332
GMAX 2	1903
GMAX 3	1283
GMED 1	1732
GMED 2	1211
GMED 3	1518
GMIN 1	685
GMIN 2	723
GMIN 3	819
GA	342
ILA	2268
PECT	562
PERI	939
PSOAS	2353
QF	805
RF	2719
SR	330
SM	2723
ST	867
TFL	493
BF-sh	1700
VI	2597
VL	3956
VM	2736
GL	1570
GM	3368
SOL	4415

Table S5- List of used physiological cross-sectional area (PCSA) for the 34 muscles incorporated into the lower extremity model (OpenSim; Delp et al. (2007)). Quadriceps components are vastus medialis obliqus (VM), rectus femoris (RF), vastus intermidus medialis (VIM) and vastus lateralis (VL). Hamstrings components include biceps femoris long head (BFLH), biceps femoris short head (BFSH), semi membranous (SM) and TRIPOD made of sartorius (SR), gracilis (GA) and semitendinosus (ST). Gastrocnemius components are gastrocnemius medial (GM) and gastrocnemius lateral (GL). Soleus (SOL) muscle is uni-articular ankle muscle. Hip joint muscles

include adductor, long (ADL), mag (3 components ADM) and brev (ADB); gluteus max (3 components GMAX), med (3 components GMED) and min (3 components GMIN), iliacus (ILA), iliopsoas (PSOAS), piriformis (PERI), superior gemellus (GEM), quadriceps femoris; pectineus (PECT), tensor facia lata (TFL), periformis, quadratus femoris (QF). The muscles PCSA have been taken from the maximum isometric muscle forces of Opensim and then scaled to our model bodyweight and bodyheight. (BH = 169 cm; BM= 61.9 kg)